Міністерство освіти і науки України
Національний університет «Запорізька політехніка»

НОВІ МАТЕРІАЛИ І ТЕХНОЛОГІЇ В МЕТАЛУРГІЇ ТА МАШИНОБУДУВАННІ

НАУКОВИЙ ЖУРНАЛ

ВИХОДИТЬ ЧОТИРИ РАЗИ НА РІК

№ 4’2025

Заснований у грудні 1997 року

Засновник та видавець – Національний університет «Запорізька політехніка»

Запоріжжя
НУ «Запорізька політехніка»
2025

Ministry of Education and Science of Ukraine
National University Zaporizhzhia Polytechnic

NEW MATERIALS AND TECHNOLOGIES IN METALLURGY AND MECHANICAL ENGINEERING

THE SCIENTIFIC JOURNAL

PUBLISHED FOUR TIMES PER YEAR

No 4’2025

Founded in December 1997

Founder and publisher – National University Zaporizhzhia Polytechnic

Zaporizhzhia
NU Zaporizhzhia Polytechnic
2025

p-ISSN 1607-6885
e-ISSN 2786-7358

УДК 669+621.002+621.002.3

Наказом Міністерства освіти і науки України № 1471 від 26.11.2020 р. «Про затвердження рішень Атестаційної колегії Міністерства щодо діяльності спеціалізованих вчених рад від 26 листопада 2020 року» журнал «Нові матеріали і технології в металургії та машинобудуванні» **(скорочена назва – НМТ)** включений до переліку наукових фахових видань України в категрії «Б»**, в яких можуть публікуватися результати дисертаційних робіт на здобуття наукових ступенів доктора наук і доктора філософії (кандидата наук).**

Інтернет-сторінка журналу: https://nmt.zp.edu.ua

Наукове видання включено до міжнародних (INSPEC, CrossRef) і національних («Джерело», Національна бібліотека України імені В. І. Вернадського НАН України) реферативних та наукометричних баз даних.

Опублікованим статтям присвоюється унікальний ідентифікатор цифрового об'єкта DOI.

Науковий журнал друкує оригінальні та оглядові статті науковців ВНЗ і установ України та інших країн відповідно до рубрик:

- теорія будови та структурних змін у металах, сплавах та композитах. Вплив термічної, хіміко-термічної та термомеханічної обробки на характер структури і фізико-механічні властивості матеріалів;
- конструкційні та функціональні матеріали. Механічні властивості сталей, сплавів та композитів. Технологічне забезпечення надійності та довговічності деталей енергетичних установок. Методи механічного оброблення. Технології зміцнювальних обробок. Характеристики поверхневих шарів та захисних покриттів деталей машин і виробів;
- металургійне виробництво. Теплофізика та теплоенергетика. Ресурсозберігальні технології. Порошкова металургія. Промтранспорт. Раціональне використання металів;
- механізація, автоматизація та роботизація. Вдосконалення методів дослідження та контролю якості металів. Моделювання процесів у металургії та машинобудуванні.

РЕДАКЦІЙНИЙ ШТАТ

Рукописи надісланих статей проходять додаткове незалежне рецензування з залученням провідних фахівців України та інших країн, за результатами якого редакційна колегія ухвалює рішення щодо можливості їх опублікування. Рукописи не повертаються.

Рекомендовано до видання Вченою радою Національного університету «Запорізька політехніка»,
протокол № 6 від 23 грудня 2025 року.

Журнал набраний та зверстаний у редакційно-видавничому відділі Національного університету «Запорізька політехніка»

Комп'ютерний дизайн та верстання Наталія Савчук

Адреса редакції: 69063, Запоріжжя, вул. Університетська, 64, тел. (061) 769-82-96, редакційно-видавничий відділ

e-mail: rvv@zp.edu.ua

p-ISSN 1607-6885
e-ISSN 2786-7358

UDC 669+621.002+621.002.3

By order of the Ministry of Education and Science of Ukraine No. 1471 of November 26, 2020 "On approval of decisions of the Attestation Board of the Ministry regarding the activities of specialized scientific councils of November 26, 2020", the journal "New materials and technologies in metallurgy and mechanical engineering" (abbreviated name - NMT) is included in the list of scientific professional publications of Ukraine in the category "B", in which the results of dissertations for the scientific degrees of Doctor of Science and Doctor of Philosophy (candidate of science) can be published.

Internet page of the journal: https://nmt.zp.edu.ua
The scientific publication is included in international (INSPEC, CrossRef) and national (Dzherelo, National Library of Ukraine named after V. I. Vernadsky of the National Academy of Sciences of Ukraine) abstract and scientometric databases.
Published articles are assigned a unique DOI digital object identifier.
The scientific journal publishes original articles by scientists from universities and organizations of Ukraine and other countries in accordance with the headings:
- theory of structure and structural changes in metals, alloys and composites. Influence of thermal, chemical-thermal and thermomechanical treatment on the nature of the structure and physical and mechanical properties of materials;
- structural and functional materials. Mechanical properties of steels, alloys and composites. Technological support of reliability and durability of parts of power plants. Methods of mechanical processing. Hardening technologies. Characteristics of surface layers and protective coatings of machine parts and products;
- metallurgical production. Thermal physics and heat power engineering. Resource-saving technologies. Powder metallurgy. Promtransport. Rational use of metals;
- mechanization, automation and robotization. Improvement of methods for research and quality control of metals. Modeling of processes in metallurgy and mechanical engineering.

EDITORIAL TEAM

Manuscripts of submitted articles undergo additional independent review with the involvement of leading experts from Ukraine and other countries, based on which the editorial board decides on the possibility of their publication. Manuscripts are not returned.

Recommended for publication by the Academic Council of the National University Zaporizhzhia Polytechnic,
Protocol N 6 Decemder 23, 2025.

The journal was typed and typeset in the editorial and publishing department of the National University Zaporizhzhia Polytechnic

Computer design and layout Nataliia Savchuk

Editorial address: 69063, Zaporizhzhia, st. University, 64, tel. (061) 769-82-96, editorial and publishing department
e-mail: rvv@zp.edu.ua

ЗМІСТ

CONTENTS

125 РОКІВ НЕЗЛАМНОСТІ ТА РОЗВИТКУ: НАЦІОНАЛЬНИЙ УНІВЕРСИТЕТ «ЗАПОРІЗЬКА ПОЛІТЕХНІКА» ВІДЗНАЧИВ ЮВІЛЕЙ

Один із найстаріших технічних університетів України – Національний університет «Запорізька політехніка» – відзначив 125-річчя від дня заснування. Ювілей став знаковою подією не лише для міста Запоріжжя, а й для всієї країни, адже заклад продовжує працювати й розвиватися за 30 кілометрів від лінії фронту, демонструючи стійкість, професіоналізм і віру в майбутнє України.

Історія університету починається у 1900 році з відкриття Олександрівського механіко-технічного училища. Саме воно стало фундаментом інженерної освіти регіону. Протягом XX століття заклад неодноразово змінював свій статус і назву, відображаючи розвиток промисловості та потреби держави: індустріальний технікум, інститут сільськогосподарського машинобудування, авто-механічний та машинобудівний інститути, Запорізький державний технічний університет (ЗДТУ), Запорізький національний технічний університет (ЗНТУ).

Сьогодні він відомий як Національний університет «Запорізька політехніка» – сучасний науково-освітній центр, що поєднує традиції та інновації.

Університет готує фахівців для ключових галузей промисловості України на всіх рівнях вищої освіти. Науково-дослідна база закладу включає сучасні лабораторії, інноваційні центри, міжнародні проєкти та партнерства з промисловими підприємствами.

У час, коли країна потребує нових інженерів, технологів, IT- спеціалістів та науковців, «Запорізька політехніка» відіграє стратегічну роль у формуванні кадрового потенціалу для відбудови держави.

За 125 років у стінах університету було підготовлено тисячі інженерів, винахідників, науковців і виробничих лідерів. Під керівництвом талановитих викладачів тут сформувалися покоління фахівців, чия праця зробила значний внесок у розвиток науки й техніки в Україні та світі.

Університет щодня доводить свою стійкість. Навчальний процес триває, наукові проєкти реалізуються, вступники продовжують обирати «Запорізьку політехніку» як місце для здобуття освіти та професії.

Ювілей став не лише нагодою підбити підсумки, а й подивитися вперед: університет розвиває цифрові технології навчання, модернізує матеріальну базу, розширює міжнародні зв'язки та готується відігравати ще значнішу роль у післявоєнній відбудові України.

125 YEARS OF RESILIENCE AND PROGRESS: ZAPORIZHZHIA POLYTECHNIC NATIONAL UNIVERSITY CELEBRATES ITS ANNIVERSARY

One of the oldest technical universities in Ukraine – Zaporizhzhia Polytechnic National University – has celebrated the 125th anniversary of its founding. This milestone has become a significant event not only for the city of Zaporizhzhia but also for the entire country, as the institution continues to operate and develop just 30 kilometers from the frontline, demonstrating resilience, professionalism, and confidence in Ukraine's future.

The history of the university dates back to 1900, when the Oleksandrivsk Mechanical and Technical School was established. It laid the foundation for engineering education in the region. Throughout the 20th century, the institution underwent several transformations, reflecting the development of industry and the needs of the state: the Industrial Technical School, the Institute of Agricultural Engineering, the Automotive and Mechanical Engineering Institutes, Zaporizhzhia State Technical University (ZSTU), and Zaporizhzhia National Technical University (ZNTU).

Today, it is known as Zaporizhzhia Polytechnic National University – a modern scientific and educational center that combines tradition and innovation.

The university trains specialists for key industrial sectors of Ukraine at all levels of higher education. Its research infrastructure includes modern laboratories, innovation centers, international projects, and partnerships with major industrial enterprises.

At a time when the country urgently needs new engineers, technologists, IT specialists, and researchers, Zaporizhzhia Polytechnic plays a strategic role in forming the human capital needed for Ukraine's reconstruction.

Over the past 125 years, the university has trained thousands of engineers, inventors, scientists, and industrial leaders. Under the guidance of talented educators, generations of professionals have been shaped here – people whose work has made a significant contribution to the development of science and technology in Ukraine and beyond.

University proves its resilience every day. The educational process continues, research projects move forward, and prospective students continue to choose Zaporizhzhia Polytechnic as a place to pursue their education and future careers.

The anniversary has become not only an opportunity to summarize past achievements but also to look ahead: the university continues to develop digital learning technologies, modernize its infrastructure, expand international cooperation, and prepare to play an even more important role in Ukraine's post-war reconstruction.

СТРУКТУРОУТВОРЕННЯ. ОПІР РУЙНУВАННЮ ТА ФІЗИКО-МЕХАНІЧНІ ВЛАСТИВОСТІ

STRUCTURE FORMATION. RESISTANCE TO DESTRUCTION AND PHYSICAL-MECHANICAL PROPERTIES

UDC 669.14.018.8-415:620.193

Volodymyr Kornienko	Postgraduate student of the Department of integrated technologies of welding and structural modeling, National University Zaporizhzhia Polytechnic, Zaporizhzhia, Ukraine, *e-mail: vkornienko268@ gmail.com*, ORCID: 0009-0007-2193-3204
Dmytro Mishchenko	Postgraduate student of the Department of Transport technologies, National University Zaporizhzhia Polytechnic, Zaporizhzhia, Ukraine, *e-mail:dvmis@ukr.net*, ORCID: 0009-0006-7372-3271
Sergiy Byelikov	Doctor of Technical Sciences, Professor of the Department of Transport Technologies, National University Zaporizhzhia Polytechnic, Zaporizhzhia, Ukraine, *e-mail: belikov@zp.edu.ua*, ORCID: 0000-0002-9510-8190
Valeriy Mishchenko	Doctor of Technical Sciences, Professor of the Department of Integrated Yechnologies of Welding and Structural Modeling, National University Zaporizhzhia Polytechnic, Zaporizhzhia, Ukraine, *e-mail: mishchen4@gmail.com*, ORCID: 0000-0003-0992-478X
Natalia Evseeva	PhD, Associate Professor of the Department of Cars, Heat Engines and Hybrid Power Plants, National University Zaporizhzhia Polytechnic, Zaporizhzhia, Ukraine, *e-mail: korskovanat@ukr.net*, ORCID: 0000-0002-3398-6537
Olexiy Kapustyan	PhD, Associate Professor of the Department of Integrated Technologies of Welding and Structural Modeling, National University Zaporizhzhia Polytechnic, Zaporizhzhia, Ukraine, *e-mail: kafedra_otzv@zntu.edu.ua*, ORCID: 0000-0002-8979-8076
Pavlo Tsokotun	Senior lecturer of the Department of Cars, Heat Engines and Hybrid Power Plants, National University Zaporizhzhia Polytechnic, Zaporizhzhia, Ukraine, *e-mail: tsokotunpv@ gmail.com*, ORCID: 0000-0002-0237-4693

COMPARATIVE STUDIES OF THE CORROSION RESISTANCE OF STAINLESS STEEL SHEETS FOR THE COATING LAYER OF BIMETALS

Purpose. *Evaluation of the influence of the chemical composition and structure on the corrosion resistance of steels of different structural classes used as a cladding layer of bimetallic reactors and other devices of titanium-magnesium production.*

Research methods. *In order to choose a rational cladding layer of the developed bimetal, a comparative analysis of the corrosion resistance of steels 12Х18Н9, 10Х14АГ15 and 08Х18Т1 and steels 04Х18ч, 03Х18ТБч and 03Х17Н3Г9МБДЮч, taken as standards for comparison, was carried out [1]. Titanium tetrachloride and a one-molar solution of sulfuric acid were used as chemically active media.*

Results. *The results of the investigation of the corrosion resistance of steels of different structural classes by gravimetric and potentiometric methods in chemically active environments showed that the most suitable option for the cladding layer is steel 03Х17Н3Г9МБДЮч, which has similar coefficients of linear thermal expansion and high corrosion resistance to the base of bimetal - 14Х17Н13МБч [2].*

Scientific novelty. *It was established that the use of bimetal with a cladding layer made of 03Х17Н3Г9МВДЮч, 03Х18Н or 04Х18ч steel reduces the nickel impurity content by 10 times or more in the titanium sponge during the reduction process.*

DOI 10.15588/1607-6885-2025-4-1

Practical value. *The use of a bimetal with a base steel of 14Х17Н13МВч in combination with a cladding layer of steel 03Х17Н3Г9МБДЮч makes it possible to obtain a titanium sponge that is particularly clean of nickel impurities and will significantly expand the scope of use in the aviation and rocket industry.*

Key words: *corrosion-resistant steel, base steel, titanium sponge, reactor, bimetal, cladding layer, impurities.*

Introduction

The modern industrial magnetothermic method of obtaining titanium in batch reactors allows the production of titanium in the form of a sponge. Smelted titanium ingots must meet strict quality standards. However, this method has a significant disadvantage – contamination of the titanium sponge with nickel entering the sponge titanium from the reactor material during the recovery process.

In this regard, the application of bimetals, which can be used in the manufacture of reactor bodies for recovery and separation in magnesiumthermic titanium production, is becoming increasingly relevant. Existing steels used for the manufacture of reactors are subject to deformation, corrosion, contamination of titanium sponge and are limited in service life.

Analysis of research and publications

The modern development of the metallurgical industry in Ukraine and abroad guides researchers to create new corrosion-resistant steels. The reactor body in titanium-magnesium production is usually made of steels capable of withstanding high temperatures and aggressive conditions of the technological process. However, during long-term operation, the reactor undergoes warping and deformation as a result of cyclic heating and cooling, corrosion damage when interacting with chlorides and reaction products, contamination of the titanium sponge. These shortcomings stimulate the search of new materials that have high heat resistance, mechanical strength, and corrosion resistance at the same time [3–8].

The use of bimetals in reactor designs for titanium-magnesium production can be a promising direction for increasing the efficiency, reliability, and economy of the technological process [9-10]. Bimetallic materials can eliminate most of the shortcomings of traditional reactor housings, provide a longer service life of the equipment, reduce costs and improve the quality of the titanium sponge. Further research in the field of selection of optimal combined metals, their joining technologies and operational tests will accelerate the introduction of bimetals into the industrial practice.

Purpose of work

The purpose of this work is to study the corrosion resistance of sheet stainless steels for the cladding layer of bimetals in aggressive environments.

To achieve this goal, the following tasks were formulated and solved:

- a comparative analysis of the corrosion resistance of steels of different structural classes in a one-mole (1M) solution of sulfuric acid H2SO4 was carried out;
- an evaluation of the behavior of selected steels in the melt of titanium tetrachloride TiCl4 was carried out.

Research material and methodology

Gravimetric and potentiometric methods were used to study the corrosion resistance of steels. The chemical composition of the studied steels is given in Table 1.

The essence of the gravimetric method is to determine the change in the mass of a sample of a certain size immersed in an aggressive environment for a certain time.

The essence of the potentiometric method is to obtain passivation characteristics by obtaining polarization diagrams using the fast scanning technique. To do this, the test sample is immersed in the test solution and cathodically polarized with a high scanning speed to a current density of 10^{-2} А/см^2 then anodically polarized at a rate of 50 V/h. Research was carried out using a PP-5848 potentiostat with a preset value current speed. The scheme of the setup for conducting polarization measurements is shown in Figure 1.

Table 1 – Chemical composition of the studied steels

Steel grade	C	Cr	Si	Mn	Ni	W	Mo	V	S	P	Al	Ti	Fe
12Х18Н9	0,12	18,2	0,65	0,4	9,4	-	-	-	0,02	0,02	-	-	bees
10Х15АГ14	0,1	15,2	0,21	14,35	-	-		-	0,03	0,03			
08Х18Т1	0,08	18,0	0,46	0,2					0,017	0,03		0,8	
03Х17Н3Г9 МБДЮч	0,029	16,6	-	9,09	2,3	0,018	0,262	0,256	0,0097	0,0219	0,14	0,042	
04Х18ч	0,04	18,4	0,26	0,31			-	-	0,01	0,023	0,001 рзм	-	
03Х18ТБчЧ	0,03	18,1	0,5	0,2		-	-	-	0,01	0,02	0,001 рзм	0,15	Nb 0,15

DOI 10.15588/1607-6885-2025-4-1

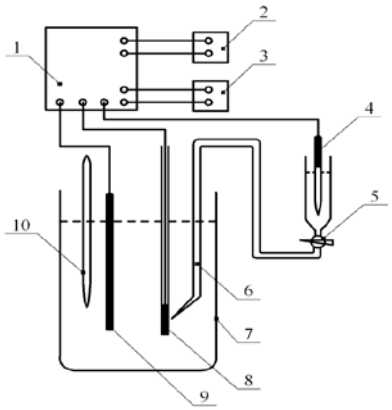

Figure 1. Scheme of the installation for conducting polarization measurements. 1 – potentiostat, 2 – electronic millivoltmeter, 3 – electronic ammeter, 4 – reference electrode, 5 – ground tap, 6 – Luggin capillary, 7 – beaker, 8 – sample, 9 – auxiliary electrode, 10 – thermometer

Research results

On the basis of the conducted research, a bimetal consisting of a cladding layer of steel 03Х17Н3Г9МБДЮч and a base steel 14Х17Н13МБч was developed, which allows to reduce nickel impurities in spongy titanium by 12 times and increase the service life of reactors by 30%.

Experimental electrode potentials are determined in relation to the hydrogen potential, which is assumed to be zero. The tests were carried out in a chemically active one-molar (1M) solution of H2SO4, and the dependence of the potential on the current was constructed for the analysis (Fig. 2–7).

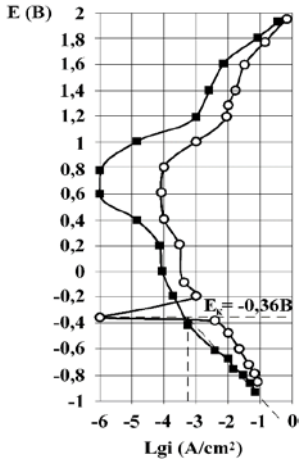

Figure 2. Polarization diagram of steel 03Х17Н3Г9МБДЮч in 1M sulfuric acid solution

It follows from the polarization diagram that the studied steel 03Х17Н3Г9МБДЮч can be transferred to a passive state with a small shift of the potential in the positive direction, which indicates its ability to passivation. The negative potential of steel 03Х17Н3Г9МБДЮч indicates that at first the steel corrodes, but soon the corrosion slows down and this is explained by passivation. The passivation current (In) of steel 03Х17Н3Г9МБДЮч indicates the steel's ability to self-passivation.

The analysis of polarization diagrams shows that in a 1M solution of H2SO4, all studied steels, with the exception of 12Х18Н9 and 03Х17Н3Г9МБДЮч, are in a stable active state (Fig. 2–7) and corrode with the release of hydrogen.

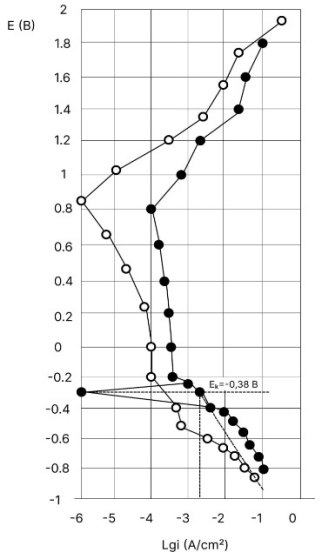

Figure 3. Polarization diagram of 12Х18Н9 steel in 1M sulfuric acid solution

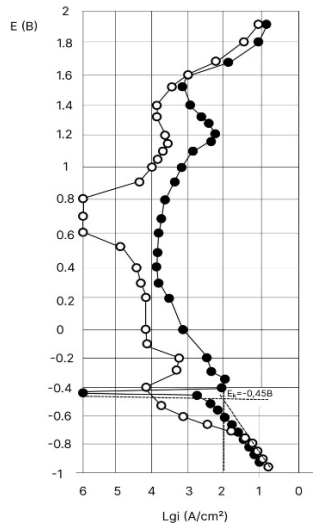

Figure 4. Polarization diagram of 10Х14АГ15 steel in 1M sulfuric acid solution

The passivation current (In) is an order of magnitude higher than 10^{-3}А·см^2 – the maximum cathode current that can be provided by dissolved oxygen in the air. Therefore, all studied steels, with the exception of 12Х18Н9 and 03Х17Н3Г9МБДЮч, are not capable to self-passivation

DOI 10.15588/1607-6885-2025-4-1

in strong acidic solutions even with intensive aeration.

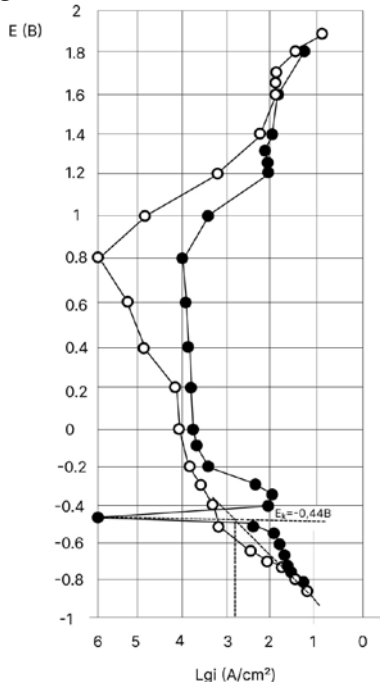

Figure 5. Polarization diagram of 08X18T1 steel in 1M sulfuric acid solution

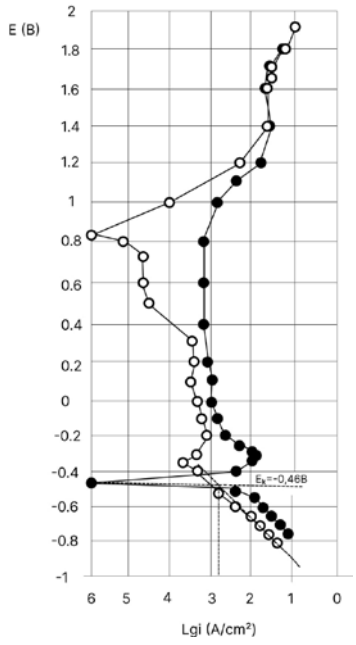

Figure 6. Polarization diagram of steel 04X18h in 1M sulfuric acid solution

This conclusion was confirmed during gravimetric tests: samples of 12X18H9 steel, actively corroded in a 1M solution of H_2SO_4, easily went into a passive state after being exposed to air for a few seconds and then immersed in the solution again. A similar effect was observed in steel 03X17H3Г9МБДЮч.

Samples of other steels began actively corrode again after abovamentioned operation. The results of determining the corrosion of steel in a 1M solution of H2SO4 by the gravimetric method correlate well with the results obtained by the extrapolation method of the Tefel part of the polarization curves (Table 2).

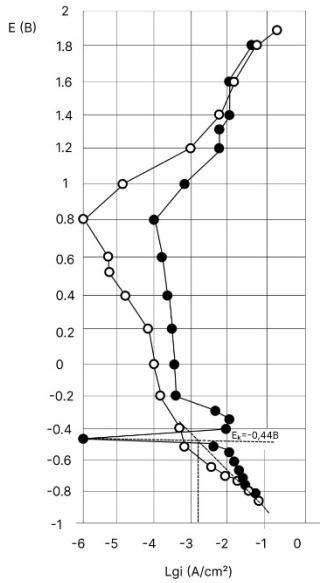

Figure 7. Polarization diagram of 03X18TБч steel in 1M sulfuric acid solution

Table 2 – Results of measurement of corrosion rate in steels in 1M H2SO4 solution

Steel brand	Δm, g/sm^2·h	П Mm/year	Lg I corr, gravim-etry	Lg I corr Po-tent. meas-ure
03X17H3Г9МБДЮч	$4{,}3\cdot10^{-4}$	4,6	-3,55	-3,6
12X18H9	$3{,}51\cdot10^{-4}$	4,1	-3,45	-3,4
10X14АГ15	$4{,}3\cdot10^{-2}$	495,5	-1,36	-1,9
08X18T1	$1{,}9\cdot10^{-3}$	22,6	-2,7	-2,8
04X18ч	$2{,}1\cdot10^{-3}$	24,1	-2,69	-2,7
03X18TБч	$1{,}3\cdot10^{-3}$	15,4	-2,87	-2,9

The corrosion rate of steel 10X14АГ15 in these conditions exceeds the corrosion rate of 08X18T1, 06X18ч and 03X18TБч by an order of magnitude. At the same time, their corrosion resistance is lower than that of 12X18H9 steel in the active, and even more so in the passive state. Some discrepancy between the measured and calculated values of Lg I corr. for steel 10X14АГ15 is explained, apparently, by the presence of a significant self-dissolution current, which is not registered by the device, and occurs at high dissolution rates.

It also follows from the polarization diagrams that all investigated steels can be transferred to a passive state with a relatively small displacement of the system potential in the positive direction. The magnitude of the corrosion current in the passive state obtained from the polarization

DOI 10.15588/1607-6885-2025-4-1

data is 0.0001–0.001 А·см^2 and is obviously overestimated, since the corrosion rate of 12Х18Н9 steel in the passive state actually measured by the gravimetric method is almost two orders of magnitude lower than the calculated value (Table 2).

This effect, apparently, is due to the fact that at such a high scanning speed, a stable passive state is not completely achieved due to the short exposure time at the potentials corresponding to the passive region. However, a relative comparison of the curves shows that the corrosion current in the passive state for steel 04Х18ч is noticeably higher than for other steels. This is a serious sign of the presence of active, poorly passivating areas on its surface and a possible tendency this steel to pitting or intergranular corrosion. Such chemically active non-passivating areas in steel 04Х18ч may be the release of excess rare earth metals, not related to oxygen and sulfur.

A comparative analysis of the corrosion resistance of steels 12Х18Н9, 10Х14АГ15 and 08Х18Т1, taken as standards of comparison with steel 03Х17Н3Г9МБДЮч and 04Х18ч, 03Х18ТБч, was carried out.

Table 3 shows comparative indicators of corrosion resistance of studied steels as a cladding layer of bimetal. does not exceed 200 °C.

Table 3 – Comparative indicators of the corrosion resistance of studied steels of molten titanium tetrachloride TiCl4 for the cladding layer of the bimetal

Steel grade	Duration of test, hour	Media	Corrosion speed g/(sm^2·h)
03Х17Н3Г9 МБДЮч	1440	$TiCl_4$	0,0000762
04Х18ч	1440	$TiCl_4$	0,000029
12Х18Н9	1440	$TiCl_4$	0,0000744

As a result of the tests carried out in the titanium tetrachloride melt, it was established that the corrosion resistance of the steels chosen as the cladding layer 03Х17Н3Г9МБДБч and 04Х18ч are not inferior to steel 12Х18Н9. In addition, due to the low content of nickel in steel 03Х17Н3Г9МБДЮч up to 3.8% and the complete absence of nickel in steel 04Х18ч, nickel impurities in the titanium sponge decreased 12 times in the process of magnesiumthermal reduction of titanium.

Conclusions

Studies of steel 03Х17Н3Г9МБДЮч fully confirm the expediency of using it as a material for the cladding layer of a bimetal for reactors of magnesithermic production of titanium, which in terms of corrosion resistance exceeds steel 12Х18Н9, and the coefficients linear thermal expansion are very close in a wide range of temperatures, in contrast to martensitic-ferritic steel 04Х18ч, nevertheless, this steel can also be used as a cladding layer of bimetals for other devices of titanium-magnesium production, the working temperature of which

References

1. Heat-resistant corrosion-resistant steel: pat. 100650 Ukraine. MPK S 22 S 38/02; appl. 17.02.12 ; publ. 10.01.13, Bull, 1, 4.

2. Heat-resistant alloy on iron-chromium-nickel basis: pat. 129577 Ukraine. MPK S 22 S 38/30, S 22 S 38/30; appl. 04.04.23 ; publ. 04.06.25, Bull, 23, 4.

3. Stainless steel grades [Електронний ресурс] // Outokumpu products. – Режим доступа: http: // www.outokumpu.com / en / stainless-steel / grades / Pages / default.aspx

4. AvestaWelding [Электронний ресурс] // Avesta welding products. – Режим доступа: http: // www.kskct.cz / images / materialy / en / avesta.pdf.

5. Akio Fuwa, Satoru Takaya (2005). Producing titanium by reducing $TiCl_2$ – $MgCl_2$ mixed salt with magnesium in the molten state, JOM Journal of the Minerals, Metals and Materials Society, 57, 10, 56–60.

6. Mishchenko V., Loskutov S., Kripak A (2022). Determining the thermoplastic deformation mechanism of titanium reduction reactors and recommendations to increase the reactor service life. Eastern-European Journal of Enterprise Technologies. ISSN 1729-3774, 5/7 (119), 14–20.

7. V. G. Mishchenko, N. A. Evseeva (2019). Influence of Metallurgical Processing on the Structure and Properties of Multicomponent Alloy Steel. Steel in Translation, 49, 5, 357–360. (Scopus)

8. V. Mishchenko, N. Evseeva, S. Shejko, V. Shalomeev (2019). Steel corrosion resistance in the technological, Materials Science and Technology Conference 2019 (MS and T 2019) : Proceedings, September 29–October 3, 2019, Portland, Oregon. (Scopus)

9. V. G. Mishchenko, S. B. Belikov, A. V. Klimov., A. O. Kripak, D. M. Tonkonog., V. V. Kornienko, A. O. Kharchenko (2023). Creation of a special structural material by rolling asymmetric packages for dual-purpose products. New materials and technologies in metallurgy and mechanical engineering, 2, 32–37.

Received 08.12.2025
Accepted 17.12.2025

DOI 10.15588/1607-6885-2025-4-1

ПОРІВНЯЛЬНІ ДОСЛІДЖЕННЯ КОРОЗІЙНОЇ СТІЙКОСТІ ЛИСТОВИХ НЕРЖАВІЮЧИХ СТАЛЕЙ ДЛЯ ПЛАКУЮЧОГО ШАРУ БІМЕТАЛІВ

Володимир Корнієнко — аспірант кафедри інтегрованих технологій зварювання та моделювання конструкцій Національного університету «Запорізька політехніка», м. Запоріжжя, Україна, *e-mail: vkornienko268@ gmail.com*, ORCID: 0009-0007-2193-3204

Дмитро Міщенко — аспірант кафедри фізичне транспортні технології Національного університету «Запорізька політехніка», м. Запоріжжя, Україна, *e-mail: dvmis@ukr.net*, ORCID: 0009-0006-7327-3271

Сергій Бєліков — д-р техн. наук, професор, професор кафедри транспортні технології Національного університету «Запорізька політехніка», м. Запоріжжя, Україна, *e-mail: belikov@zp.ed.ua*, ORCID: 0000-0002-9510-8190

Валерій Міщенко — д-р техн. наук, професор, професор кафедри інтегрованих технологій зварювання та моделювання конструкцій Національного університету «Запорізька політехніка», м. Запоріжжя, Україна, *e-mail: mishchen4@gmail.com*, ORCID: 0000-0003-0992-478X

Наталія Євсєєва — канд. техн. наук, доцент, доцент кафедри автомобілі, теплові двигуни та гібридні енергетичні установки Національного університету «Запорізька політехніка», м. Запоріжжя, Україна, *e-mail: korskovanat@ukr.net*, ORCID: 0000-0002-3398-6537

Олексій Капустян — канд. техн. наук, доцент, доцент кафедри інтегрованих технологій зварювання та моделювання конструкцій Національного університету «Запорізька політехніка», м. Запоріжжя, Україна, *e-mail: kafedra_otzv@zntu.edu.ua*, ORCID: 0000-0002-8979-8076

Павло Цокотун — старший викладач кафедри автомобілі, теплові двигуни та гібридні енергетичні установки, Національного університету «Запорізька політехніка», м.Запоріжжя, Україна, *e-mail: tsokotunpv@gmail.com*, ORCID: 0000-0002-0237-4693

Мета роботи. *Оцінка впливу хімічного складу та структури на корозійну стійкість сталей різних структурних класів, що використовуються як плакувальний шар біметалів реакторів та інших пристроїв титаномагнієвого виробництва.*

Методи дослідження. *З метою вибору раціонального плакуючого шару біметалу, що розробляється, проведено порівняльний аналіз корозійної стійкості сталей 12Х18Н9, 10Х14АГ15 і 08Х18Т1 і взятих як еталони порівняння сталей 04Х18ч, 03Х18ТБч також 03Х17Н3Г9МБДЮч. Як хімічно активне середовище використовували тетрахлорид титану і одномольний розчин сірчаної кислоти.*

Отримані результати. *Результати дослідження корозійної стійкості сталей різних структурних класів гравіметричним і потенціометричним методами в хімічно активних середовищах показали, що найбільш прийнятим варіантом для шару, що плакує, є сталь 03Х17Н3Г9МБДЮч, що має близькі коефіцієнти лінійного термічного розширення та високою корозійну стійкість з основою біметалу - 14Х17Н13МБч [2].*

Наукова новизна. *Встановлено, що використання біметалу з плакувальним шаром з 03Х17Н3Г9МБДЮч, 03Х18Н або сталі 04Х18гч, знижує вміст домішки нікелю в 10 разів і більше в титановій губці при відновлювальному процесі.*

Практична цінність. *Застосування біметалу з основою сталь 14Х17Н13МБч у поєднанні з плакувальним шаром із сталі 03Х17Н3Г9МБДЮч дає можливості отримувати особливо чисту за домішками нікелю титанову губку та суттєво розширить сферу використання в авіаційній та ракетній промисловості.*

Ключові слова: *корозійностійка сталь, сталь основи, титанова губка, реактор, біметал, плакуючий шар, домішки.*

Список літератури

1. Heat-resistant corrosion-resistant steel: pat. 100650 Ukraine. MPK S 22 S 38/02; appl. 17.02.12 ; publ. 10.01.13, Bull. No. 1. – 4 p.

2. Heat-resistant alloy on iron-chromium-nickel basis: pat. 129577 Ukraine. MPK S 22 S 38/30, S 22 S 38/30; appl. 04.04.23 ; publ. 04.06.25, Bull. No. 23. – 4 p.

DOI 10.15588/1607-6885-2025-4-1

3. Stainless steel grades [Електронний ресурс] // Outokumpu products. – Режим доступа: http: // www.outokumpu.com / en / stainless-steel / grades / Pages / default.aspx

4. AvestaWelding [Электронний ресурс] // Avesta welding products. – Режим доступа: http: // www.kskct.cz / images / materialy / en / avesta.pdf.

5. Akio Fuwa. Producing titanium by reducing $TiCl_2$ – $MgCl_2$ mixed salt with magnesium in the molten state [Текст] / Akio Fuwa, Satoru Takaya // JOM Journal of the Minerals, Metals and Materials Society. – 2005. – Vol. 57. – No. 10. – P. 56 – 60.

6. Mishchenko V. Determining the thermoplastic deformation mechanism of titanium reduction reactors and recommendations to increase the reactor service life. / Mishchenko V., Loskutov S., Kripak A. // Eastern-European Journal of Enterprise Technologies. ISSN 1729-3774, 2022, 5/7 (119), P. 14–20.

7. Mishchenko, V. G. Influence of Metallurgical Processing on the Structure and Properties of Multicomponent Alloy Steel [Текст] / V. G. Mishchenko, N. A. Evseeva // Steel in Translation. – 2019. – Vol. 49. – No. 5. – P. 357–360. (Scopus)

8. Steel corrosion resistance in the technological process / V. Mishchenko, N. Evseeva, S. Shejko, V. Shalomeev // Materials Science and Technology Conference 2019 (MS and T 2019) : Proceedings, September 29–October 3, 2019. – Portland, Oregon. (Scopus)

9. Creation of a special structural material by rolling asymmetric packages for dual-purpose products / V. G. Mishchenko, S. B. Belikov, A. V. Klimov et al. // New materials and technologies in metallurgy and mechanical engineering. – 2023. – No. 2. – C. 32–37.

.

DOI 10.15588/1607-6885-2025-4-1

КОНСТРУКЦІЙНІ І ФУНКЦІОНАЛЬНІ МАТЕРІАЛИ

STRUCTURAL AND FUNCTIONAL MATERIALS

UDC 669.715:669.018.25:620.186

Serhii Puchek — Postgraduate student of the Department of Transport Technologies, National University Zaporizhzhia Polytechnic, Zaporizhzhia, Ukraine, *e-mail: puchek777@gmail.com*, ORCID: 0009-0007-8077-6106

Sergiy Byelikov — Doctor of Technical Sciences, Professor of the Department of Transport Technologies, National University Zaporizhzhia Polytechnic, Zaporizhzhia, Ukraine, *e-mail: belikov@zp.edu.ua*, ORCID: 0000-0002-9510-8190

STRUCTURE AND PROPERTIES OF HEAT-RESISTANT ALLOY ZHS-26VI FOR THE PRODUCTION OF RELEVANT PARTS OF GAS TURBINE ENGINES

Purpose. *To study the macro- and microstructural state of a series of research samples of the heat-resistant alloy ZhS26-VI for the production of critical components of a gas turbine engine, namely rotor blades of a high-pressure turbine (HPT), and to evaluate the mechanical properties and heat resistance in accordance with the technical specifications of the materials of the gas turbine hot part .*

Research methods. *Macro- and microstructural analysis and phase composition studies were carried out by optical metallography using an optical microscope. Mechanical properties at room temperature were determined in accordance with ISO 6892-84 and ST SEV 471-88. Tensile tests were carried out on a ZDMY30 machine.*

Results. *The structure and properties of samples of experimental melts of the ZhS-26VI alloy obtained in the FM-1-2-100 vacuum furnace of the "ULMAC" company by the method of equiaxed crystallization were studied. Significant grinding of the macrograin was established due to intensive heat removal and high crystallization rate. The microstructure of the samples before heat treatment corresponds to the cast state of the alloy, and after heat treatment in the standard mode satisfies the technical conditions and corresponds to the approved microstructure scale. The mechanical and heat-resistant properties of the samples meet the requirements of the regulatory documentation for responsible heat-resistant casting.*

Scientific novelty. *New data on the structure and phase state of the ZhS26-VI alloy of experimental and serial melts were obtained. The fine structure of the nickel-based heat-resistant alloy, which is traditionally used to produce high-pressure turbine blades of an aviation gas turbine engine, was studied.*

Practical value. *The results obtained provide an opportunity to expand the use of the ZhS26-VI heat-resistant alloy for the production of castings for critical purposes.*

Key words: *heat-resistant alloy, macro- and microstructure, heat treatment, mechanical properties, heat resistance, gas turbine blade.*

Introduction

The development of new-generation gas turbine engines (GTEs) requires improved performance characteristics, including power, service life, reliability, durability, and fuel efficiency. Achieving the required GTE performance is ensured by the application of heat-resistant nickel alloys as the primary materials for hot-gas path components [1-5]. Heat-resistant alloys used in gas turbine construction must have an optimal combination of mechanical properties and heat resistance with sufficient ductility, which generally ensures high component performance under conditions of uneven stress distribution across the cross-section. In the works [1–6, 10, 11] special attention was paid to the study and improvement of the long-term strength and creep properties of heat-resistant alloys, and the authors [7–9, 12, 13] paid special attention to the development of principles for alloying heat-resistant alloys operating in high-temperature corrosive environments, which is more typical for gas turbine units in land and marine engine building, although it is also inherent in aircraft engines operating in marine environments or desert regions [8, 9]. Ensuring improved characteristics of hot tract parts and, in general, the operational life of a gas turbine engine is usually carried out in two main directions: the development of new complex heat-resistant alloys with a high content of elements, having low diffusion coefficients under high temperature conditions and increasing the range of service characteristics through additional alloying, modification and microalloying of industrial alloys that have demonstrated reliability in long-term operation [16].

DOI 10.15588/1607-6885-2025-4-2

For modern gas turbine engines, the base material for both uncooled and air-cooled blades are high-strength cast nickel alloys, which, in addition to the nickel base, may contain chromium, cobalt, titanium, aluminum, tungsten, and other elements. An example of such alloys is the nickel alloy ZhS26-VI [14].

Material and Methodology

Fragments of a rod blank produced in a ULMAC FM-1-2-100 vacuum furnace using equiaxed crystallization of the ZhS26-VI alloy were studied.

The chemical composition of the material, as well as the macro- and microstructure of the test samples, were determined. The macrostructure was revealed by chemical etching in a reagent consisting of 80 % HCl and 20 % H_2O_2.

Using high-speed directional solidification, 15mm-diameter, 135mm-long specimens were cast from 90mm-diameter rod blanks of ZhS26-VI alloy obtained from fresh components to determine their mechanical and heat-resistant properties.

The mechanical and heat-resistant properties were determined on unheat-treated specimens, as well as after heat treatment using the standard mode—homogenization at 1265 ± 100 °C in a vacuum.

After processing according to the specified options, the blanks were machined to ensure the dimensions specified in the technical documentation for the manufacture of mechanical testing specimens. Mechanical properties at room temperature (tensile strength, yield strength, elongation, and reduction in area) were determined in accordance with ISO 6892-84 and ST SEV 471-88. Tensile testing was performed on a ZDVY30 testing machine.

Long-term strength testing was conducted in accordance with DSTU ISO 204:2019 using an Instron M3 testing machine at 945 °C and a load of 260 MPa until complete failure of the specimens.

Research Results and Discussion

The chemical composition of the ZhS26-VI alloy for all tested variants, with respect to the main elements, meets the requirements of the scientific and technical documentation for the material (Table 1).The macrostructure of the transverse cut of fragments of workpieces, taken from a vacuum furnace FM-1-2 from OLVAC using the equiaxial crystallization method, is presented in Fig. 1.The structure of the workpiece-fork is presented by the following crystallization zones:

- Zone of fine subcortical crystals;
- Zone of columnar crystals;
- Zone of equiaxed crystals.

The zone of columnar crystals, which expand from the surface of the samples to the central zone at a 12–23 mm distance (Fig. 1). According to the authors [15, 16], this zone is formed under influence of cobalt aluminate, which is introduced into the first ceramic-shaped working layer and ensures increased thermal conductivity [16, 17]. The advancing zone is the zone of equiaxed grains, grown at the center of the fork with a diameter of 4–61 mm. Intensive fragmentation of grains in this zone can be associated with the action of dispersed particles of titanium carbides, which are additional centers of crystallization, which promotes the formation of a more finely dispersed structure of the alloy [16].

Table 1 – Chemical composition of tested variants of ZhS26-VI nickel-based alloy

№ melt	Content of elements, %															
	C	Cr	Co	W	Al	Ti	Mo	Fe	Nb	V	Si	Mn	S	P	B	Ni
1	0,144	5,08	9,05	11,54	5,86	0,98	0,98	0,06	1,54	1,03	0,090	0,008	0,003	0,005		Base
2	0,16	5,10	9,06	11,58	5,90	0,99	1,01	0,06	1,54	1,00	0,080	0,006	0,005	0,004		Base
3	0,144	4,95	9,10	11,46	5,84	1,02	1,06	0,06	1,60	1,05	0,080	0,009	0,005	0,004	0,014	Base
4	0,143	4,98	8,93	11,52	5,90	1,00	1,03	0,06	1,60	1,04	0,080	0,010	0,005	0,004	0,012	Base
5	0,14	5,03	9,00	11,45	5,76	1,02	1,04	0,06	1,65	1,03	0,080	0,010	0,005	0,004	0,011	Base
6	0,143	5,12	9,13	11,51	5,77	1,02	1,06	0,06	1,65	1,05	0,070	0,009	0,005	0,004	0,014	Base
7	0,144	5,16	9,15	11,42	5,66	1,02	1,05	0,06	1,63	1,07	0,080	0,009	0,005	0,004	0,014	Base
8	0,14	4,98	9,03	11,59	5,82	1,05	1,09	0,06	1,60	0,99	0,085	0,008	0,005	0,004	0,013	Base
9	0,15	5,02	9,10	11,49	5,78	1,09	1,11	0,06	1,71	1,08	0,065	0,009	0,005	0,004	0,015	Base
10	0,133	4,80	8,84	11,75	6,05	0,92	1,00	0,06	1,50	1,00	0,10	0,008	0,005	0,004	0,010	Base
11 Series	0,15	5,04	8,89	11,65	5,86	0,93	1,00	0,06	1,63	0,99	0,11	0,009	0,005	0,004	0,010	Base
Norms TU 1-92-177-91	0,12-0,17	4,3-5,3	8,7-9,3	11,2-12,0	5,6-6,1	0,8-1,2	0,8-1,2	≤0,5	1,4-1,8	0,8-1,2	≤0,2	≤0,3	≤ 0,005	≤ 0,010	≤ 0,015	Base

DOI 10.15588/1607-6885-2025-4-2

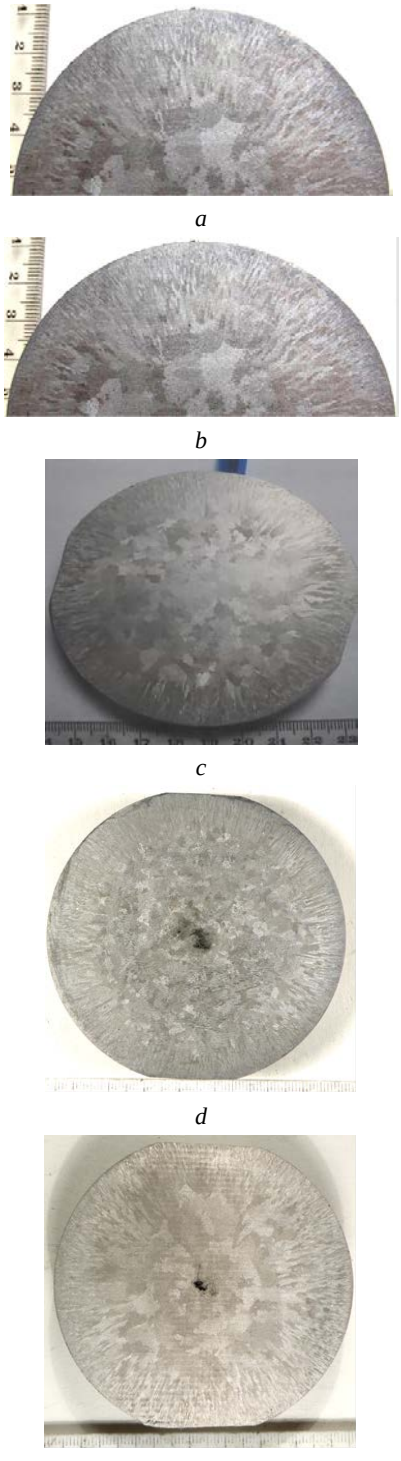

a

b

c

d

e

Figure 1. Macrostructure in the cross-section of the bar blank of the ZhS26-VI alloy samples:
a – variant 1 before heat treatment; *b* – variant 1 after heat treatment; *c* – variant 2 in the initial state; *d* – variant 10 in the initial state; *e* – variant 11 in the initial state

The results of measuring the parameters of the macrostructure of the blanks of different variants of the melts of the ZhS26-VI alloy samples are given in Table 2.

Table 2 – Parameters of the macrostructure of the blanks made of ZhS26-VI metal in the initial state

Option number	Size of crystallization zones, mm			macrograin, size mm
	zone of fine subcortical crystals	columnar crystal zone	zone of equiaxed crystals	
1	1…2	17…23	44…56	3,0…8,0
2	1…2	12…15	52…58	2,0…10,0
10	1…3	18…20	47…51	2,0…5,0
11	1…2	10…12	57…61	1,0…2,5

Metallographic examination of the test samples revealed no metal contamination in the form of films, coarse slag inclusions, or accumulations thereof.

The microstructure of the alloy samples cast made of the ZhS26-VI alloy, in all test variants, is a γ-solid solution with an intermetallic γ′- phase and a eutectic (γ-γ′) phase with carbides and carbonitrides, corresponding to the as-cast state of the ZhS26-VI alloy (Fig. 2).

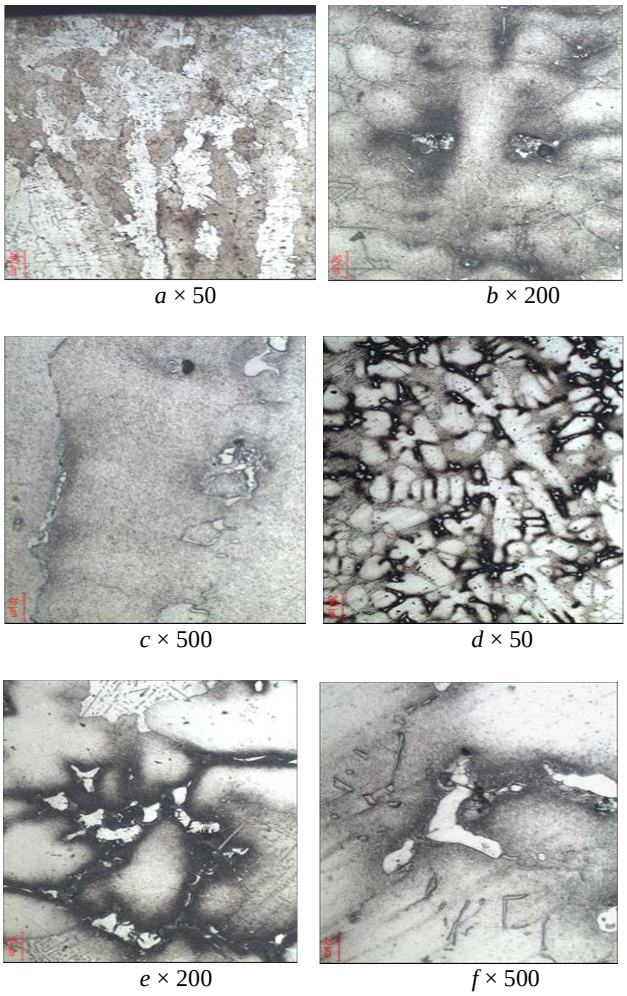

a × 50 *b* × 200

c × 500 *d* × 50

e × 200 *f* × 500

Figure 2. Microstructure in the edge (*a*, *b*, *c*) and central (*d*, *e*, *f*) zones of sample 1

DOI 10.15588/1607-6885-2025-4-2

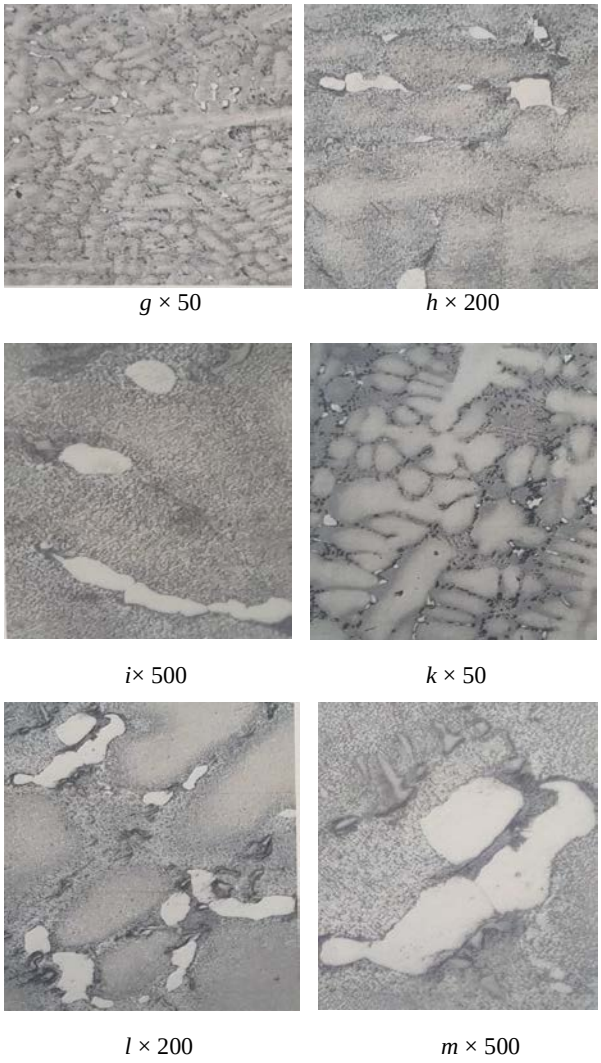

g × 50 *h* × 200

i× 500 *k* × 50

l × 200 *m* × 500

Figure 2. Continuation, in the edge (*g*, *h*, *i*) and central zones of sample 2 (*k*, *l*, *m*) before heat treatment

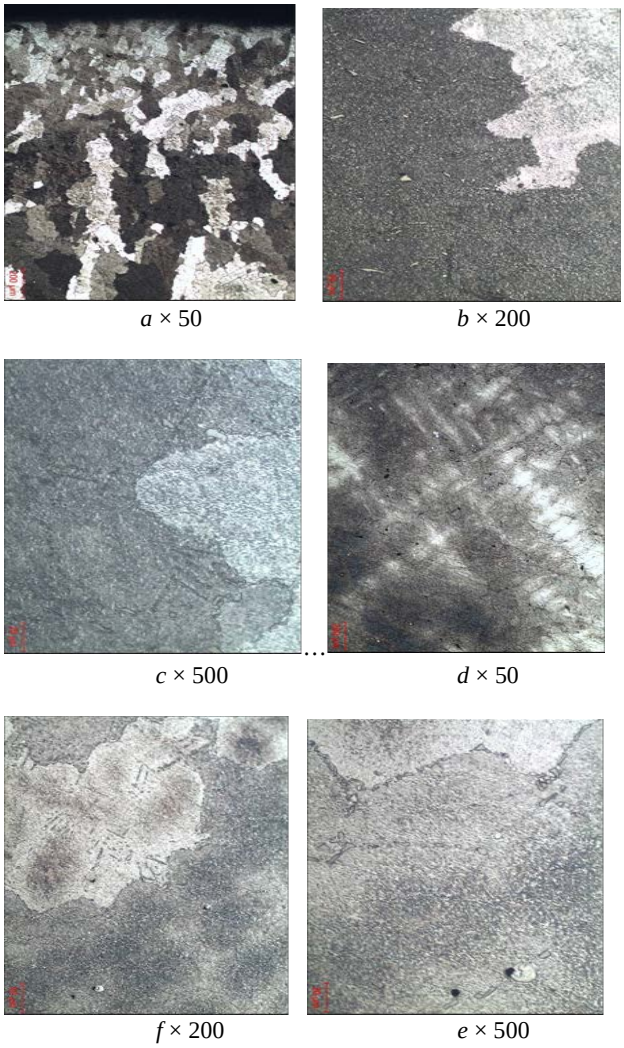

a × 50 *b* × 200

c × 500 *d* × 50

f × 200 *e* × 500

Figure 3. Microstructure in the edge (*a*, *b*, *c*) and central (*d*, *f*, *e*) zones of sample 1

The microstructure after heat treatment is characterized by greater homogeneity due to the equalization of the particle sizes of the intermetallic γ′- phase between the axes and interaxial space of the dendrites and almost complete dissolution of the eutectic (γ-γ′) -phase in the γ-solid solution (Fig. 3). It can be considered that the microstructure of all samples is satisfactory for a normally heat-treated condition of this alloy.

TCP phases were not detected in the studied alloy samples (either before or after heat treatment according to the standard mode). To determine the mechanical and heat-resistant properties, samples (diameter 15 mm, length 135 mm) were cast from rod blanks with a diameter of 90 mm using the high-speed directional crystallization method.

Mechanical and heat-resistant properties were determined according to 18T-TU-165 on unheat-treated samples, as well as after heat treatment using the standard mode (homogenization at 1265 ± 100 °C for 1 hour 15 minutes, in a vacuum). The results of mechanical tests, including long-term strength tests, are presented in Table 3.

Mechanical tests showed that all studied variants provide mechanical properties that meet the requirements of regulatory and technical documentation. The most pronounced indicators of material ductility are those obtained, as the obtained values exceed the requirements by 1.5 to 3 times (see Table 3).

DOI 10.15588/1607-6885-2025-4-2

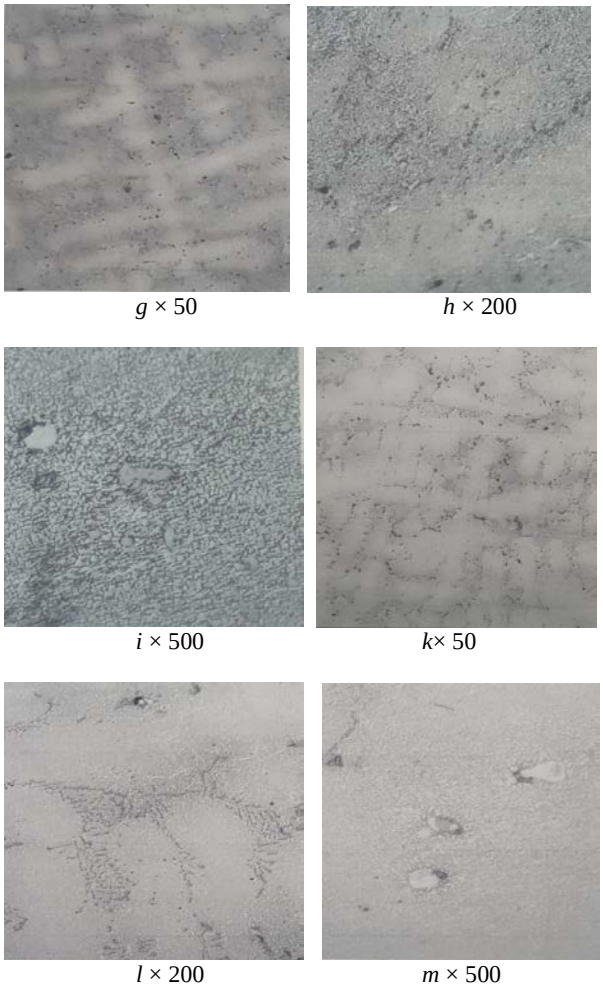

g × 50 *h* × 200

i × 500 *k*× 50

l × 200 *m* × 500

Figure 3. Continuation, as well as in the edge (*g*, *h*, *i*) and central (*k*, *l*, *m*) zones of the sample 2 after heat treatment

The time to high-temperature failure of the studied samples also complies with regulatory requirements and exceeds them by 1.5 to 2.5 times (see Table 3). The favorable morphology of grain-boundary carbides and the uniform distribution of the carbonitride component throughout the alloys, along with traditional strengthening by the intermetallic γ′- phase, characteristic of alloys of this class, were the reasons for the high time to failure.

The sizes of the structural components in the original 90mm diameter blank of the ZhS26-VI alloy, as well as in the samples (15mm in diameter and 135mm in length) before and after heat treatment, are presented in Table 4.

In the alloy structure, carbides and carbonitrides are present as small, dispersed particles of spherical and plate-like shapes, generally uniformly distributed throughout the material. Standard calculations of the quantitative and dimensional properties of the intermetallic γ′- phase did not reveal any significant differences between the alloys studied.

Table 3 – Mechanical and high-temperature properties of studied metals

Melt number	State of the material	Mechanical properties at 20°C		Hour before the failure (at Tisp = 9 75°C and Ϭ = 260 MPa), τ_f, hour
		$Ϭ_в$, МПа	δ, %	
1	without heat treatment	914	10,0	94^{15}
	after heat treatment	875	9,4	100^{30}
2	without heat treatment	1094	8,6	72^{30}
	after heat treatment	913	9,8	82^{30}
3	without heat treatment	928	9,2	40^{00}
4	without heat treatment	874	14,8	40^{00}
5	without heat treatment	727	24,8	91^{00}
6	without heat treatment	1108	13,2	67^{30}
7	without heat treatment	1085	10,8	53^{30}
8	without heat treatment	897	17,0	79^{30}
9	without heat treatment	866	17,2	68^{30}
Norms of TC		≥ 850	≥ 6,0	$\geq 40^{00}$

Conclusions

A series of experimental melts of ZhS26-VI alloy samples revealed significant macrograin refinement due to intensive heat removal and high crystallization rates. The macrostructure of all studied samples is satisfactory and meets technical specifications. The microstructure of the samples before heat treatment corresponds to the as-cast state of the alloy, and after heat treatment under standard conditions, it also meets technical specifications and conforms to the approved microstructure scale

It can be concluded that the normally heat-treated structure of the studied samples was achieved due to the conformity of the alloy's chemical composition. Heat treatment and hot isostatic pressing completely eliminated internal microporosity. The structure of all studied alloys exhibited the precipitation of carbides and carbonitrides in the form of small particles of spherical and lamellar morphology, generally distributed uniformly throughout the material.

DOI 10.15588/1607-6885-2025-4-2

The mechanical and high-temperature properties of the samples meet the requirements of regulatory documentation for critical heat-resistant castings. To confirm the sufficiency of the demonstrated level of mechanical properties, it is recommended to conduct technical tests (motor, full-scale) of parts as part of a gas turbine engine according to the accepted methodology of aviation regulations.

Table 4 – Dimensions of structural components for work pieces with a diameter of 90 mm and in samples (diameter 15 mm, depth 135 mm) of studied alloys

Melt number	Naymenuvan nya	State of the material	Place of measurement	Size of structural components, microns			Distance between axes of 2nd order dendrites, μm
				carbides		Eutectic type (γ-γ')	
				Globular type MeC	Plate type Me_6C		
11	Workpiece, diameter 90mm	without h/t	edge	1,5…6	6…27	4…18	25…35
			center	2…8	6…30	9…65	65…90
		after h/t	edge	1,5…6	6…25	-	25…35
			center	2…8	6…30	До 16	65…90
	sample, diameter 15 mm	without h/t	center	3…12	5…25	7…60	50…90
		after h/t	center	3…9	5…28	-	50…90
22	Workpiece, diameter 90 mm	without h/t	edge	3…11	4…34	11…52	20…40
			center	2…13	6…32	15…50	45…90
		after h/t	center	4…9	3…30	-	20…40
			center	2…9	6…30	5…22	45…90
	Sample, diameter 15 mm	without h/t	center	3…9	7…44	8…43	60…90
			center	3…18	7…40	-	60…90

References

1. Okada, I., Torigoe, T., Takahashi, K., & Izutsu, D. (2004). Development of Ni base superalloy for industrial gas turbine. Proceedings of the International Symposium on Superalloys, 707–712.

2. Perrut, M., Caron, P., Thomas, M., & Couret, A. (2018). High temperature materials for aerospace applications: Ni-based superalloys and γ-TiAl alloys. Comptes Rendus Physique, 19(8), 657–671. https://doi.org/10.1016/j.crhy.2018.10.003

3. Sims, C. T., Stoloff, N. S., & Hagel, W. C. (1987). Superalloys II: High-temperature materials for aerospace and industrial power (2nd ed.). John Wiley & Sons, 615.

4. Epishin, A., Link, T., Nazmy, M., et al. (2008). Microstructural degradation of CMSX-4: Kinetics and effect on mechanical properties. Proceedings of the International Symposium on Superalloys, 725–731.

5. Reed, R. C. (2006). The superalloys: Fundamentals and applications. Cambridge University Press, 372.

6. Paton, B. E. (1987). Zharoprochnost' liteynykh nikelevykh splavov i zashchita ikh ot okisleniya [Heat resistance of cast nickel alloys and their protection against oxidation]. Naukova Dumka, 256.

7. Koval, A. D., Belikov, S. B., Sanchugov, E. L., & Andrienko, A. G. (1990). Nauchnyye osnovy legirovaniya zharoprochnykh nikelevykh splavov, stoykikh protiv vysokotemperaturnoy korrozii (VTK) [Scientific foundations of alloying heat-resistant nickel alloys resistant to high-temperature corrosion]. UKMK VO, 56.

8. Bielikov, S. B. (1996). Rozvytok naukovykh pryntsypiv lehuvannia lyvarnykh zharomitsnykh nikelevykh splaviv z metoiu pidvyshchennia korozijnoi stijkosti detalei v umovakh vysokotemperaturnoho seredovyshcha hazoturbinnykh ustanovok [Development of scientific principles of alloying cast heat-resistant nickel alloys to improve the corrosion resistance of parts in the high-temperature environment of gas turbine installations] [Doctoral dissertation, Zaporizhzhia National Technical University], 439.

9. Koval, A. D., Belikov, S. B., & Sanchugov, E. L. (2001). Principles of alloying of high-temperature nickel alloys resistant to high-temperature corrosion. Metal Science and Heat Treatment, 43(9–10), 373–377. https://doi.org/10.1023/A:1013245225944, 9, 373–377.

10. Boguslaev, V. A., Muravchenko, F. M., Zhemanyuk, P. D., et al. (2007). Tekhnolohichne zabezpechennia ekspluatatsiinykh kharakterystyk detalei

DOI 10.15588/1607-6885-2025-4-2

HTD. Lopatky turbyny. Chastyna 2 [Technological assurance of operational characteristics of GTE parts. Turbine blades. Part 2]. Zaporizhzhia, 493.

11. Solntsev, Yu. P., Bielikov, S. B., Volchok, I. P., & Sheiko, S. P. (2010). Spetsialni konstruktsiini materialy [Special structural materials]. Valpis-Polihraf, 536.

12. Gaiduk, S. V., & Belikov, S. B. (2017). Nauchnyye osnovy proyektirovaniya liteynykh zharoprochnykh nikelevykh splavov s neobkhodimym kompleksom sluzhebnykh svoystv [Scientific basis for the design of cast heat-resistant nickel alloys with the necessary set of service properties]. Zaporizhzhia National Technical University, 79.

13. Gaiduk, S. V. (2018). Razvitiye i primeneniye nauchnykh printsipov legirovaniya dlya razrabotki zharoprochnykh nikelevykh splavov s garantirovannymi svoystvami [Development and application of scientific principles of alloying for the development of heat-resistant nickel alloys with guaranteed properties] [Doctoral dissertation, Zaporizhzhia National Technical University], 404.

14. Zhemanyuk, P. D., Klochikhin, V. V., Lysenko, N. A., & Naumik, V. V. (2015). Structure and properties of cast blades of aircraft engines made of heat-resistant nickel alloy ZhS26-VI after hot isostatic pressing. Bulletin of Engine Building, (1), 139–146.

15. Zhemanyuk, P. D., Pedash, A. A., Tsivirko, E. I., & Pedash, A. F. (2013). Combination of modification in the production of gas turbine engine parts. Bulletin of Engine Building, (1), 75–78.

16. Danilov, S., Pedash, O., Naumik, V., Tyomkin, D., & Naumik, O. (2024). Complex modification of a heat-resistant nickel alloy with dispersed parts of refractory joints. New Materials: Technologies in Metallurgy and Mechanical Eng, 4, 6–14.

17. Pedash, A. A., Bialik, G. A., & Tsivirko, E. I. (2015). Increasing the thermal conductivity of local ceramic molds with cobalt aluminate. Aviation and Space Technology and Technology, (10), 40–44.

Received 14.10.2025
Accepted 03.11.2025

СТРУКТУРА ТА ВЛАСТИВОСТІ ЖАРОМІЦНОГО СПЛАВУ ЖС-26ВІ ДЛЯ ВИРОБНИЦТВА ВІДПОВІДАЛЬНИХ ДЕТАЛЕЙ ГАЗОТУРБІННИХ ДВИГУНІВ

Сергій Пучек — аспірант кафедри транспортних технологій Національного університету «Запорізька політехніка», м. Запоріжжя, Україна, *e-mail: puchek777@gmail.com*, ORCID: 0009-0007-8077-6106

Сергій Бєліков — д-р техн. наук, професор, професор кафедри транспортних технологій Національного університету «Запорізька політехніка», м. Запоріжжя, Україна, *e-mail: belikov@zp.edu.ua*, ORCID: 0000-0002-9510-8190

***Мета роботи**. Вивчити макро- та мікроструктурний стан серії дослідницьких зразків жароміцного сплаву ЖС26-ВІ для виробництва критичних компонентів газотурбінного двигуна, а саме роторних лопаток турбіни високого тиску (ТВТ), та оцінити механічні властивості та жароміцність у відповідності до технічних специфікацій матеріалів гарячої частини газової турбіни.*

***Методи дослідження**. Макро- і мікроструктурний аналіз та дослідження фазового складу проводили методом оптичної металографії на оптичному мікроскопі. Механічні властивості при кімнатній температурі визначали у відповідності до ISO 6892-84 та СТ СЭВ 471-88. Випробування на розрив здійснювали на машині ZDMY30.*

***Отримані результати**. Проведено дослідження структури та властивостей зразків дослідних плавок сплава ЖС-26ВІ, отриманих у вакуумній печі FM-1-2-100 фірми «ULMAC» методом рівновісної кристалізації. Установлене суттєве подрібнення макрозерна за рахунок інтенсивного тепловідводу та високої швидкості кристалізації. Мікроструктура зразків до термічної обробки відповідає литому стану сплава, а після термообробки по стандартному режиму задовольняє технічні умови та відповідає затвердженій шкалі мікроструктури. Механічні та жароміцні властивості зразків відповідають вимогам нормативної документації до відповідального жароміцного лиття.*

***Наукова новизна**. Одержано нові дані щодо структури та фазового стану сплаву ЖС26-ВІ дослідних та серійних плавок. Вивчено тонку будову жароміцного сплаву на основі нікелю, що традиційно використовується для отримання лопаток турбіни високого тиску газотурбінного двигуна авіаційного призначення.*

***Практична цінність**. Отримані результати надають можливість розширити використання жароміцного сплаву ЖС26-ВІ для виробництва виливків відповідального призначення.*

***Ключові слова**: жароміцний сплав, макро- та мікроструктура, термічна обробка, механічні властивості, жароміцність, лопатка газової турбіни.*

DOI 10.15588/1607-6885-2025-4-2

Список літератури

1. Development of Ni Base Superalloy for Industrial Gas Turbine [Text] / I. Okada, T. Torigoe, K. Takahashi, D. Izutsu // Proceedings of the International Symposium on Superalloys. – 2004. – P. 707–712.

2. High temperature materials for aerospace applications: Ni-based superalloys and γ- TiAl alloys / M. Perrut, P. Caron, M. Thomas, A. Couret // Comptes Rendus Physique. – 2018. – No. 19. – P. 657–671.

3. Sims, Ch.T. Superalloys II: High-Temperature Materials for Aerospace and Industrial Power (2nd edition) [Text] / Ch.T. Sims, Norman S. Stoloff, William C. Hagel. - New York: John Wiley & Sons, 1987. – 615 p.

4. Microstructural Degradation of CMSX-4: Kinetics and Effect on Mechanical Properties / A. Epishin, T. Link, M. Nazmy et al. // Proceedings of the International Symposium on Superalloys. – 2008. - P. 725–731.

5. Reed R. C. The Superalloys: Fundamentals and Applications / R. C. Reed. – Cambridge, University Press. - 2006. – 372 p.

6. Патон Б. Е. Жаропрочность литейных никелевых сплавов ы защита их от окисления. - К., Наукова думка. – 1987. – 256 с.

7. Научные основы легирования жаропрочных никелевых сплавов, стойких против высокотемпературной коррозии (ВТК): Научное издание – препринт / А. Д. Коваль, С. Б. Беликов, Е. Л. Санчугов, А. Г. Андриенко, ЗМИ. – К. : УМК ВО, 1990. – 56 с.

8. Бєліков С. Б. Розвиток наукових принципів легування ливарних жароміцних нікельових сплавів з метою підвищення корозійної стійкості деталей в умовах високотемпературного середовища газотурбінних установок : дис. докт. техн. наук: 05.02.01 / С. Б. Бєліков. – Запоріжжя :ЗНТУ, 1996. – 439 с.

9. Koval A.D. Principles of Alloying of High-Temperature Nickel Alloys Resistant to High-Temperature Corrosion / A. D. Koval, S. B. Belikov, E. L. Sanchugov // Metal science and heat treatment. – 2001. – No. 9–10. – P. 373–377.

10. Технологическое обеспечение эксплуатационных характеристик деталей ГТД. Лопатки турбины. Часть 2: монография [Текст] / Богуслаев В. А., Муравченко Ф. М., Жеманюк П. Д. и др. – Запорожье, 2007. – 493 с.

11. Спеціальні конструкційні матеріали : підручник / Ю. П. Солнцев, С. Б. Бєліков, І. П. Волчок, С. П. Шейко; ред.: І. П. Волчок. – Запоріжжя : Валпіс-Поліграф, 2010. – 536 с.

12. Гайдук, С. В. Научные основы проектирования литейных жаропрочных никелевых сплавов с необходимым комплексом служебных свойств / С. В. Гайдук, Беликов С. Б. – Запорожье, ЗНТУ. – 2017. – 79 с.

13. Гайдук, С. В. Развитие и применение научных принципов легирования для разработки жаропрочных никелевых сплавов с гарантированными свойствами [Текст]: дис. д-ра техн. наук: 05.02.01 / Гайдук С.В. Запорож. нац. техн. ун-т.- Запорожье, 2018. – 404 с.

14. Structure and properties of cast blades of aircraft engines made of heat-resistant nickel alloy ZhS26-VI after hot isostatic pressing / P. D. Zhemanyuk, V. V. Klochikhin, N. A. Lysenko, V. V. Naumik // Bulletin of Engine Building. – 2015. – No. 1. – P. 139–146.

15. Combination of modification in the production of gas turbine engine parts [Text] / P. D. Zhemanyuk, A. A. Pedash, E. I. Tsivirko, A. F. Pedash // Bulletin of Engine Building. – 2013. – No. 1. – P. 75–78.

16. Complex modification of a heat-resistant nickel alloy with dispersed parts of refractory joints [Text] / S. Danilov, O. Pedash, V. Naumik, D. et al. // New materials: technologies in metallurgy and mechanical engineering. – 2024. – No. 4. – P. 6–14.

17. Pedash A. A. Increasing the thermal conductivity of local ceramic molds with cobalt aluminate [Text] / A. A. Pedash, G. A. Bialik, E. I. Tsivirko //Aviation and space technology and technology. – 2015. – No. 10. – P. 40–44.

DOI 10.15588/1607-6885-2025-4-2

ТЕХНОЛОГІЇ ОТРИМАННЯ ТА ОБРОБКИ КОНСТРУКЦІЙНИХ МАТЕРІАЛІВ

TECHNOLOGIES OF OBTAINING AND PROCESSING OF CONSTRUCTION MATERIALS

UDC 621.438:620.193/.199:621.793.7

Yevhen Vyshnepolskiy — Candidate of Technical Sciences, Associate Professor of the Department of Mechanical Engineering Technology, National University Zaporizhzhia Polytechnic, Zaporizhzhia, Ukraine, *e-mail: evishnepolskiy@gmail.com*, ORCID: 0000-0002-8048-7976

Andrii Bondariev — Postgraduate student of the Department of of Mechanical Engineering Technology, National University Zaporizhzhia Polytechnic, Zaporizhzhia, Ukraine, *e-mail: bondarev@gmail.com*, ORCID: 0009-0004-9429-4050

ENHANCING WEAR RESISTANCE OF COMPLEX-SHAPED DUAL-USE MECHANICAL COMPONENTS

Purpose. *To provide a scientific foundation for a technological approach to significantly increase the wear resistance of gas turbine engine (GTE) nozzle guide vanes (NGVs) by applying advanced protective coating deposition methods.*

Research methods. *The research methods included the selection of typical materials for investigation (ZhS6U and Inconel 718 alloys), a review of multifunctional coating systems and their classifications (Thermal Barrier Coatings (TBCs), wear resistant metallo ceramic coatings (Wear-Resistant Cermet Systems), an analysis of spraying methods (Detonation Spraying (D-Gun), High-Velocity Oxygen Fuel (HVOF), and Atmospheric Plasma Spraying (APS)), and a review of scientific studies that confirm the effectiveness of these methods.*

Results. *The analysis of existing research and literature has shown that the detonation spraying technology is uniquely and most suitably applicable for solving the stated problem, as it is capable of forming a Cr_3C_2-NiCr system coating with the required combination of properties: high density, excellent adhesion, and, most important, a favorable field of residual compressive stresses.*

Scientific novelty. *The systematic approach to solving the complex problem of protecting NGV blades (dual-use parts and mechanisms) by applying the detonation spraying technology, which is known for its ability to form exceptionally dense and wear-resistant coatings.*

Practical value. *Potential possibility to increase significantly the time between overhauls, reliability, and combat readiness of critically important GTE components.*

Key words: *GTE, NGV blade, superalloy, Solid Particle Erosion (SPE), high-temperature gas corrosion, oxidation, TBC, D-Gun, HVOF, APS.*

Introduction

Gas turbine engines are the basis of modern aviation, energy and maritime transport, playing a key role in both the civil and military sectors. The efficiency, power and reliability of these dual-purpose mechanisms directly depend on the durability of the components that are operating in the hot section (exhaust tract) of the engine [1]. Among such components, a special place hold parts with complex geometric shape, in particular the blades of the nozzle apparatus (NGV, Fig. 1), which are one of the most loaded structural elements. The high cost of their manufacture from heat-resistant superalloys and difficulty of replacement makes the task of extending their operational life extremely relevant from an economic and strategic point [2].

The main problem limiting the service life of NGVs is the complex multimodal degradation of their surfaces, which are simultaneously exposed to extreme thermal, mechanical and chemical loads [3]. Monolithic heat-resistant superalloys, despite their unique properties, are not able to independently withstand such an aggressive environment for a long time without the use of special protective measures [4].

Traditionally, thermal barrier coatings (TBC) [5] are used to protect hot section elements, which are applied mainly by the atmospheric plasma spraying (APS) method [6]. Although they effectively reduce the thermal load on

DOI 10.15588/1607-6885-2025-4-3

the base material, their porous structure, necessary for low thermal conductivity, makes them vulnerable to intense erosion by solid particles (Solid Particle Erosion, SPE) [7]. This leads to rapid destruction of the protective layer and premature failure of the part, which indicates the need to develop more reliable and comprehensive solutions.

Despite many years of research and significant progress in the development of surface hardening materials and technologies, the complex problem of increasing the wear resistance of complex-profile parts remains only partially solved. The complex geometry of parts limits the application of many traditional and even some advanced surface treatment technologies, creating “shadow zones” [8] or uneven coating [9].

Figure 1. Typical view of a one-part solid-metal NGV of GTE (3D Model)

Analysis of Research and Publications

NGV, as a subject of research, should be considered not only as a solid-metal complex-profile part, but also as an assembly unit (AU) [1, 2]. It is due to its diversity (but not only) the purpose of the GTE is formed, which directly affects the application: flight environment, selection of operating modes, accuracy and quality obtained during manufacturing.

NGVs are located directly behind the combustion chamber and is the first fixed element of the turbine that comes into contact with the combustion products. Its main purpose is to convert the thermal energy of the hot gas flow into kinetic energy and to form and direct the flow at an optimal angle to the working blades of the first stage of the turbine. The temperature of the gas flow can exceed 1300…1600°C, which is significantly higher than the melting point of structural materials. To prevent degradation of the main structural elements, namely the path surfaces of the blades, an internal complex air cooling system is designed, which directly affects the path or passes through the entire unit (if made as a AU), but even with that, the temperature and pressure still remain quite high, and the gas flow speed reaches supersonic values (depending on the application: M > 1…1.2). In this case, the application of protective coatings is not just a measure to extend the resource, but a necessary condition for engine operation over the entire range of modes. It allows to increase the turbine inlet temperature, which is a key factor for increasing the thermal and fuel efficiency of the GTE [2].

Degradation of the surface of the NGV blades is a complex process, which is caused not by the sequential, but by the simultaneous action of several destructive mechanisms. An effective protective coating must comprehensively resist each of them, precisely:

1) Erosion by solid particles (Solid Particle Erosion, SPE). SPE is the mechanical removal of material from a surface as a result of bombardment by solid particles contained in a gas stream. The sources of these particles can be sand, dust, volcanic ash that sucked into the engine from the environment, as well as soot formed in the combustion chamber. The intensity of erosive wear depends on the kinetic energy of the particles (their mass and velocity), the angle of contact with the surface (angle of attack), and temperature [10].

The mechanisms of erosive failure may differ for ductile and brittle materials. For metal substrates, a ductile mechanism is typical, which includes the processes of plowing and cutting. For ceramic coatings, such as TBC, a brittle mechanism is more typical, which consists in the formation and joining of microcracks with subsequent chipping off of material fragments. Erosion not only thins the part, changing its aerodynamic profile, but can also completely remove the protective coating, exposing lesser resistant layers and the substrate for further degradation [10].

2) High-temperature gas corrosion and oxidation. Chemical degradation is an equally significant factor in destruction. The gas stream is a chemically aggressive medium containing oxygen, water vapor and impurities such as sulfur, sodium and vanadium compounds (especially when operating on the seas or using low-quality fuel). At high temperatures, these components actively interact with the surface of the material, causing intense oxidation and hot corrosion [3, 11].

In systems with TBCs, the critical element is the interface between the ceramic top and the metal bonding layers. During operation, a layer of Thermally Grown Oxide (TGO), mainly Al_2O_3, is formed and grows on the surfaces. The accumulation of stresses in this layer is one of the main mechanisms leading to TBC delamination [3]. For cermet coatings similar to the Cr_3C_2-NiCr system, the degradation mechanism may be the oxidation of chromium and the carbide phase at temperatures exceeding their operating conditions [12].

3) Thermomechanical fatigue and creep. The operation of a gas turbine engine is characterized by cyclicity: start-ups, ramp-ups, power reductions, shutdowns etc. Each of the cycles is accompanied by rapid temperature changes, which causes cyclic thermal stresses in the materials. These stresses arise, in particular, due to the difference in the coefficients of thermal expansion (CTE) between the metal substrate and the ceramic or cermet coating. Repeating of such cycles leads to the accumulation of fatigue damage, the initiation and propagation of cracks. This process is called thermomechanical fatigue [3, 13].

At the same time, at high temperatures, under the constant mechanical loads (from the pressure of the gas flow), the material undergoes creep – slow plastic deformation.

2025 DOI 10.15588/1607-6885-2025-4-3

The combination of thermomechanical fatigue and creep is one of the most dangerous mechanisms of gradual degradation, which can lead to the destruction of the part.

It is important to understand that these mechanisms do not act in isolation, but synergistically, creating a cascade of interconnected destruction. For example, erosive damage to the surface does not simply remove material, but creates microscopic defects and areas of increased roughness. These defects act as concentrators and, as a result, sharply accelerate the initiation of fatigue cracks. At the same time, by removing the protective oxide layer or the top layer of the coating, erosion opens access to aggressive gases to the «fresh» surfaces, repeatedly intensifying the corrosion and oxidation processes. Thus, the initial mechanical damage from SPE acts as a catalyst for further chemical and mechanical destruction. This proves that an effective coating must be not only dense (to resist erosion), but also viscous, dense and firmly bonded to the base to prevent the formation of primary damage that triggers this destructive cascade. Such a model of synergistic degradation also indicates the insufficiency of single-factor laboratory tests (for example, only for erosion or only for oxidation) to adequately predict the behavior of the material in real operating conditions.

Purpose of the Work

The main goal of this work is to scientifically substantiate the technological approach of significantly increasing the wear resistance of the NGVs of the GTE by applying advanced methods of applying protective coatings. To achieve this goal, the following tasks were set:

1. To analyze the complex wear mechanisms acting on the surface of the NGVs blades under operating conditions.

2. To review and select the optimal materials of the substrate and protective coating.

3. To perform a comparative analysis of modern coating technologies, considering the choice of detonation spraying method as the most promising one.

4. To develop a comprehensive methodology for experimental research and evaluation of the properties of the proposed coatings, based on international standards.

Materials and Research Methods

The basis for the manufacture of NGVs blades are cast or deformed nickel superalloys. These are complex multicomponent systems based on nickel with a face-centered cubic (FCC) crystal lattice, capable of maintaining strength, creep resistance and corrosion resistance at temperatures approaching 80...85 % of its own melting point. Their unique properties are achieved through complex alloying. Elements such as chromium (Cr) and aluminium (Al) form protective oxide films (Cr_2O_3 and Al_2O_3) on the surface, which provide resistance to oxidation. Molybdenum (Mo), tungsten (W), tantalum (Ta) and rhenium (Re) strengthen the solid solution (matrix). However, the key role is played by aluminum (Al), titanium (Ti) and niobium (Nb), which are dispersed particles of the intermetallic γ′-phase (for example, $Ni_3(Al, Ti)$), which is the main strengthening element that effectively blocks the movement of dislocations at high temperatures [2, 3].

As typical representatives of materials for NGV, one of the following can be noted:

а) ЖС6У (ZhS6U) is a cast heat-resistant nickel-based alloy widely used in post-soviet GTE manufacturing. It demonstrates high long-term strength: it is able to withstand a stress of 230 MPa at a temperature of 975 °C for at least 40 hours. The short-term strength limit at room temperature was 830 MPa [14].

б) Inconel 718 is one of the most common deformed superalloys on an iron-nickel basis in the world. Its feature is the strengthening by γ″-phase (Ni_3Nb), which provides high strength at temperatures up to 700 °C, as well as good weldability and processability. This alloy is often used as a model substrate material in the study of coatings [2, 3]. In the following consideration and as the main material, this material will be chosen.

To ensure reliable operation of superalloys in the conditions of the hot gas turbine tract, multifunctional coating systems are used, which can be classified according to their main purpose, namely:

1) thermal protective coatings (Thermal Barrier Coatings, TBC). The main task of TBC is to create a thermal barrier between the hot gas flow and the cooled metal part. Such a coating is able to reduce the temperature on the metal surface by 100…170 °C, which allows either to increase the gas temperature in the turbine (increasing efficiency), or to increase the service life of the part at the same temperature. Classical TBC has a multilayer structure [3, 5]:

- top ceramic layer (Top Coat). Usually made of zirconium dioxide stabilized with 7…8 % yttrium oxide (YSZ). The material provides low thermal conductivity, high melting point and thermal expansion coefficient close to the CTE of the metal base. To reduce thermal conductivity, controlled porosity is created in the structure of this layer (up to 15…20 %);

- metal bonding layer (Bond Coat). Applied between the substrate and the ceramic layer. Performs two functions: provides strong adhesion of ceramics to the metal and protects the substrate from high-temperature oxidation. Usually these are alloys of the MCrAlY type (where M is Ni, Co or their combination).

Despite the high efficiency of thermal protection, its porosity, that is key to thermal insulation properties, which becomes the main weakness of TBC under conditions of intense erosion. Erodent particles easily destroy the fragile ceramic structure, penetrating into the pores and causing destruction by the «tunnelling» mechanism. This creates a fundamental conflict of properties: a coating optimized for thermal insulation is vulnerable to mechanical wear.

2) Wear-Resistant Cermet Systems. To counteract mainly erosive and corrosive wear, cermet coatings are

used that combine a hard ceramic phase and a plastic metal matrix bond. The most widespread are:

- Cr_3C_2-NiCr system identified as one of the best candidates for protection against wear at high temperatures (up to 850…900 °C). The hard chromium carbide (Cr_3C_2) particles provide high hardness and resistance to abrasive wear, while the nickel-chromium alloy (NiCr) matrix provides the coating with the necessary ductility, fracture toughness, and excellent resistance to oxidation and hot corrosion due to the formation of a stable Cr_2O_3 oxide film. However, during prolonged operation at very high temperatures, phase transformations may occur in the structure of this coating, in particular, the release of secondary carbides, which leads to the creation of brittleness and a decrease in crack resistance [6, 7];

- WC-Co system is considered as a reference for protection against abrasive and erosive wear at low and moderate temperatures (not exceeding 500 °C). Extremely hard tungsten carbide (WC) particles provide exceptional wear resistance, and the cobalt (Co) binder provides high viscosity. By changing the cobalt content, the balance between hardness and viscosity of the coating can be adjusted. The main disadvantage of this system is its low resistance to oxidation at high temperatures, which makes it unsuitable for use in the hot tract of a gas turbine engine, but useful for comparative studies [6, 7].

The above analysis reveals the key dilemma of «insulation versus integrity». Dense, wear-resistant metal-ceramic coatings have significantly higher thermal conductivity than porous TBCs, which leads to a higher thermal load on the substrate. Conversely, TBCs optimized for thermal insulation quickly fail due to erosion. This contradiction indicates that the monolithic single-layer coating structure is inherently a compromise. The optimal solution probably lies in the creation of multilayer or functionally graded materials (FGM) [15]. Such an architecture could combine, for example, an inner, more porous layer for thermal insulation and an outer, dense, hard and erosion-resistant layer deposited using a high-energy process. This shifts the focus of the research from the question of «Which material?» to the question of «What is material architecture?».

Consideration of types of protective coatings should be carried out in tandem with modern methods and surface technologies that allow to control the stability of the process of application to the material. The most advanced method today can be considered the detonation spraying method. Detonation Spraying (D-Gun) is a thermal spraying method invented in 1955 by a group of researchers consisting of H.B. Sargent, R.M. Poorman and H. Lamprey [2, 16]. This process is fundamentally different from other spraying methods due to the use of energy from a controlled explosion.

The working tool is a detonation gun – a long water-cooled barrel, closed on one side. A precisely dosed portion of an explosive gas mixture (usually acetylene + oxygen) and powder coating material are fed into the gun chamber. The mixture is ignited by a spark, which initiates detonation – a combustion process that propagates at supersonic speed and is accompanied by the formation of a shock wave. This detonation wave heats the powder particles to a plastic or molten state and accelerates them to extremely high speeds, reaching 1200 m/s. With high kinetic energy, the particles hit the surface of the part, undergo significant plastic deformation, and form a dense layer of coating. The process is cyclical: the frequency of «shots» is in range from 1 to 10 Hz. After each shot, the barrel is purged with inert gas (nitrogen) to remove combustion products and prepare for the next cycle. This method has the following advantages [2]:

1. High density and low porosity. Due to the enormous kinetic energy of the particles during collision, occurs effective compaction. As a result, coatings with extremely low porosity are formed, which often does not exceed 1…2 % and is critically important for preventing the penetration of corrosive agents deep into the coating and for achieving maximum wear resistance;

2. Extremely high bond strength (adhesion). High-velocity impact not only provides strong mechanical engagement of particles with irregularities of the prepared surface, but can also initiate local metallurgical processes (like «microwelding») at the surface. This results in the formation of coatings with bond strengths that significantly exceed those of other thermal spraying methods (often over 70 MPa);

3. Creation of residual compressive stresses. Bombarding the surface with high-velocity particles creates an effect similar to shot-peening. Favorable residual compressive stresses are formed in the surface layer of the coating. This is a unique and extremely important advantage, since the compressive stresses counteract the tensile stresses arising from thermal mismatch and external loads, effectively inhibiting the initiation and propagation of cracks and, thus, increasing fatigue life;

4. Minimal thermal load on the substrate. Despite the high temperature in the detonation wave, the interaction time of hot gases and particles with the substrate is very short due to the pulsed nature of the process. The total heat flux transferred to the part is significantly less than with plasma spraying. This minimizes the risk of part distortion, undesirable structural changes in the substrate material and the size of the heat affected zone (HAZ).

To justify the choice of detonation spraying technology, it is necessary to compare it with the main alternative high-energy methods: high-velocity oxygen-fuel (HVOF) and atmospheric plasma (Atmospheric Plasma Spraying, APS) spraying (Table 1):

DOI 10.15588/1607-6885-2025-4-3

Table 1 – Comparative characteristics of high-energy thermal spraying methods

Parameter	Spraying methods		
	D-Gun	HVOF	APS
Heat Source	Detonation of the O_2-fuel mixture	Continuous combustion O_2-fuel	Direct current electric arc (plasma)
Velocity of the Gas (particles)	Very high (~ 1200 m/s)	High (~ 600…1000 m/s)	Middle (~ 200…500 m/s)
Temperature of the Gas (Particles)	High (~ 3000…4000 °C)	High (~ 2800…3300 °C)	Very high (up to 16000 °C)
Porosity of the coating	Very low (< 1…2%)	Low (1…3 %)	Moderate high (5…15 % and higher)
Grip Strength	Very high (> 70 MPa)	High (> 60 МПа)	Moderate (20…40 MPa)
Residual Stresses	Compressive	From weakly compressive to tensile	Mostly tensile
Main Application	Extreme wear and erosion resistance	Wear and corrosion resistance	Thermal barrier coatings (TBC)

1) High-velocity oxy-fuel spraying (HVOF). This process also uses the combustion of a fuel-oxygen mixture to heat and accelerate particles, but unlike detonation, continuous combustion occurs in a high-pressure chamber, the products of which are accelerated to supersonic speeds in a specially designed nozzle. HVOF allows for very high-quality, dense coatings with high adhesion and is considered a direct competitor to D-Gun. However, as a rule, particle velocities in the D-Gun process are even higher, which provides an advantage in density, adhesion and compressive stress levels. Analysis of the case of the failure of a Cr_3C_2–NiCr HVOF coating due to thermal embrittlement shows that even a small improvement in coating quality (density, residual stresses) that detonation spraying can provide will be crucial for extending the service life [6, 17, 18].

2) Atmospheric Plasma Spraying (APS). With this method, a plasma jet generated by an electric arc in a plasma-forming gas flow (argon, nitrogen, hydrogen) is used to heat the material. The temperature in the plasma can reach about 16000 °C, which allows melting all, even the most refractory materials. However, the particle velocity in APS is significantly lower than in D-Gun and HVOF. This leads to the formation of coatings with higher porosity and lower adhesive strength. Such properties make APS coatings less suitable for applications requiring maximum wear resistance, but ideal for applying TBC, where porosity is functionally necessary [6, 9, 19].

The choice of coating technology is determined not only by the desire to obtain «good» properties, but also by the necessity to create a specific stress-strain state in the «coating-substrate» system. The residual compressive stresses, which are an inherent property of detonation coatings, give them a unique mechanistic advantage. They directly counteract the main driving forces of coating failure – tensile stresses from thermal mismatch and fatigue loads. While the HVOF process can also produce high-quality coatings, the level of compressive stresses in them is usually lower, or they may even be tensile, making them more vulnerable to thermomechanical fatigue, as demonstrated in the analyzed failure case. This emphasizes that when evaluating and comparing coatings, measuring residual stresses is as important as determining hardness or adhesion.

Discussions

To validate the proposed technological solution and quantitatively assess the effectiveness of protective coatings, it is necessary to develop and implement a comprehensive program of experimental research and methods for assessing the properties of coatings, based on the recognized international standards ISO 2063 [20, 21] and ASTM C633 [22], as well as described in the literature [3, 4]. Let's consider in stages:

1) Stage I – formation of experimental samples: selection of the «substrate-coating» system. It includes:

- choice of substrate material. As a substrate material for experimental samples, it is advisable to choose the heat-resistant superalloy Inconel 718 or the alloy ZhS6U, which are representative of real NGVs (or in particular NGVs blades). The samples are made in the form of plates with standard sizes (for example, 25×25×5 mm);
- surface preparation. The quality of adhesion of the coating to the base critically depends on the condition of the - - surface. Therefore, before spraying, a mandatory blast-abrasive treatment with an abrasive powder (for example, Al_2O_3 based electrocorundum) is performed to clean it from dirt and oxides and create a matte and smooth relief, which improves mechanical adhesion;
- selection of coating material. Based on the analysis, a metal-ceramic powder of the Cr_3C_2-25(Ni20Cr) system was selected as the main candidate, which has proven its effectiveness in high-temperature wear-resistant applications;
- application process. The coating is applied by detonation spraying to a specified thickness (e.g. 200…400 μm). Key process parameters (oxygen/acetylene ratio, shot frequency, spraying distance) should be documented to ensure reproducibility.

Stage II – analysis of microstructural and physical-mechanical characteristics. The structure and properties of the obtained coatings are studied using the following standardized methods:

DOI 10.15588/1607-6885-2025-4-3

2.1) checking microstructure, porosity and phase composition using:

- scanning electron microscopy (SEM) [24]. It is used for visual analysis of the microstructure of the coating on a cross-sections. SEM allows to estimate the thickness of the coating, its layered (or lamellar) structure, the quality of the coating-substrate interface, as well as to qualitatively assess the presence of pores and other defects;

- energy-dispersive X-ray spectroscopy (EDS/EDX) [25]. It is used as a complementary instrument to SEM to map the distribution of chemical elements across a sample cross-section. This method allows to confirm the composition of the coating, to detect the presence of oxide inclusions and to investigate possible diffusion of elements at the interface with the substrate;

X-ray diffraction (XRD) [26]. A key method for identifying crystalline phases in a coating (e.g. Cr_3C_2, Ni-based and Cr-based phases). XRD also allows for the detection of undesirable phase transformations after thermal treatment and is one of the main methods for quantitatively measuring residual stresses in a coating.

2.2) microhardness measurement. Microhardness measurement is one of the main methods for assessing the mechanical properties of a coating. Testing is performed on a cross-section of the sample using the Vickers method in accordance with ISO 6507 or ASTM E384 standards. A diamond indenter in the form of a tetrahedral pyramid is used, which is pressed into the surface under a given load (for example, 300 gf or 2.94 N). Measurements are carried out at different distances from the surface to the substrate, which allows you to build a hardness distribution profile over the thickness of the measured coating.

2.3) assessment of adhesive and cohesive strength. It is carried out in two ways:

- peel test (according to ASTM C633) – this is the main quantitative method for measuring the adhesion strength of a coating to a substrate. The essence of the method is to glue a special cylindrical pin to the surface of the coating, which is then torn off on a tearing machine, and the maximum load at which the fracture occurred is recorded. It is also important to analyze the fracture surface: if it occurred at the «coating-substrate» boundary, then the measured value is the adhesion strength; if the fracture occurred inside the coating layer – cohesive;

- by the grid incision method (according to ISO 2409). A simpler, qualitative method for rapid assessment of adhesion. A grid of mutually perpendicular lines is cut on the surface of the coating, onto which adhesive tape is glued and sharply torn off. Adhesion is assessed visually using a classification scale depending on the area of the peeled coating.

2) Stage III – assessment of operational properties. Let's divide this stage into two components:

3.1) erosion resistance test. This test is carried out on a specialized gas erosion machine according to the procedure specified in ASTM G76 [23]. This standard describes a well-established method for comparing the erosion resistance of different materials. It consists of:

- test parameters. To simulate real operating conditions, it is necessary to set key parameters: erodent material (e.g., Al_2O_3), particle size (e.g., 50 μm), flow rate, angle of attack (e.g., 30° to simulate tangential erosion and 90° to simulate direct impact), and test temperature (up to 850…950 °C);

- evaluation criterion. Erosion resistance is quantified by the loss of mass or volume of the sample relative to the total mass of abrasive that interacted with the surface.

3.2) analysis of degradation mechanisms under high temperature exposure. To assess the thermal stability of the coating, isothermal or cyclic oxidation resistance tests are proposed. The coated samples are kept in a furnace at a high temperature (e.g. 900 °C) for a long time. After the exposure, metallographic analysis (SEM/EDS, XRD) is performed to detect changes in the microstructure, phase composition (e.g. the precipitation of secondary carbides, which was observed for HVOF coatings) and to study the oxidation kinetics.

The proposed methodology poses a direct, scientifically speaking «challenge», to noted failure mechanisms. The experimental design is not arbitrary: it is specifically designed to demonstrate that the proposed solution (detonation coating of the Cr_3C_2-NiCr system) overcomes the known weaknesses of alternative technologies (HVOF Cr_3C_2-NiCr). By subjecting the detonation coating to the same thermal stress that caused the failure of the HVOF counterpart and by analyzing its phase stability and microstructure, this experiment directly tests the hypothesis that the superior microstructural quality and favorable stress state of the detonation coating prevents or slows down this specific failure mechanism. This translates the research from the general statement «detonation spraying is better» to the specific, scientific question «Does the detonation spraying process suppress the high-temperature embrittlement observed in HVOF coatings of the Cr_3C_2-NiCr system?». A positive result of such an experiment will not only confirm the choice for this application, but will also be a significant contribution to materials science regarding the comparative thermal stability of coatings obtained by various high-energy methods (Table 2).

The synthesis of the above data allows us to suggest that the detonation spraying technology is unique and most suitable for solving the problem, since it is able to form a coating of the Cr_3C_2-NiCr system with the necessary combination of properties: high density, excellent adhesion and, most importantly, a favorable field of residual compressive stresses [27]. This combination allows us to effectively resist the synergistic destructive effects of erosion, corrosion and thermomechanical fatigue. It is cardinally differs detonation spraying from APS, which forms porous structures, and HVOF, the coatings of which may have less pronounced compressive stresses or even tensile stresses, which makes them more vulnerable to thermal instability and cracking [27, 28].

DOI 10.15588/1607-6885-2025-4-3

Table 2 – Standardized test methods for the characterization of coatings

The property that is found	Standard	Principle of the Method	Output indicator
Erosion Resistance	ASTM G76	Bombardment of a surface with solid particles in a gas stream at a controlled angle and speed.	Loss of mass or volume per unit mass of erodent (e.g., mg/g).
Adhesive Strength	ASTM C633	A pull-off test in which a pin glued to the surface of a coating is pulled off by tensile force.	Failure stress (MPa) and failure location.
Adhesion (qualitative assessment)	ISO 2409	A grid is cut on the coating, then adhesive tape is applied and peeled off. Adhesion is assessed by the amount of coating removed.	Classification score (at a scale from 0 to 5) based on visual inspection.
Microhardness	ISO 6507, ASTM E384	A diamond indenter (Vickers pyramid) is pressed into the surface under a certain load. The size of the imprint is measured.	Hardness value (HV) with load indication (e.g. 0.3 HV).

Despite the advantages, when implementing the technology, potential challenges must be taken into account, namely:

thermal mismatch. Even in the presence of compressive stresses, the significant difference in the coefficient of thermal expansion (CTE) between the nickel superalloy substrate (CTE $\approx 15.5\times10^{-6}$ K^{-1}) and the Cr_3C_2–NiCr coating (CTE $\approx 10.9\times10^{-6}$ K^{-1}) remains a risk factor that generates high interface stresses during thermal cycling. To mitigate this effect, one can consider using an intermediate, more ductile sublayer (e.g., NiCr) [6]. A more advanced solution is to use CCDS technology to create a functional gradient transition that will ensure smooth changes in properties from the substrate to the surface [15, 29];

process quality control. Stability of coating performance requires thorough control of the spraying process parameters. It is necessary to implement modern quality management methodologies, such as failure mode and effects analysis (FMEA) and «Six Sigma» to ensure high reproducibility and reliability of coatings [30];

complexity of geometry. Applying a coating of uniform thickness and properties to the aerodynamic profile of the NGVs blades is a complex technological task. Its solution requires the use of robotic multi-axis manipulators to move the detonation gun due to the complex spatial trajectory [6].

Based on the analysis of the exceptional properties of detonation coatings, it is possible to predict a significant increase in the operational life of the NGV. Creating a more damage-resistant surface that effectively resists the formation of primary defects (erosion ulcers, microcracks), the proposed coating destroys the degradation cascade. This leads to a nonlinear, significant increase of the durability of the component, which, in turn, increases the reliability of the engine as a whole mechanism, reduces maintenance and repair costs and increases the technical availability factor (TAF).

Conclusions

Based on the analysis, the following conclusions can be formulated:

The operational resource of the NGV of the GTE is limited by the simultaneous action of a complex of destructive factors, such as erosion by solid particles, high-temperature corrosion and thermomechanical fatigue.

A comparative analysis of modern technologies has shown that detonation spraying is the most promising method for application, does not allow the formation of a coating with practically zero porosity, extremely high adhesion and favorable residual compressive stress indicators.

As an optimal solution, a metal-ceramic coating based on Cr_3C_2-NiCr, applied by the detonation spraying method, is proposed. It provides a better balance of the strength, toughness and resistance to aggressive environments, compared to traditional or other metal-ceramic systems.

A comprehensive experimental validation program based on international ASTM and ISO standards is proposed, which allows for a comprehensive assessment of the microstructural, physical-mechanical and operational properties of the proposed coating.

The implementation of this application technology will lead to a significant increase in the durability and reliability of critically important components of dual-purpose mechanisms, which provides significant economic advantages both during manufacturing and operation.

References

1. Skubachevsky, G. S. (1981). Aviatsionnye gazoturbinnye dvigateli. Konstruktsiia i raschet detalei. 4th ed., rev. and enl. Moscow: Mashinostroenie. 552 p.

2. Inozemtsev, A. A., Nikhamkin, M. A., & Sandratsky, V. L. (2008). Osnovy konstruirovaniia aviatsionnykh dvigatelei i energeticheskikh ustanovok. T. 2: Kompressory. Kamery sgoraniia. Forsazhnye kamery. Turbiny. Vykhodnye ustroistva. Moscow : Mashinostroenie. 464 p.

3. Reed, R. C. (2006). The Superalloys: Fundamentals and Applications. Cambridge University Press. https://doi.org/10.1017/CBO9780511541285.

DOI 10.15588/1607-6885-2025-4-3

4. Donachie, M. J., & Donachie, S. J. (2002). Superalloys: A Technical Guide (2nd ed.). ASM International. https://doi.org/10.31399/asm.tb.stg.9781627082335.

5. Padture, N. P., Gell, M., & Jordan, E. H. (2012). Thermal Barrier Coatings for Gas-Turbine Engine Applications. MRS Bulletin, 37(10), 891–897. https://doi.org/10.1557/mrs.2012.232.

6. Pawlowski L. The Science and Engineering of Thermal Spray Coatings. 2nd ed. Chichester : John Wiley & Sons, 2008. 642 p. ISBN 978-0-471-49049-4.

7. Holmberg K., Matthews A. Coatings Tribology: Properties, Techniques and Applications in Surface Engineering. 2nd ed. Amsterdam: Elsevier, 2009. 732 p. ISBN 978-0-444-52750-9.

8. Panjan, P., Čekada, M., & Panjan, M. (2013). The shadowing effect in PVD hard coatings. Coatings, 3(1), 23-34.

9. Padture, N. P., Gell, M., & Jordan, E. H. (2002). Thermal barrier coatings for gas-turbine engine applications. Science, 296(5566), 280-284.

10. Hutchings, I. M., & Shipway, P. H. (2017). Tribology: Friction and Wear of Engineering Materials (2nd ed.). Butterworth-Heinemann.

11. Birks, N., Meier, G. H., & Pettit, F. S. (2006). Introduction to High-Temperature Oxidation and Corrosion (2nd ed.). Cambridge University Press. https://doi.org/10.1017/CBO9780511617541.

12. S. Matthews, B. James, M. Hyland. The role of microstructure in the high temperature oxidation mechanism of Cr_3C_2–NiCr composite coatings. Corrosion Science. 2009. Vol. 51, no. 5. P. 1172-1180. DOI: https://doi.org/10.1016/j.corsci.2009.02.027.

13. Hertzberg, R. W., Vinci, R. P., & Hertzberg, J. L. (2013). Deformation and Fracture Mechanics of Engineering Materials (5th ed.). John Wiley & Sons.

14. Zubchenko, A. S. (Ed.). (2003). Marochnik stalei i splavov (2nd ed., rev. & enl.). Moscow: Mashinostroenie.

15. Aifantis, E.C. Gradient material mechanics: Perspectives and Prospects. Acta Mech 225, 999–1012 (2014). https://doi.org/10.1007/s00707-013-1076-y.

16. Sargent, H. B., Poorman, R. M., & Lamprey, H. (1955). U.S. Patent No. 2,714,563.

17. Lakhwinder, S., Vikas, C., & Grewal, J. S. (2012). A Review on Detonation Gun Sprayed Coatings. Journal of Minerals and Materials Characterization and Engineering, 11(3), 243–265.

18. Thorpe, M.L., Richter, H.J. A pragmatic analysis and comparison of HVOF processes. JTST 1, 161-170 (1992). https://doi.org/10.1007/BF02659017.

19. Vagge, S. T., & Ghogare, S. (2022). Thermal barrier coatings: Review. Materials Today: Proceedings, 56, 1201–1216. https://doi.org/10.1016/j.matpr.2021.11.170.

20. ISO 2063-1:2019. Thermal spraying — Zinc, aluminium and their alloys – Part 1: Design considerations and quality requirements for corrosion protection systems.

21. ISO 2063-2:2017. Thermal spraying — Zinc, aluminium and their alloys – Part 2: Execution of corrosion protection systems.

22. ASTM C633-13(2022). Standard Test Method for Adhesion or Cohesion Strength of Thermal Spray Coatings.

23. ASTM International. (2023). Standard Test Method for Conducting Erosion Tests by Solid Particle Impingement Using Gas Jets (Standard No. ASTM G76-18(2023)).

24. W. Zhou, R. Apkarian, Z. L. Wang and D. Joy, “Fundamentals of Scanning Electron Microscopy (SEM),” in Scanning Microscopy for Nanotechnology, Springer, 2007, pp. 1-40.

25. Girão, A. V., Caputo, G., & Ferro, M. C. (2017). Application of Scanning Electron Microscopy-Energy Dispersive X-ray Spectroscopy (SEM-EDS). In Comprehensive Analytical Chemistry (Vol. 75, pp. 153–166). Elsevier. https://doi.org/10.1016/bs.coac.2016.10.002.

26. Singh, P. K. (2024, June). X-Ray Diffraction (XRD)-Basic principle, instrumentation, sample preparation, XRD plots, applications of XRD, XRD sample based errors. ResearchGate.

27. Lakhwinder, S., Vikas, C., & Grewal, J. S. (2012). A Review on Detonation Gun Sprayed Coatings. Journal of Minerals and Materials Characterization and Engineering, 11(3), 243–265.

28. Verma, A. K., Singh, H., & Kumar, D. (2012). A Comparative Study of Mechanical and Thermo-Mechanical Properties of Cr3C2-NiCr Coatings Deposited by HVOF, D-Gun and Cold Spraying. Journal of Minerals and Materials Characterization and Engineering, 11(3), 221–228.

29. Yu, H.; Liu, Y.; Hu, Y.; Ta, M. Experimental Study on the Effect of Gradient Interface on the Mechanical Properties of Cu/WC_P Functionally Gradient Materials Using Digital Image Correlation Technique. Materials 2022, 15, 4004. https://doi.org/10.3390/ma15114004.

30. Shrestha, T. (2024, January). Gas turbine coating's life cycle. Thermal Processing, 20–22.

Received 10.11.2025
Accepted 24.11.2025

ПІДВИЩЕННЯ ЗНОСОСТІЙКОСТІ СКЛАДНОПРОФІЛЬНИХ ДЕТАЛЕЙ МЕХАНІЗМІВ ПОДВІЙНОГО ПРИЗНАЧЕННЯ

DOI 10.15588/1607-6885-2025-4-3

Євген Вишнепольский — канд. техн. наук, доцент кафедри технологіїї машинобудування, Національний університет «Запорізька політехніка», м. Запоріжжя, Україна, *e-mail: evishnepolskiy@gmail.com,* ORCID: 0000-0002-8048-7976

Андрій Бондарєв — аспірант кафедри технологіїї машинобудування, Національний університет «Запорізька політехніка», м. Запоріжжя, Україна, *e-mail: bondarev@gmail.com,* ORCID: 0009-0004-9429-4050

Мета роботи. *Метою даної роботи є наукове обґрунтування технологічного підходу до значного підвищення зносостійкості лопаток соплового апарату(СА) ГТД шляхом застосування передових методів нанесення захисних покриттів.*

Методи дослідження. *Методи дослідження включали підбір типових матеріалів для проведення досліджень (сплави ЖС6У та Inconel 718), розгляд багатофункціональних систем покриттів та їх класифікацій (теплозахисні покриття (Thermal Barrier Coatings, TBC), зносостійкі металокерамічні системи (Wear-Resistant Cermet Systems)), методи напилення (детонаційне напилення (Detonation Spraying, D-Gun), високошвидкісним киснево-паливним (High Velocity Oxygen Fuel, HVOF, атмосферним плазмовим напиленням (Atmospheric Plasma Spraying, APS) та аналіз наукових досліджень, що підтверджують ефективність зазначених методів.*

Отримані результати. *Аналіз наявних досліджень та літератури показав, що технологія детонаційного напилення є унікальною та найбільш придатною для вирішення поставленої задачі, оскільки вона здатна сформувати покриття системи Cr_3C_2-NiCr з необхідною комбінацією властивостей: високою щільністю, відмінною адгезією та, що найважливіше, сприятливим полем залишкових напружень стиснення.*

Наукова новизна. *Наукова новизна роботи полягає у системному підході до вирішення складної проблеми захисту лопаток СА (деталей та механізмів подвійного призначення) шляхом застосування технології детонаційного напилення, яка відома своєю здатністю формувати надзвичайно щільні та зносостійкі покриття.*

Практична цінність. *Практичне значення дослідження полягає у потенційній можливості суттєвого збільшення міжремонтного ресурсу, надійності та боєготовності критично важливих елементів ГТД.*

Ключові слова: *ГТД, лопатка соплового апарату (СА), суперсплав, ерозія твердими частинками, високотемпературна газова корозія, окислення, TBC, D-Gun, HVOF, APS.*

Список літератури

1. Скубачевский Г. С. Авиационные газотурбинные двигатели. Конструкция и расчет деталей: учебник. 4-е изд., перераб. и доп. / Скубачевский Г. С. М. : Машиностроение, 1981. – 552 с.

2. Иноземцев А. А. Основы конструирования авиационных двигателей и энергетических установок. Т. 2: Компрессоры. Камеры сгорания. Форсажные камеры. Турбины. Выходные устройства: учебник / Иноземцев А. А., Нихамкин М. А., Сандрацкий В. Л. – М. : Машиностроение, 2008. – 464 с.

3. Reed, R. C. The Superalloys: Fundamentals and Applications / Reed, R. C. // Cambridge University Press, 2006. https://doi.org/10.1017/CBO9780511541285.

4. Donachie, M. J. Superalloys: A Technical Guide (2nd ed.) / Donachie, M.J., & Donachie, S.J. // ASM International, 2002. https://doi.org/10.31399/asm.tb.stg.9781627082335.

5. Padture, N. P. Thermal Barrier Coatings for Gas-Turbine Engine Applications / Padture, N. P., Gell, M., & Jordan, E. H. // MRS Bulletin, 2012. – 37(10), P. 891–897. https://doi.org/10.1557/mrs.2012.232.

6. Pawlowski L. The Science and Engineering of Thermal Spray Coatings. 2nd ed. Chichester : John Wiley & Sons, 2008. – 642 p. ISBN 978-0-471-49049-4.

7. Holmberg K. Coatings Tribology: Properties, Techniques and Applications in Surface Engineering / Holmberg K., Matthews A. // 2nd ed. Amsterdam: Elsevier, 2009. – 732 p. ISBN 978-0-444-52750-9.

8. Panjan, P. The shadowing effect in PVD hard coatings / Panjan, P., Čekada, M., & Panjan, M. // Coatings, 2013. – 3(1)/ – P. 23–34.

9. Padture, N. P. Thermal barrier coatings for gas-turbine engine applications / Padture, N. P., Gell, M., & Jordan, E. H. // Science, 2002. – 296(5566). – P. 280–284.

10. Hutchings, I. M. Tribology: Friction and Wear of Engineering Materials (2nd ed.) / Hutchings, I. M., & Shipway, P. H. // Butterworth-Heinemann, 2017.

11 Birks, N. Introduction to High-Temperature Oxidation and Corrosion (2nd ed.) / Birks, N., Meier, G. H., & Pettit, F. S. // Cambridge University Press, 2006. https://doi.org/10.1017/CBO9780511617541.

12. S. Matthews The role of microstructure in the high temperature oxidation mechanism of Cr_3C_2-NiCr composite coatings / S. Matthews , B. James , M. Hyland . // *Corrosion Science*. – 2009. – Vol. 51, No 5. – P. 1172–1180. DOI: https://doi.org/10.1016/j.corsci.2009.02.027.

13. Hertzberg, R. W. Deformation and Fracture Mechanics of Engineering Materials (5th ed.) / Hertzberg, R. W., Vinci, R. P., & Hertzberg, J. L. // John Wiley & Sons, 2013.

DOI 10.15588/1607-6885-2025-4-3

14. Зубченко, А. С. Марочник сталей и сплавов (2-е изд., доп. и испр.) / Зубченко, А. С. – М. : Машиностроение. – 2003.

15. Aifantis, E. C. Gradient material mechanics: Perspectives and Prospects / Aifantis, E. C. // Acta Mech 225, 2014. – P. 999–1012. https://doi.org/10.1007/s00707-013-1076-y.

16. Sargent, H. B., Poorman, R. M., & Lamprey, H. (1955). U.S. Patent No 2, 714,563.

17. Lakhwinder, S. A Review on Detonation Gun Sprayed Coatings / Lakhwinder, S., Vikas, C., & Grewal, J. S. // Journal of Minerals and Materials Characterization and Engineering, 2012. – 11(3). – P. 243–265.

18. Thorpe, M. L. A pragmatic analysis and comparison of HVOF processes / Thorpe, M. L., Richter, H.J. // JTST 1, 1992. – P. 161–170. https://doi.org/10.1007/BF02659017.

19. Vagge, S. T. Thermal barrier coatings: Review / Vagge, S. T., & Ghogare, S. // Materials Today: Proceedings, 2022. – 56. – P. – 1201–1216. https://doi.org/10.1016/j.matpr.2021.11.170.

20. ISO 2063-1:2019. Thermal spraying – Zinc, aluminium and their alloys – Part 1: Design considerations and quality requirements for corrosion protection systems.

21. ISO 2063-2:2017. Thermal spraying – Zinc, aluminium and their alloys – Part 2: Execution of corrosion protection systems.

22. ASTM C633-13(2022). Standard Test Method for Adhesion or Cohesion Strength of Thermal Spray Coatings.

23. ASTM International. (2023). Standard Test Method for Conducting Erosion Tests by Solid Particle Impingement Using Gas Jets (Standard No. ASTM G76-18(2023)).

24. W. Zhou “Fundamentals of Scanning Electron Microscopy (SEM),” in Scanning Microscopy for Nanotechnology / W. Zhou, R. Apkarian, Z. L. Wang and D. Joy // Springer, 2007. – P. 1–40.

27. Girão, A. V. Application of Scanning Electron Microscopy-Energy Dispersive X-ray Spectroscopy (SEM-EDS) / Girão, A. V., Caputo, G., & Ferro, M. C. In Comprehensive Analytical Chemistry, 2017. – Vol. 75 – P. 153–166). Elsevier. https://doi.org/10.1016/bs.coac.2016.10.002.

28. Singh, P. K. (2024, June). X-Ray Diffraction (XRD)-Basic principle, instrumentation, sample preparation, XRD plots, applications of XRD, XRD sample based errors. ResearchGate.

29. Lakhwinder, S. A Review on Detonation Gun Sprayed Coatings / Lakhwinder, S., Vikas, C., & Grewal, J. S. // Journal of Minerals and Materials Characterization and Engineering, 2012. – 11(3). – P. 243–265.

30. Verma, A. K. A Comparative Study of Mechanical and Thermo-Mechanical Properties of Cr_3C_2-NiCr Coatings Depositedby HVOF, D-Gun and Cold Spraying / Verma, A. K., Singh, H., & Kumar, D. // Journal of Minerals and Materials Characterization and Engineering, 2013. – 11(3)/ – P. 221–228.

25. Yu, H. Experimental Study on the Effect of Gradient Interface on the Mechanical Properties of Cu/WC_P Functionally Gradient Materials Using Digital Image Correlation Technique / Yu, H., Liu, Y., Hu, Y., Ta, M. // Materials 2022. – 15, 4004. https://doi.org/10.3390/ma15114004.

26. Shrestha, T. (2024, January). Gas turbine coating's life cycle / Shrestha, T. // Thermal Processing, (2024, January). – P. 20–22.

DOI 10.15588/1607-6885-2025-4-3

UDC 621.793:620.178

Volodymyr Pleskach — Candidate of Technical Sciences, Associate Professor of the Department of Composite Materials, Chemistry and Technologies, Zaporizhzhia Polytechnic National University, Zaporizhia, Ukraine, *e-mail: vmpayzp@gmail.com*, ORCID: 0000-0002-6182-4332

Ivan Akimov — Candidate of Technical Sciences, Associate Professor of the Department of Composite Materials, Chemistry and Technologies, Zaporizhzhia Polytechnic National University, Zaporizhia, Ukraine, *e-mail: akimovi@ukr.net*, ORCID: 0000-0001-6076-0149

Svitlana Kyrylakha — Master's student of the Department of Integrated Welding Technologies and Structural Modeling, Zaporizhia Polytechnic National University, Zaporizhzhia, Ukraine, *e-mail: lanakirilaha@gmail.com*, ORCID: https://orcid.org/0009-0001-5688-5616

PROTECTION OF MACHINE PARTS MADE OF ALUMINUM ALLOYS FROM GAS ABRASIVE WEAR

Purpose. *Analyzing the patterns of gas abrasive wear of the aluminum alloy VD17, applying protective coatings that can provide effective wear resistance, providing recommendations of the optimal type of protective coating.*

Research methods. *The study usedinstallation, the design of which allows changing the parameters of gas-abrasive wear within wide limits, that as best reproduce the wear conditions of machine parts under different operating conditions. The study was conducted on samples of aluminum alloy VD17 with metal protective layers applied by galvanic and chemical methods. The study was conducted using metallographic analysis to identify the structure that provides optimal protection against gas-abrasive wear.*

Results. *Analysis of the nature and magnitude of materials wear was carried out, in the flow of free abrasive depending on the velocity of the abrasive flow and its angle of attack. The degree of reduction in wear of the aluminum alloy VD17 when using chromium and nickel protective coatings was determined. Based on the comparative assessment of the quantitative characteristics of the protective layers, the ability of coatings to reduce wear of the alloy VD17 under the action of a gas abrasive flow was determined.*

Scientific novelty. *The angle of attack corresponding to maximum wear was determined for both the VD17 alloy and the proposed protective chromium and nickel coatings. Based on the analysis of the obtained results, it was revealed how applied metal protective coatings react to gas-abrasive wear depending on the composition and adhesion to the base.*

Practical value. *The results of the work can be used by designers involved in products that operate under conditions of gas-abrasive wear.Based on the obtained dependences of the wear of the materials depending on the angle of attack, it is possible to choose the optimal material and product configuration in such a way that wear is minimal, as well as to choose the optimal type and method of coating application depending on the configuration of the part and production capabilities.*

Key words: *reliability, wear resistance, gas abrasive wear, wear, electroplating chrome plating, chemical nickel plating.*

Introduction

The main concern of any manufacturer to be successful in the market is to ensure the release of reliable products. Reliability is usually understood as the ability of a certain product to perform its functions according to its intended purpose under certain operating conditions [1, 2]. In practice, one of the most important indicators of reliability in operation is durability. It, in turn, is determined by the time that the product will be able to perform its functions until it enters the so-called limit state. The limit state occurs when repair becomes impossible or impractical. Most often, during operation, the long-term operation of a product is affected by various types of wear, which can affect the product daily and constantly. Wear is understood as the process of gradual destruction of the surface of a product, which leads to a change in its size, shape or mass [3].

In the literature on wear, the greatest attention is paid to mechanical wear. Under different operating conditions, it can take different forms. Within the general science of wear – tribology [4, 5], the greatest attention is paid to the study of wear due to sliding or rolling friction [6, 7].

One of the important mechanical types of wear is abrasive wear, and in particular, gas abrasive wear. Nowadays, many structures and products are made of high-strength aluminum alloys. In particular, they are used for the manufacture of fan and compressor blades of aircraft engines. Achieving a long service life of such engines is

DOI 10.15588/1607-6885-2025-4-4

prevented by the relatively rapid wear of aluminum alloys under the influence of air flow with suspended particles of free abrasive (dust, soot, ice particles, etc.). Protection of aluminum parts from gas-abrasive wear will allow not only to increase the engine service life, but also to reduce its mass.

Analysis of research and publications

Abrasive wear is one of the most common and destructive types of damage to machine parts during operation. In general, it consists in the fact that abrasive particles - bodies with a hardness significantly higher than the hardness of the metal - under different conditions of interaction with the surface of the part lead to its local destruction. The particles themselves can be very diverse in origin, shape, size and hardness. These can be grains of sand, dust, oxides, intermetallics, metal wear products, etc.

Depending on the interaction of abrasive particles with a metal surface, several types of abrasive wear are distinguished: with the participation of fixed and moving particles, with and without lubrication, impact interaction or under low pressure, with high or low speed of mutual movement, etc. Abrasive wear occurs in sliding bearings for various purposes, in parts of construction, agricultural and mining equipment, etc.

Ukrainian scientists [8] have made a significant contribution to the study of the mechanism of abrasive wear, such as B.I. Kostetsky, I.V. Kragelsky and others, and ways to prevent it.

One of the types of abrasive wear is gas abrasive wear. It consists in process of abrasive particles destroy metal, moving at a greater or lesser speed in a gas stream. Gas abrasive wear occurs in buildings under certain meteorological conditions, helicopter engines over sandy unprepared airfields, etc. The features and basic patterns of gas abrasive wear under various conditions were studied by such scientists as G. Evans,I.V. Kragelsky, I.R. Kleis and others [9].

Today it is known that the intensity of gas abrasive wear depends on the flow velocity V and its angle of attack α.

The dependence of wear on the velocity of the gas-abrasive flow is related to the kinetic energy of the abrasive particle at the moment of impact. Therefore, the intensity of wear depends on both the mass of the particle and the speed of its movement in the second degree. It increases with increasing velocity and flow of the carrier gas, and the size and mass of the abrasive particles. In addition, the hardness and shape of the abrasive particles affect the amount of wear.

The change in wear intensity when the angle of attack of the gas abrasive flow α changes depends on the mechanism of destruction of the surface material. The latter, in turn, depends on the properties of the material being worn.

If a plastic material is destroyed, then at small values of the angle α the particles remove metal by cutting and scratching. With an increase in the angle α to 60° and more, destruction due to repeated plastic deformation begins to prevail. In the surface layer, slag gradually appears and accumulates, and the amount of wear begins to decrease.

When it comes to high-strength brittle materials, at small angles of attack the particles slide along the surface and often cannot scratch it. As the angle α increases, the wear rate gradually increases. The brittle fracture mechanism begins to operate, and with a vertical direction of particle impact it comes into full force. That is, at α = 90° the wear reaches a maximum.

Purpose of work

The task of this work is to analyze the patterns of gas-abrasive wear of aluminum alloys of fan blades and compressors of aircraft engines and to find proposals for protecting them from gas-abrasive wear.

Research material and methodology
Gas abrasive wear testing facility

This study used a gas-abrasive wear test rig that fairly well reproduces the wear conditions that exist in aircraft engines.

Currently, there are no specific standards or special methods for studying gas-abrasive wear of structural materials. Therefore, quite diverse installations are used in the research, the main task of which is to create test conditions that are as close as possible to the operating conditions of the relevant machine parts.

According to literature data, existing test rigs are divided into gravitational, mechanical, and pneumatic, based on the principle of the abrasive flow.

In gravity installations, the speed of abrasive particles is created due to their free fall. In such installations, it is difficult to create a high speed at the moment of impact of particles, but it is possible to calculate it quite accurately at the moment of impact. Most often, such installations are used to assess the stability of various coatings, in particular enamel ones.

In mechanical type installations, the speed of abrasive particles is created due to centrifugal forces. The basis of these installations is a rotor rotating around a vertical axis, through the channels of which abrasive particles are accelerated to the required speed. Several stationary samples are installed around the rotor at one angle or another. During testing, it is relatively easy to establish the parameters of the particles at the moment of impact. However, the installation requires accurate dosing of the abrasive supply. In addition, the test result is negatively affected by the flow of abrasive around the edges of the sample.

In pneumatic installations, the required speed is set to the particles by a stream of air or gas, and a flat sample, moving or stationary, is installed at a certain angle to the gas-abrasive jet flowing from the nozzle. Such installations have the ability to change the wear parameters in a wide range, adapting to the operating conditions of the material being studied. Their disadvantage is that the speed of the particles at the moment of impact may not exactly correspond to the speed of the gas flow. There are also difficulties in creating angles of attack close to zero.

DOI 10.15588/1607-6885-2025-4-4

Nevertheless, today this type of installation is the most common, since they make it relatively easy to reproduce any test conditions that are close to operating conditions: in terms of speed and angle of attack of the gas abrasive flow; type, size and concentration of abrasive particles in the flow; composition and temperature of the gas flow, etc.

In this study, a pneumatic type installation was used. During the research, gas-abrasive wear conditions were created in it, close to the operation of compressor blades and fans of aircraft engines (Fig. 1).

The main element of the installation is a rotor with a diameter of 700 mm, which serves to fix 60 samples simultaneously and give them a circular speed. On the front side of the disk, an annular groove of a special shape is machined for fixing the samples. The samples are installed tightly to each other so that only the surface of the samples is worn during the tests. Using a three-stage pulley, the disk can be given the following rotation speeds: 700, 1500 and 3000 rpm. The rotor with the samples is carefully balanced. To eliminate imbalance when testing samples that differ significantly from each other in mass, samples of the same mass are installed on the rotor at diametrically opposite places around the circumference.

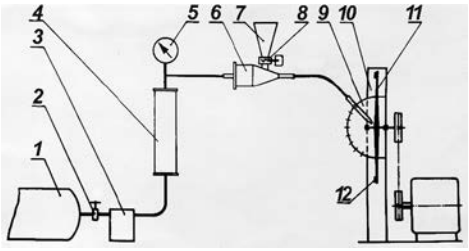

Figure 1. Scheme of the gas abrasion wear test setup:

1 – compressor; 2 – tap; 3 – oil-water separator;
4 – rotameter; 5 – manometer; 6 – mixing chamber;
7 – bunker; 8 – dispenser; 9 – abrasive chamber;
10 – housing; 11 – sample; 12 – rotor

The sample is a flat plate with dimensions of 35×20×2 mm. On the upper edge it has a chamfer that enters the groove of the rotor. The sample is fixed on the rotor with a screw (Fig. 2). To prevent abrasion of the sample when screwing and unscrewing the screw, a conical brass washer is installed between the screw and the sample.

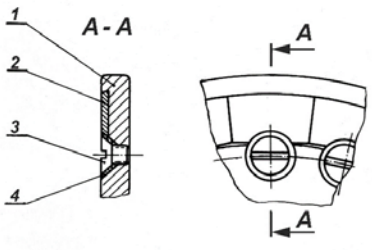

Figure 2. Sample mounting diagram:

1 – rotor; 2 – sample; 3 – screw; 4 – washer

The air flow is created by a compressor. The air supplied to the unit is cleaned in an oil-water separator. The valve sets the volume of spent air necessary to create a given gas flow rate. Its value is determined using a rotameter RS-7.

The unit for feeding abrasive into the gas stream consists of a hopper, a dispenser and a mixing chamber. The dispenser is a profiled screw, which is rotated by an electric motor through a gearbox and thereby ensures continuous feeding of abrasive into the mixing chamber. Using replaceable screws, the concentration of abrasive in the gas stream can be varied within wide limits. In the mixing chamber, a flow velocity sufficient to capture abrasive particles is created. In addition, the abrasive feeding unit provides the possibility of heating the gas stream or introducing additional components (for example, moisture) into it.

In the abrasive chamber, the actual wear of the samples occurs with a gas-abrasive flow with specified parameters. Structurally, it is a flat box, the end part of which includes the edge of the disk with the samples. On its semicircular wall, there are cut holes for a pipe with a replaceable nozzle, from which the flow of abrasive particles is directed to the samples. The cut holes allow the nozzle to be installed in nine fixed positions (every 15°) at an angle relative to the plane of the disk at the same distance from the theoretical point of contact of the abrasive with the sample.

The shape and dimensions of the nozzle outlet ensure that abrasive particles only hit the samples and eliminate wear of the rotor and sample mounting parts. Due to the sufficiently small size of the nozzle outlet and the small distance between it and the sample surface, there is no significant dispersion of the collision parameters of individual abrasive particles in the flow during testing.

At the moment of interaction of abrasive particles and the sample, two types of motions act on them: the circular velocity of the sample and the velocity of particles with the gas flow. Therefore, the actual velocity of particles at the moment of collision was found by geometric addition of the vectors of the corresponding motions (Fig. 3).

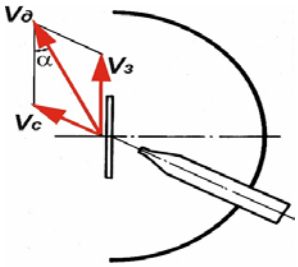

Figure 3. Diagram of the velocities of abrasive particles relative to the sample:

Vs – sample velocity; Vs – jet velocity of the gas abrasive flow;
Vd – actual collision velocity; α – angle of attack

The circular velocity of the point in the center of the sample was taken as the sample velocity Vc. The deviation of the velocities of the extreme points of the sample from the one adopted in the calculations does not exceed 3%. The

DOI 10.15588/1607-6885-2025-4-4

jet velocity of the gas abrasive flow Vc was calculated according to the laws of gas dynamics using the readings of the air volume flow rate by the rotameter and the pressure in the flow by the manometer (Fig. 1). The angle of attack α was calculated according to the data of the velocity triangle.

Research methodology

According to the characteristics of the air flow in the compressors of most aircraft engines [10], the speed of the gas-abrasive flow during the tests varied from 95 to 280 m/s. The installation allows you to change the angle of attack of the abrasive flow from 20 to 860.

For the tests, quartz sand with a particle size of 100...200 microns was used. The sieved and prepared sand for testing was dried in a drying cabinet at a temperature of 120 °C before loading into the batcher and weighed with an accuracy of 0.1 g. At all test speeds, a constant sand concentration in the flow was maintained: 20 g/m^3.

The used sand was not reused because after contact with the samples, the sand particles are crushed, their shape, size, edge sharpness, etc. change. Therefore, the wear results when using fresh and used sand will be different.

In each test mode, 4...6 samples of the same type were simultaneously examined. The samples were weighed before and after the test on an analytical balance with an accuracy of 0.1 mg. The difference in the mass of the sample before and after the test determined the mass wear of the sample. But in order to compare the results of tests of different durations carried out on samples made of materials that differ significantly in density, the obtained mass wear, depending on the density of the tested material, was converted into volumetric and measured in mm3 of the sample material removed from 1 sm^2 of the outer surface of the sample at a consumption of 1 kg of abrasive during the test (mm^3/ sm^{2}kg).

Aluminum alloy VD17

The basis for the research was the aluminum deformed alloy VD17 of the aluminum-copper-magnesium system, which has the following chemical composition: aluminum – the base, copper – 2.6...3.2%, magnesium – 2.0...2.4%, manganese – 0.45...0.70%, iron and silicon – up to 0.3% each.

Alloy VD17 is duralumin with increased heat resistance; it is usually subjected to hardening and natural aging. At room temperature, it has a tensile strength of up to 500 MPa and a relative elongation of 10%, and is characterized by high fatigue strength and fracture toughness.

Duralumin VD17 is used in many branches of engineering. It is used to make truck bodies, building structures, parts in the refrigeration and food industries, etc. In aircraft construction, it is used to make propeller blades, compressors and engine fans operating at temperatures up to 250°C, frames, control rods, etc. [11–13].

Metal protective coatings

Based on the analysis of literary sources, metal protective coatings were selected to protect the VD17 aluminum alloy: electroplating chrome plating and chemical nickel plating.

For electroplating, a standard electrolyte is usually used, which contains: 250 g/l CrO_3, 2.5 g/l H2SO4 at t = 45...55°C and current density i_k = 20...60 A/dm^2.

Temperature and current density significantly affect the current output and properties of cathode chromium deposits. Depending on these parameters, the chromium deposit varies from pale milky and soft to shiny and hard. Different types of coatings are obtained at high current densities and different temperatures. At relatively low temperatures, matte coatings are obtained, and with increasing temperature at constant current density, shiny coatings are obtained.

The following parameters were chosen for chromium plating of the samples: electrolyte containing 300 g/l CrO3, 2.5 g/l H2SO4, current density ik = 45…50 A/dm2, and at a temperature of t = 45...500 °C, matte coatings were obtained, and at a temperature of t = 50...65°C, shiny ones were obtained [14, 15]. The microstructure of the electroplated chromium coating on the VD17 alloy is shown in Fig. 4.

One of the main advantages of chemical nickel plating is the ability to obtain a uniform coating layer on parts of any complex configuration (including compressor blades). Chemically deposited nickel has certain advantages: the surface of the coating is shiny, its hardness is higher than that of electrolytic nickel deposits, the coating does not reduce fatigue strength.

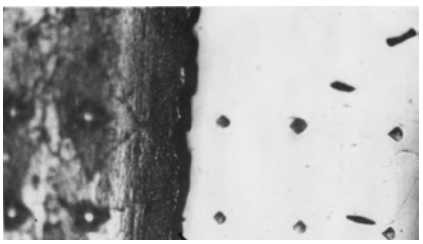

Figure 4. Microstructure of electroplated chromium coating on VD17 alloy

For chemical nickel plating of aluminum alloys, alkaline solutions (pH = 8...10) are used due to more favorable conditions for the process on the surface of light alloys [16]. Nickel plating of samples was carried out in a solution of the following composition: nickel chloride (II) $NiCl_2$ – 21 g/l; sodium hypophosphate – 24 g/l; sodium citrate – 45 g/l; ammonium chloride NH_4Cl – 30 g/l; ammonium hydroxide NH4OH – 50 g/l at an acidity of pH = 8.5...9.5 and a temperature of 75...800 °C. The process lasted 6...8 hours with regular adjustment of the acidity of the solution using ammonium hydroxide.

The resulting coating, 40...60 microns thick, is actually a solid solution of phosphate in nickel with small inclusions of phosphides. Chemical analysis showed that the precipitate contains 96...97 % nickel and 3...4 % phosphorus.

Nickel-plated samples were divided into two groups. The samples of the first group were annealed at a temperature of 2300 °C for 45 min. in order to improve the adhesion of the coating to the base. The samples of the second group, in addition to similar annealing, were subjected to hardening and aging according to the regime usual for the VD17 alloy (Fig. 5).

DOI 10.15588/1607-6885-2025-4-4

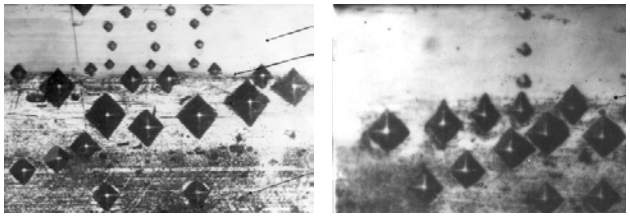

a *b*

Figure 5. Microstructure of nickel coatings processed in the first mode (*a*) and in the second mode (*b*)

Research results

The study showed that the main influence on the wear rate of a structural material under the action of a gas abrasive flow is the velocity of the abrasive flow and the angle at which the abrasive flow acts on the surface of the material. The dependence of the wear rate on the angle of attack for all the studied materials was typical for plastic materials: with an increase in the angle of attack, wear increases and, having reached a maximum, smoothly decreases (Fig. 6).

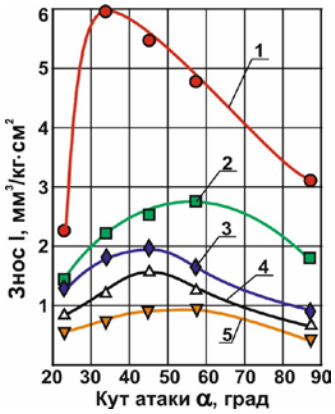

Figure 6. Dependence of wear of VD17 alloy and coatings on the angle of attack at a gas abrasive flow velocity of 95 m/s:

1 – VD17 alloy, 2 – nickel coating, h/t 1,
3 – nickel coating, h/t 2; 4 – matte chrome coating,
5 – shiny chrome coating

The angle of attack of the flow α, which corresponds to the maximum wear, depends on the mechanical properties of the material of the samples. The smallest angle of attack is for the VD17 alloy. The angles of maximum wear of the coatings are somewhat larger, being in approximately the same range. This is due to the increase in the hardness of the worn material.

Also, with increasing gas-abrasive flow velocity, a shift of the wear maximum towards larger angles of attack is observed. In this case, the greater the hardness of the worn material and the greater the abrasive flow velocity, the less clearly the maximum on the wear-angle of attack curve is manifested (Fig. 7).

Discussion

There is a noticeable difference in the wear of the aluminum alloy and nickel and chromium coatings. This is due to the significantly different physical and mechanical properties of the coating metals and aluminum. At the same time, the study showed a sufficiently high quality of adhesion of such different metal coatings to the aluminum surface.

The angle α, which corresponds to the maximum wear at a certain flow rate, is different for all materials. The smallest angle α of maximum wear is for the aluminum alloy VD17. With increasing material hardness, the maximum shifts towards larger angles. The same shift is observed with increasing gas abrasive flow rate. In this case, the greater the hardness of the material being worn and the greater the flow rate, the less clearly the maximum appears on the wear-angle of attack curve.

As for the quantitative characteristics, the degree of wear reduction of metal coatings depends on the hardness of the corresponding coating, and the order of the wear curves is preserved at all angles of attack and velocities of the gas abrasive flow.

The protective properties of nickel coatings are quite stable at all speeds: nickel coating heat-treated according to the first mode increases wear resistance by 2.3...2.7 times, and heat-treated according to the second mode - by 3...4 times. The difference between the wear of both nickel coatings is 15...35%.

The difference in maximum wear of chrome coatings is 40...60 %. The effectiveness of protection of aluminum alloy by chrome coatings increases with increasing abrasive flow rate. Shiny chrome coating increases the wear resistance of VD17 alloy by 6.5...9.0 times, matte – by 4...7 times.

The intensity of wear growth of nickel coatings with increasing flow velocity is somewhat higher than that of chromium coatings. The most sensitive to the increase in abrasive flow velocity is alloy VD17.

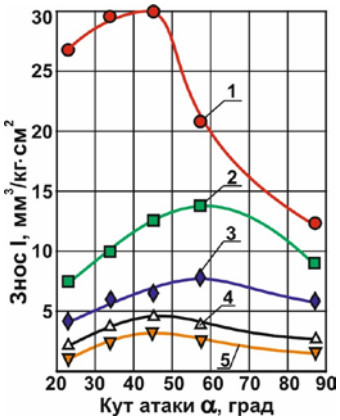

Figure 7. Dependence of wear of VD17 alloy and coatings on the angle of attack at a gas abrasive flow velocity of 280 m/s

1 – VD17 alloy, 2 – nickel coating, h/t 1, 3 – nickel coating, h/t 2, 4 – chrome matte coating, 5 – chrome shiny coating

Conclusions

1. A detailed analysis of the regularities of gas abrasive wear of the VD17 alloy was carried out.

2. To increase the wear resistance of the VD17 alloy,

DOI 10.15588/1607-6885-2025-4-4

galvanic chromium and chemical nickel coatings were proposed and the patterns of their wear in a gas-abrasive flow were studied.

3. The influence of the physical and mechanical properties of coatings on resistance to gas abrasive wear was analyzed.

4. Based on the comparative evaluation of the quantitative wear characteristics of protective coatings, it can be concluded that both coatings can be used to protect machine parts made of VD17 alloy from gas-abrasive wear. The choice depends both on the conditions of interaction of the part with the flow and on the possibility of applying a high-quality galvanic or chemical coating to the part.

References

1. DSTU 2860-94 Nadiynist tekhniki. Terminy ta vyznachennya (1994) [Reliability of equipment. Terms and meanings] [in force since 1996-01-01] Kyiv, Derzhstandart Ukrainy,75. [in Ukrainian].

2. Ivshchenko L.Yo., Petrykin V.V. (2006). Derzhavni standarty v mashynobuduvanni i menaloobrobtsi [State standards in mechanical engineering and metalworking] Kharkiv: „Kompaniya CMIT", 320. [in Ukrainian].

3. DSTU 2823-94. Znosostiykist vyrobiv. Tertya, znoshuvannya ta zmashchuvannya. Terminy ta vyznachennya (1995) [Wear resistance of products. Friction, wear and lubrication. Terms and meanings] [in force since 1996-01-01] Kyiv, Derzhstandart Ukrainy, 18. [in Ukrainian].

4. Kondrachuk M.V., Khabubel V.F., Pashechko M.I., Korbut Ye.V. (2009). Trybologiya [Tribology] Kyiv, vyd. Natsionalnogo Aviatsiynogo universytetu „NAU-druk". 232. [in Ukrainian].

5. Bhushan B. (2002). Introduction to tribology, New York : John Whiley & Sons, 732. [in English].

6. Zakalov O.V., Zakalov I.O. (2011). Osnovy tertya i znoshuvannya v mashynach [Basics of friction and wear in machines] Ternopil, vyd. TNTU im. I.Puluya.322. [in Ukrainian].

7. Dmytrychenko M.F., Mnatsakanov R.G., Mikosyanchyk O.O. (2006). Osnovy tertya ta znoshuvannya [Basics of friction and wear] Kyiv, Informavtodor, 216. [in Ukrainian].

8. Dubrovskiy S.S., Rebrova S.V. (2019). Vykorystannya suchasnykh tekhnologiy pry vygotovlenni t remonti elementiv konstruktsiy girnycho-zbagachuvalnogo obladnanya [The use of modern technologies in the manufacture and repair of structural elements of mining and beneficiation equipment] Visnyk Kryvorozkogo natsionalnogo universytetu, 48, 79–83. [in Ukrainian].

9. Pokhmurska G.V., Voytovych A.A. Udarno-abrazyvne znoshuvannya poverkhnevykh shariv, naplavlenykh drotamy systemy Fe-Cr-B-C [Impact-abrasive wear of surface layers welded with wires of the Fe-Cr-B-C system] Naukovyy visnyk NLTU Ukrainy, 25.3, 129–135. [in Ukrainian].

10. Pleskach Volodyvyr, Akimov Ivan (2025). Nadiynist detaley mashyn pry gazoabrazyvnomu znoshuvanni [Reliability of machine parts under gas-abrasive wear] Novi materialy i tekhnologii v metalurgii ta mashynobuduvanni, 1, 44–49. [in Ukrainian].

11. Solntsev Yu.P., Belikov S.B., Volchok I.P., Sheyko S.P. (2010). Spetsialni konstruktsiyni msterialy [Special construction materials] Zaporizhzhya, "VALPIS-POLIGRAF", 536. [in Ukrainian].

12. Popovsch V.V., Popovsch V.V. (2006). Tekhologiya konstruktsiynykh materialiv i manerialoznavstvo [Structural materials technology and materials science] Lviv, Svit. 624. [in Ukrainian].

13. Boguslayev V.O., Kachan O.Ya., Kalinina N.Ye., Mozgovyy V.F., Kalinin V.T. (2009). Aviatsiyno-kosmichni materialy ta tekhnologii [Aerospace materials and technologies] Zaporizhzhya, vyd. VAT „Motor-Sich", 383. [in Ukrainian].

14. Kutiy O.I. (2004). Galvanotekhnika [Electroplating technology] Lviv, vyd. NU "Lvivska politekhnika", 236. [in Ukrainian].

15. Yakymenko G.Ya., Artemenko V.M. (2006). Tekhnichna ekektrokhimiya, ch. III. Galvanichni vyrobnytstva, Technical electrochemistry, part III. Galvanic production, Kharkiv, NTU "KhPI", 272. [in Ukrainian].

16. Rulova A.V., Kislova O.V. (2019). Modyfikatsiya kislotnykh rozchyniv khimichnogo nikeluvannya aluminiyu ta yogo splaviv [Modification of acidic solutions for chemical nickel plating of aluminum and its alloys] Tekhnologii ta dyzayn, № 1 (30), 2019, 1–7. [in Ukrainian].

Received 05.11.2025
Accepted 12.11.2025

ЗАХИСТ ДЕТАЛЕЙ МАШИН З АЛЮМІНІЄВИХ СПЛАВІВ ВІД ГАЗОАБРАЗИВНОГО ЗНОШУВАННЯ

Володимир Плескач — канд. техн. наук, доцент кафедри композиційних матеріалів, хімії та технологій, Національний університет «Запорізька політехніка», м. Запоріжжя, Україна, *e-mail: vmpayzp@gmail.com*, ORCID: 0000-0002-6182-4332

Іван Акімов — канд. техн. наук, доцент кафедри композиційних матеріалів, хімії та технологій, Національний університет «Запорізька політехніка», «Запорізька політехніка», м. Запоріжжя, Україна, *e-mail: akimovi@ukr.net*, ORCID: 0000-0001-6076-0149

Світлана Кирилаха — магістрант кафедри інтегрованих технологій зварювання та моделювання конструкцій, Національний університет «Запорізька політехніка», м. Запоріжжя, Україна, *e-mail: lanakirilaha@gmail.com*, ORCID: 0009-0001-5688-5616

DOI 10.15588/1607-6885-2025-4-4

Мета роботи. *Полягає в аналізі закономірностей газоабразивного зношування алюмінієвого сплаву ВД17, у знаходженні захисних покриттів, які можуть забезпечити ефективне зменшення зносу, та надання рекомендацій щодо оптимального типу захисного покриття.*

Методи дослідження. *При дослідженні використовувалася установка, конструкція якої дозволяє змінювати параметри газоабразивного зношування у широких межах, які б якнайкраще відтворювали умови зношування деталей машин за різних умов експлуатації. Дослідженню піддавалися зразки з алюмінієвого сплаву ВД17 і металеві захисні шари, нанесені на нього гальванічним і хімічним способами. Дослідження проводилося із застосуванням металографічного аналізу з метою виявлення структури, яка забезпечує оптимальний захист від газоабразивного зношування.*

Отримані результати. *У ході роботи проведений аналіз характеру і величини зносу матеріалів, що досліджувалися, у потоці вільного абразиву залежно від швидкості абразивного потоку і його кута атаки. Визначено ступінь зменшення зносу алюмінієвого сплаву ВД17 при використанні хромового і нікелевого захисних покриттів. На підставі порівняльного оцінювання кількісних характеристик захисних шарів визначено можливості цих покриттів зменшити знос сплаву ВД17 при дії газоабразивного потоку.*

Наукова новизна. *Визначена величина кутів атаки, які відповідають максимальному зношуванню, як для сплаву ВД17, так і для запропонованих захисних хромового і нікелевого покриттів. На підставі аналізу отриманих результатів виявлено, як реагують використані металеві захисні покриття на газоабразивне зношування залежно від складу і зчеплення з основою.*

Практична цінність. *Результати роботи можуть бути використані конструкторами, що займаються виробами, які працюють в умовах газоабразивного зношування. На підставі отриманих залежностей зносу матеріалів, що досліджувалися, від кута атаки є можливість обрати оптимальні матеріал і конфігурацію виробу таким чином, щоб зношування було мінімальним, а також обрати оптимальний вид і спосіб нанесення покриття залежно від конфігурації деталі та виробничих можливостей.*

Ключові слова: *надійність, зносостійкість, газоабразивне зношування, знос, гальванічне хромування, хімічне нікелювання.*

Список літератури

1. ДСТУ 2860-94 Надійність техніки. Терміни та значення. – [Чинний від 1996-01-01]. – К. : Держстандарт України, 1994. – 75 с.

2. Івщенко Л.Й., Петрикін В.В. Державні стандарти в машинобудуванні і металообробці: навч. посібник – Харків : «Компанія СМІТ», 2006. – 320 с.

3. ДСТУ 2823 – 94. Зносостійкість виробів. Тертя, зношування та мащення. Терміни та визначення. [Чинний від 1996-01-01] – К.: Держстандарт України, 1995. – 18 с.

4. Трибологія / Кондрачук М. В., Хабутель В. Ф., Пашечко М. І., Корбут Є. В. – К. : вид-во Національного Авіаційного університету «НАУ-друк», 2009. – 232 с.

5. Bhushan B. Introduction to tribology / Bhushan B. – New York : John Whiley & Sons, 2002. – 732 p.

6. Закалов О.В. Основи тертя і зношування в машинах: навч. посібник / Закалов О.В., Закалов І. О. – Тернопіль : вид-тво ТНТУ ім. І. Пулюя, 2011.– 322 с.

7. Дмитриченко М. Ф. Основи тертя та зношування / Дмитриченко М. Ф., Мнацаканов Р. Г., Мікосянчик О. О. – К. : Інформавтодор, 2006 – 216 с.

8. Дубровський С. С. Використання сучасних технологій при виготовленні та ремонті елементів конструкцій гірничо-збагачувального обладнання / Дубровський С. С., Реброва С. В. // Вісник Криворозького національного унуверситету/ – Вип. 48. – 2019. – С. 79–83.

9. Похмурська Г. В. Ударно-абразивне зношування поверхневих шарів, наплавлених дротами системи Fe-Cr-B-C / Похмурська Г. В., Войтович А. А. // Науковий вісник НЛТУ України. – 2015. – Вип. 25.3. – С. 129–135.

10. Плескач Володимир Надійність деталей машин при газоабразивному зношуванні /Плескач Володимир, Акімов Іван// Нові матеріали і технології в металургії та машинобудуванні. – 2025. – № 1. – С. 44–49.

11. Спеціальні конструкційні матеріали : підручник / Ю. П. Солнцев, С. Б. Беліков, І. П. Волчок, С. П. Шейко. – Запоріжжя : «ВАЛПІС-ПОЛІГРАФ», 2010.– 536 с.

12. Попович В.В. Технологія конструкційних матеріалів і матеріалознавство: підручник / Попович В. В., Попович В. В. – Львів : Світ, 2006. – 624 с.

13. Авіаційно-космічні матеріали та технології: підручник / Богуслаєв В.О., Качан О. Я., Калініна Н. Є. та ін.–Запоріжжя : вид. ВАТ «Мотор-Січ», 2009.–383 с.

14. Кутій О.І. Гальванотехніка / Кутій О.І.– Львів: вид. НУ «Львівська політехніка», 2004. – 236 с.

15. Якименко Г. Я. Технічна електрохімія, ч. ІІІ. Гальванічні виробництва : підручник за ред. Б. І. Байрачного / Якименко Г. Я., Артеменко В. М. – Харків : НТУ «ХПІ», 2006. – 272 с.

16. Рульова А. В. Модифікація кислотних розчинів хімічного нікелювання алюмінію та його сплавів / Рульова А. В., Кислова О. В. // Технології та дизайн. – № 1 (30). – 2019. – С. 1–7.

DOI 10.15588/1607-6885-2025-4-4

МОДЕЛЮВАННЯ ПРОЦЕСІВ В МЕТАЛУРГІЇ ТА МАШИНОБУДУВАННІ

MODELING OF PROCESSES IN METALLURGY AND MECHANICAL ENGINEERING

UDC 621.941.08

Pavlo Tryshyn — PhD, Associate Professor of the Department of Mechanical Engineering Technology, National University Zaporizhzhia Polytechnic, Zaporizhzhia, Ukraine, *e-mail: trishin@zp.edu.ua*, ORCID: 0000-0002-3301-5124

Olena Kozlova — Candidate of Technical Sciences, Associate Professor of the Department of Mechanical Engineering Technology, National University Zaporizhzhia Polytechnic, Zaporizhzhia, Ukraine, *e-mail: kozlova@zp.edu.ua*, ORCID: 0000-0002-3478-5913

Yuriy Vnukov — Doctor of Technical Sciences, Professor, Independent scientist, California, USA, *e-mail: ypahar@ukr.net*, ORCID: 0000-0002-4297-9646

CALCULATION OF PARAMETERS OF A CUTTER-OSCILLATOR WITH TWO DEGREES OF FREEDOM

Purpose. *The main purpose of the work is to conduct a comprehensive assessment of the parameters of a cutter-oscillator with two degrees of freedom using three methods: analytical, computer, and experimental.*

Research methods. *The analytical approach included determining the natural frequency of oscillations and the angle of the resulting displacement of the cutter-oscillator with two degrees of freedom. For numerical modeling of the cutter-oscillator, the SolidWorks and NX software packages were used. The research was also conducted by an experimental method, within which the oscillograms of the oscillations of the cutting edge were recorded. On their basis, the static deflection of the cutter-oscillator and the frequency of its free oscillations were determined.*

Results. *As a result of the study, it was found that the use of an cutter-oscillator is effective for determining the dynamic characteristics of the turning process. The analytical method made it possible to obtain preliminary estimates of the frequencies of natural oscillations and the direction of the resulting displacement. Computer modeling in SolidWorks and NX provided increased accuracy of calculations and allowed varying the system parameters without additional experiments. Experimental measurements based on the analysis of the oscillograms of the cutting edge oscillations confirmed the consistency of the theoretical and model data. The obtained results prove the reliability of the adopted models and the feasibility of using computer modeling for further improvement of the dynamic analysis of the turning process.*

Scientific novelty. *The scientific novelty of the work lies in the integrated approach to the study of the dynamic characteristics of a cutter-oscillator with two degrees of freedom, which combines analytical, numerical and experimental methods of evaluation.*

Practical value. *The practical value of the work lies in the development and justification of a methodology for evaluating the dynamic parameters of a two degree of freedom cutter-oscillator, which can be used during the design and adjustment of tool systems in the turning process. The use of computer modeling allows you to change quickly the design parameters of the tool without conducting a significant number of experiments, reducing the cost of time and resources. The obtained results can be implemented in production practice and used to improve dynamic control systems in metalworking.*

Key words*: oscillogram, self-oscillations, angle of the resulting displacement, regenerative self-oscillations, the natural frequency of oscillations.*

Introduction

Vibrations during turning largely determine the quality of processing, dimensional accuracy and tool durability. One of the effective tools for studying vibrations is the cutter-oscillator. Such tools make it possible to assess the influence of the design parameters of the tool, the material being processed and the cutting modes on the dynamics of

DOI 10.15588/1607-6885-2025-4-5

the cutting process. Accurate determination of the parameters of the cutter-oscillator is necessary for a qualitative study of the parameters of vibrations during turning.

Modern research methods include analytical calculations, computer modeling and experimental measurements. Each of these approaches has its advantages: analytical methods allow for a quick assessment of system parameters, computer modeling allows for the consideration of complex design and physical factors, and experimental studies ensure the verification of models in real conditions.

Analysis of research and publications

The most undesirable and difficult to eliminate vibrations during cutting are self-oscillations – self-sustaining vibrations that arise due to the internal feedback between the cutting process and the vibrations of the tool. Today, a number of reasons for the excitation of self-oscillations during turning are distinguished: the regenerative effect (regenerative self-oscillations) [1, 2], the coordinate coupling (mode coupling) [3, 4], the decreasing characteristic of the cutting force from the processing speed (tangential self-oscillations) [5]. At the same time, it is important to note that in real conditions of cutting, oscillations are always coupled and consist of different types of oscillation, including self-oscillation, of different directions of action, depending on the direction of the degree of freedom of the tool.

To study self-oscillation, various methods and means of measurement: acoustic emission [6, 11, 12], dynamometers [10, 14], variation of the torque of the electric motor of the machine tool [7, 8, 9], etc. are used. However, the most methodically correct study of self-oscillation is with cutters-oscillators, the oscillatory movement of the cutting edge of which corresponds to the law of oscillatory motion of the self-oscillating system. Works [14, 16] present the design of an oscillator cutter with two degrees of freedom in the direction of changing the thickness of the cut and the cutting speed. Accelerometers are used as sensors. The use of accelerometers does not allow to estimate the direction of the resulting movement of the cutting edge. Works [13, 15] present the design of the cutter-oscillator with one degree of freedom in the direction of change in the thickness of the cut. As a means of measuring the oscillating cutting edges, the moved sensors are used. The impact method [17], which requires the production of full-scale samples, is mainly used to study the natural frequencies of oscillating cutters-oscillators. Most of the investigated authors do not pay due attention to the calculation of the direction of the resulting movement of the cutting edge of the cutter-oscillator. That leads to failure to take into account all causes of self-oscillatory excitation in models of oscillatory motion.

The work [5] proposed the design of a cutter-oscillator with two degrees of freedom along the X and Z axes, with the same stiffness in any direction in the XOZ plane. The cutting edge is located on the axis of the holder, which excludes torsional vibrations. However, only analytical formulas for calculating the displacement of the cutting edge are given to calculate the parameters of the cutter-oscillator. Currently, the use of 3D modeling allows you to automate these calculations.

In the works of the authors [18, 19], the results of calculations of the main dynamic characteristics of cutter-oscillators with one degree of freedom are presented by the modeling method, using modern computer programs. This method showed a number of advantages compared to analytical and experimental methods.

Analysis of the dynamic characteristics of the cutter-oscillator with two degrees of freedom allows you to qualitatively assess the dynamic picture of the turning process, predict the behavior of the system under the influence of vibrations, and develop measures to prevent them.

Purpose of work

The purpose of this work is a comprehensive study of the parameters of a cutter-oscillator with two degrees of freedom using three evaluation methods - analytical, computer and experimental.

Research material and methodology

Method for determining the frequency of natural oscillations of the cutter-oscillator and determining the angle of direction of the resulting movement of the cutting edge.

Analytical method

The approximate value of the natural oscillation frequency (NOF) of the first mode of the cutter-oscillator can be found using the formula from the classical Euler–Bernoulla model using the empirical approximation $0 \leq \mu \lesssim 10$:

$$f \approx \frac{1}{2\pi} \cdot \frac{1{,}875^2}{L^2} \cdot \sqrt{\frac{EI}{\rho A}} \cdot \frac{1}{\sqrt{1+0{,}236\mu+0{,}024\mu^2}}, \text{Hz}, \quad (1)$$

where L – the length of the cutter-oscillator overhang, m;

E – Young's modulus of the material of the cutter-oscillator holder, Pa;

I – moment of inertia of the cutter-oscillator cross-section, m⁴;

$$I = I_x = I_z = \frac{\pi d^4}{64}, \quad (2)$$

A – cross-sectional area of the cutter-oscillator holder, m²;

$$A = \frac{\pi d^2}{4}. \quad (3)$$

ρ – material density of the holder of the cutter-oscillator, kg/m³;

m – mass of the cutter-oscillator head, kg;

μ – the dimensionless ratio of the mass of the head to the mass of the cutter-oscillator holder;

$$\mu = \frac{m}{\rho A L} \quad (4)$$

d – cross-sectional diameter of the cutter-oscillator holder, m;

DOI 10.15588/1607-6885-2025-4-5

Based on the data: L = 0.08, 0.1, 0.12 m, $E = 2 \cdot 10^{11}$Pa, ρ = 7850 kg/m³, m = 0.46 kg, d = 0.025 m, were fined:

$$A = \frac{3{,}14 \cdot 0{,}025^2}{4} = 4{,}9 \cdot 10^{-4}\text{m}^2.$$

$$I = I_x = I_z = \frac{3{,}14 \cdot 0{,}025^4}{64} = 1{,}9 \cdot 10^{-8}\text{m}^4.$$

$$\mu_{0{,}08} = \frac{0{,}46}{7850 \cdot 4{,}9 \cdot 10^{-4} \cdot 0{,}08} = 1{,}49.$$

$$\mu_{0{,}1} = \frac{0{,}46}{7850 \cdot 4{,}9 \cdot 10^{-4} \cdot 0{,}1} = 1{,}19.$$

$$\mu_{0{,}12} = \frac{0{,}46}{7850 \cdot 4{,}9 \cdot 10^{-4} \cdot 0{,}12} = 0{,}99.$$

$$f_{0{,}08} \approx \frac{1}{2 \cdot 3{,}14} \cdot \frac{1{,}875^2}{0{,}08^2} \times \sqrt{\frac{2 \cdot 10^{11} \cdot 1{,}9 \cdot 10^{-8}}{7850 \cdot 4{,}9 \cdot 10^{-4}}} \times$$

$$\times \frac{1}{\sqrt{1 + 0{,}236 \cdot 1{,}49 + 0{,}024 \cdot 1{,}49^2}} = 2327 \text{ Hz}.$$

$$f_{0{,}1} \approx \frac{1}{2 \cdot 3{,}14} \times \frac{1{,}875^2}{0{,}1^2} \times \sqrt{\frac{2 \cdot 10^{11} \cdot 1{,}9 \cdot 10^{-8}}{7850 \cdot 4{,}9 \cdot 10^{-4}}} \times$$

$$\times \frac{1}{\sqrt{1 + 0{,}236 \cdot 1{,}19 + 0{,}024 \cdot 1{,}19^2}} = 1535 \text{ Hz}.$$

$$f_{0{,}12} \approx \frac{1}{2 \cdot 3{,}14} \times \frac{1{,}875^2}{0{,}12^2} \times \sqrt{\frac{2 \cdot 10^{11} \cdot 1{,}9 \cdot 10^{-8}}{7850 \cdot 4{,}9 \cdot 10^{-4}}} \times$$

$$\times \frac{1}{\sqrt{1 + 0{,}236 \cdot 0{,}99 + 0{,}024 \cdot 0{,}99^2}} = 1090 \text{ Hz}.$$

For a cutter-oscillator with two degrees of freedom, the bending occurs in two main mutually perpendicular planes of inertia and can be represented as the joint action of two axial bendings f_x and f_z. The magnitude of the total bending of the cutter-oscillator is calculated by the formula [5]:

$$f = \sqrt{f_x^2 + f_z^2} \quad (5)$$

The plane in which the bending of the cutter-oscillator occurs is inclined at an angle γ to the Z axis, the value of which can be found by equation [6]:

$$\gamma = arctg\left(\frac{f_x}{f_z}\right) = arctg\left[\text{tg}(\alpha) \cdot \frac{I_x}{I_z}\right] = \alpha, \quad (6)$$

where α – the angle of action of the cutting force.

The direction of the resulting displacement (DRD) of the cutting edge of the cutter-oscillator coincides with the direction of action of the cutting force (DAF) γ = α, since the holder has a circular cross-section, the stiffness K and the moments of inertia I along the X and Z axes are the same (Fig. 1)

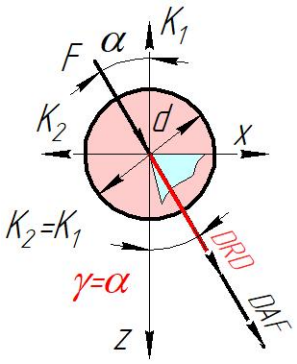

Figure 1. Scheme for calculating the angle of the DRD

The angle of action of the cutting force is found by the ratio of the components of the cutting force:

$$\alpha = F_x / F_z. \quad (7)$$

The components of the cutting force were calculated using the formula [19]:

$$F_{z,x} = 10 C_p t^x S^y v^n K_p, \quad (8)$$

where Cp – a constant that takes into account the processing conditions;

x, y, n – exponents;

t – the cutting depth, mm;

S – the feed, mm/rev;

v – the cutting speed, m/min;

K_p – the generalized correction factor that takes into account changes in processing conditions relative to the tabular values.

The following cutting modes were adopted for calculating the force: t = 1 mm, S = 0.2 mm/rev, v = 150 m/min, the workpiece material is Steel 45 (σ = 600 MPa), without a cooling medium. Cutting insert parameters: material - T15K6, γ = 0°, α = 10°, φ = 90°, λ = 0°, r = 0.5 mm.

According to equations (7), (8), the values of the components of the cutting forces and the angle of inclination of the cutting force were determined: F_x = 279.9 N, F_z = 304.6 N, α = 46.2°.

Modeling method

Using a 3D model of the cutter-oscillating created in *Unigraphics*, a frequency analysis was performed in the *SolidWorks Simulation* module, resulting in the calculated NOF as a function of the cutter's oscillating projection (L), with deformation visualization. The initial data for the calculations were the model material (65G steel) and constraints (cantilever clamping). The 3D model of the oscillating cutter is shown in (Fig. 2).

DOI 10.15588/1607-6885-2025-4-5

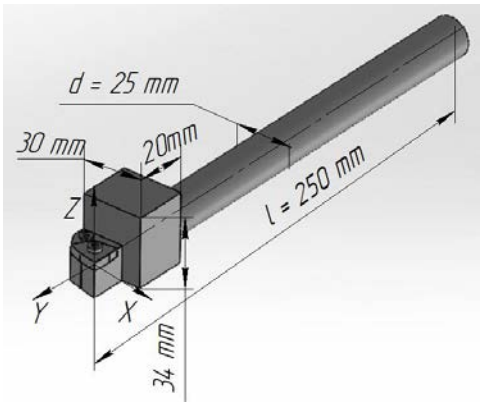

Figure 2. 3D model of a cutter-oscillator with two degrees of freedom

The angle of the cutting edge of the cutter-oscillator was determined by calculating the axial displacements from the action of the cutting force components using the SolidWorks Simulation software module. Further, according to formula (6), the angle of the cutting edge of the cutter-oscillator was determined using the formula for the cutting edge of the cutter-oscillator.

Experimental method

The experimental technique for determining the NOF, described in the authors' work [5]. The cutter-oscillator was fixed in a special device installed in the tool holder of a Zenitech WL 320 CNC lathe (Fig. 3). Two contactless displacement sensors mod. Schneider Electric XS4P12AB110 were installed in the housing of the special device along the X and Z axes. The sensors measured the axial deflections of the cutter-oscillator and were connected via an L-Card E14-140-M ADC to a personal computer. The cutter-oscillator was calibrated using a dynamometer and a dial indicator.

Figure 3. Image of devices for conducting experiments

During the experiments, the cutter-oscillator overhang length, *L*, was varied. The NOF was measured using the impact hammer test. The vibration displacement of the cutter-oscillator after the impact was recorded and stored as oscillograms. The NOF was measured using the oscillograms obtained and processed in *PowerGraph*. To experimentally investigate the direction of the resulting displacement of the cutter-oscillator under the action of turning, longitudinal turning of a rigid part was performed. Cutting edge movements during turning were recorded as oscillograms (Fig. 4), from which static deflections along the X and Z axes were measured.

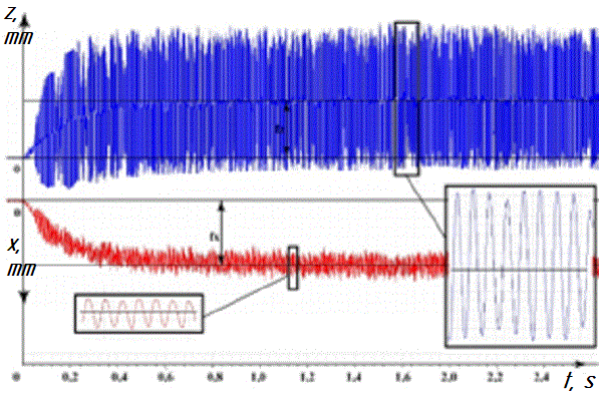

Figure 4. Oscillogram of the cutter-oscillator oscillation during turning

Research results and discussion

Fig. 5 shows a visualization of the calculation of the NOF (a) and static analysis (b) of the cutter-oscillator in the *SolidWorks Simulation* module.

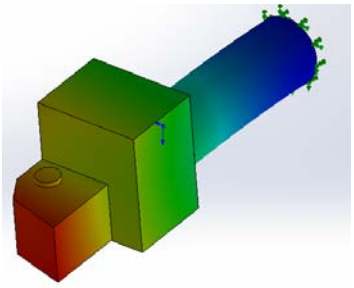

a

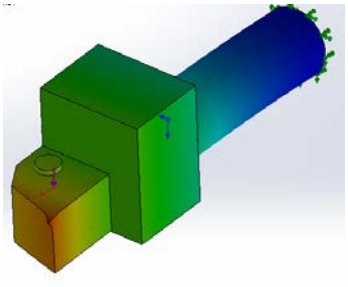

b

Figure 5. Visualization of the calculation of the NOF (*a*) and the angle - γ of the DRD (*b*) of the cutter-oscillator (*L*=120 mm)

Table 1 and Fig. 6 present the results of calculations of the NOF of the cutter-oscillator depending on the over-

DOI 10.15588/1607-6885-2025-4-5

hang L using analytical, experimental and modeling methods.

Table 1 – Results of the calculation of the NOF

L, mm	f_{an}, Hz	f_{exp}, Hz	f_{mod}, Hz
80	2327	1400…1430	1441
100	1535	1111…1250	1094
120	1090	714…769	725

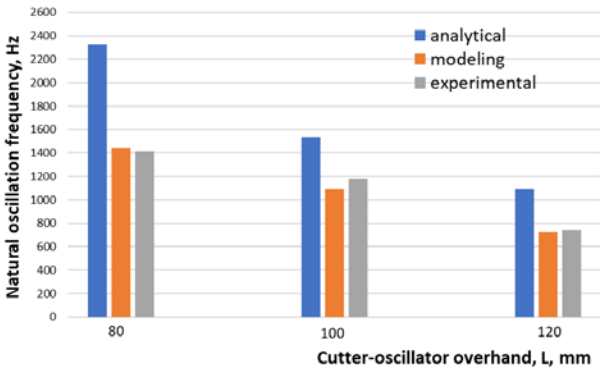

Figure 6. Results of calculating the NOF using different methods

The results demonstrate consistency between the experimental and modeling data. As the cutter-oscillator overhang increased from L = 80 mm to L = 120 mm, the oscillation frequency decreased by more than 2 times. The calculated values exceed the experimental values because the simplified oscillation frequency calculation used, based on the classical Euler-Bernoulli model, is well suited for thin, long bars. For bars with a short length relative to their diameter ($L/d \lesssim 10$), the effects of shear deformation and rotational inertia of the sections have a greater impact on the oscillation frequency, leading to a reduction (Timoshenko theory). The actual geometry of the cutter-oscillator and the rigidity of the actual mounting also influence the experimental values, which can often also reduce the frequency.

Table 2 and Fig. 7 show the results of calculating the angle of the DRD γ depending on the overhang of the cutter-oscillator, obtained by analytical method, experimentally and using computer modeling.

Table 2 – Results of calculating the angle of the NRP

Parameter	**Cutter-oscillator overhang**		
L, mm	80	100	120
	Analytical method		
γ,°	46,2	46,2	46,2
	Computer modeling method		
f_x, mm	0,01411	0,03135	0,05108
f_z, mm	0,01525	0,03395	0,05495
γ,°	42,8	42,7	42,9
	Experimental method		
f_x, mm	0,02…0,023	0,06…0,073	0,103…0,093
f_z, mm	0,026…0,033	0,06…0,08	0,1…0,096
γ,°	46,9	45,6	45,0

The obtained results demonstrated good consistency between the various calculation methods. As the tool overhang increases from L = 80 mm to L = 120 mm, the DRD angle remains virtually unchanged.

The computer simulation results are in good agreement with the experimental results, compared to the analytical method, indicating the potential for this calculation method to be effectively used to predict the parameters of cutter-oscillating of any design.

Conclusions

The dynamic characteristics of the turning process should be investigated using cutter-oscillators, which provide the ability to measure accurately both static and dynamic components of cutting forces. The work evaluated the parameters of the cutter-oscillator with two degrees of freedom using three methods – analytical, computer simulation, and experimental. The obtained results showed consistency between theoretical calculations and experimental data, which confirmed the correctness of the adopted models and assumptions.

A comparison of different approaches demonstrated that the choice of a specific method may depend on the available equipment, the required accuracy, and the ease of implementation in the conditions of a specific experiment. The analytical method provides a quick preliminary assessment, the experiment most fully takes into account real cutting conditions, and the computer simulation method combines high accuracy with the ability to vary system parameters without conducting a large number of physical tests.

The results of the study confirmed the effectiveness and feasibility of using the computer modeling method to determine the angle of the resulting cutting edge movement and the natural frequency of oscillations of the cutter-oscillator, which makes it a promising tool for further improving dynamic analysis systems for the turning process.

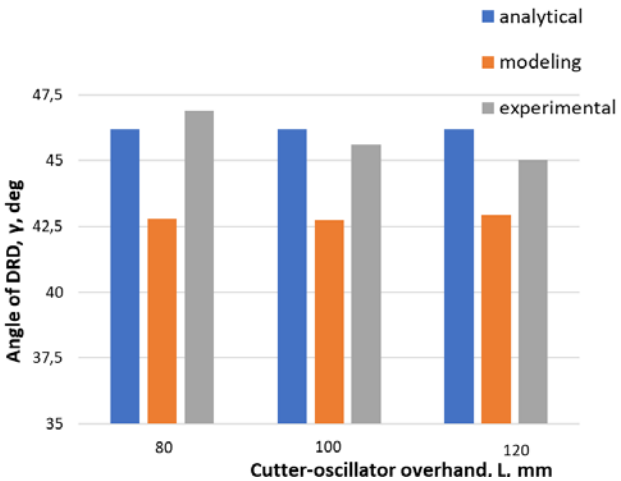

Figure 7. Results of calculating the angle - γ of DRD at L = 80, 100, 120 mm

References

1. Tobias, S. A., Fishwick, W. (1958). Theory of regenerative machine tool chatter. The engineer, 205(7),

DOI 10.15588/1607-6885-2025-4-5

199-203. https://doi.org/10.1115/1.4012609

2. Schmitz, T. L., Smith, K. S. (2019). Machining dynamics. Springer, 382. https://doi.org/10.1007/978-3-319-93707-6

3. Tlustý, J. (2000). Manufacturing processes and equipment. Prentice-Hall, 928.

4. Kudinov, V.A. (1967). Dynamics of machine tools. Mechanical engineering, 357.

5. Tryshyn, P. (2025). Theory of the Cutter-oscillators Design. Shock and Vibration. Shock and Vibration, 6679342. https://doi.org/10.1155/vib/6679342

6. Liao, Y., Ragai, I., Huang, Z., Kerner, S. (2021). Manufacturing process monitoring using time-frequency representation and transfer learning of deep neural Journal of Manufacturing Processes, 67, 231–248. https://doi.org/10.1016/j.jmapro.2021.05.046

7. Shaoke, W., Xiaohu, L., Wenjun, S., Junpeng, Y., Jun, H. (2020). Active chatter suppression for milling process with sliding mode control and electromagnetic actuator. Mechanical Systems and Signal Processing. 136, 106528. https://doi.org/10.1016/j.ymssp.2019.106528

8. Cao, L., Xiaoming, Zh., Tao,H., Xiaojian, Zh., Han, D. (2019). An adaptive chatter signal enhancement approach for early fault diagnosis in machining process. Procedia CIRP, 82, 308–313. https://doi.org/10.1016/j.procir.2019.03.273

9. Albertelli, P., Braghieri, L., Torta, M., Monno, M. (2019). Development of a generalized chatter detection methodology for variable speed machining. Mechanical Systems and Signal Processing, 123, 26–42. https://doi.org/10.1016/j.ymssp.2019.01.002

10. Li, K., He, S.,Liu, H., Mao, X., Li, B., Luo, B. (2020). Bayesian uncertainty quantification and propagation for prediction of milling stability lobe. Mechanical Systems and Signal Processing, 138, 106532. https://doi.org/10.1016/j.ymssp.2019.106532

11. Shrivastava, Y., Singh, B. A (2019). A comparative study of EMD and EEMD approaches for identifying chatter frequency in CNC turning. European Journal of Mechanics, 73, 381–393. https://doi.org/10.1016/j.euromechsol.2018.10.004

12. Pedro, J., Papandrea, E., Frigieri, P., Maia, P., Oliveira, G., Paiva, P. (2020). Surface roughness diagnosis in hard turning using acoustic signals and support vector machine: A PCA-based approach. Applied Acoustics, 159, 107102. https://doi.org/10.1016/j.apacoust.2019.107102

13. Taylor, C. M., Turner, S., Sims, N. D. (2010). Chatter, process damping, and chip segmentation in turning: A signal processing approach. Journal of Sound and Vibration, 329(23), 4922–4935. https://doi.org/10.1016/j.jsv.2010.05.025

14. Emami, M., Karimipour, A. (2021). Theoretical and experimental study of the chatter vibration in wet and MQL machining conditions in turning process. Precision Engineering, 72, 41–58. https://doi.org/10.1016/j.precisioneng.2021.04.006

15. Ma, H., Wu, J., Xiong, Z. (2020). Active chatter control in turning processes with input constraint. Int. J Adv. Manuf. Technol., 108, 3737–3751. https://doi.org/10.1007/s00170-020-05475-8

16. Nam, S., Hayasaka, T., Jung, H., Shamoto, E. (2020). Proposal of novel chatter stability indices of spindle speed variation based on its chatter growth characteristics. Precision Engineering, 62, 121–133. https://doi.org/10.1016/j.precisioneng.2019.11.018

17. Gök, F. S., Orak, M., Sofuoğlu, A. (2020). The effect of cutting tool material on chatter vibrations and statistical optimization in turning operations. Soft Computing, 24, 17319–17331. https://doi.org/10.1007/s00500-020-05022-3

18. Tryshyn P., Kozlova, O., Honchar N., Levchenko A. (2025). Modeling of processes in metallurgy and mechanical engineering. New materials and technologies in metallurgy and mechanical engineering, 3, 49–56. https://doi.org/10.15588/1607-6885-2025-3-7

19. Tryshyn P., Kozlova, O., Kazurova A. (2025). Research of natural frequencies of the cutter-oscillator during turning. New materials and technologies in metallurgy and mechanical engineering, 2, 75–83 https://doi.org/10.15588/1607-6885-2025-2-9

Received 17.11.2025
Accepted 03.12.2025

РОЗРАХУНОК ПАРАМЕТРІВ РІЗЦЯ-ОСЦИЛЯТОРА З ДВОМА СТУПЕНЯМИ СВОБОДИ

Павло Тришин — д-р філософії, доцент кафедри технології машинобудування Національного університету «Запорізька політехніка», м. Запоріжжя, Україна, *e-mail: trishin@zp.edu.ua*, ORCID: 0000-0002-3301-5124

Олена Козлова — канд. техн. наук, доцент, доцент кафедри технології машинобудування Національного університету «Запорізька політехніка», м. Запоріжжя, Україна, *e-mail: kozlova@zp.edu.ua*, ORCID: 0000-0002-3478-5913

Юрій Внуков — д-р техн. наук, професор, незалежний науковець, Каліфорнія, США, *e-mail: yprahar@ukr.net*, ORCID: 0000-0002-4297-9646

DOI 10.15588/1607-6885-2025-4-5

Мета. *Основною метою роботи є проведення комплексної оцінки параметрів різця-осцилятора з двома ступенями свободи за допомогою трьох методів: аналітичного, комп'ютерного та експериментального.*

Методи дослідження. *Аналітичний підхід включав визначення власної частоти коливань та кута результуючого переміщення різця-осцилятора з двома ступенями свободи. Для числового моделювання різця-осцилятора використовувалися програмні пакети SolidWorks та NX. Дослідження також проводилося експериментальним методом, в рамках якого реєструвалися осцилограми коливань різальної кромки. На їх основі визначався статичний вигин різця-осцилятора та частота його вільних коливань.*

Результати. *В результаті дослідження було встановлено, що використання різця-осцилятора є ефективним для визначення динамічних характеристик процесу точіння. Аналітичний метод дозволив отримати попередні оцінки частот власних коливань та кута напрямку результуючого переміщення. Комп'ютерне моделювання в SolidWorks та NX забезпечило підвищення точності розрахунків та дозволило варіювати параметри системи без додаткових експериментів. Експериментальні вимірювання, засновані на аналізі осцилограм коливань різальної кромки, підтвердили узгодженість теоретичних та модельних даних. Отримані результати доводять надійність прийнятих моделей та доцільність використання комп'ютерного моделювання для подальшого вдосконалення динамічного аналізу процесу точіння.*

Наукова новизна. *Наукова новизна роботи полягає в комплексному підході до дослідження динамічних характеристик різця-осцилятора з двома ступенями свободи, який поєднує аналітичні, числові та експериментальні методи оцінки.*

Практична цінність. *Практична цінність роботи полягає в розробці та обґрунтуванні методології оцінки динамічних параметрів різця-осцилятора з двома ступенями свободи, яка може бути використана під час проектування та налаштування інструментальних систем у процесі точіння. Використання комп'ютерного моделювання дозволяє швидко змінювати конструктивні параметри інструменту без проведення значної кількості експериментів, зменшуючи витрати часу та ресурсів. Отримані результати можуть бути впроваджені у виробничу практику та використані для вдосконалення систем динамічного керування в металообробці.*

Ключові слова: *осцилограма, автоколивання, кут результуючого переміщення, регенеративні автоколивання, власна частота коливань.*

Список літератури

1. Tobias S. A. Theory of regenerative machine tool chatter / S. A. Tobias, W. Fishwick // The engineer. – 1958.– 205(7). – P. 199–203. https://doi.org/10.1115/1.4012609

2. Schmitz T. L. Machining dynamics / T. L. Schmitz, K. S. Smith // Springer. 2019. – 382 p. https://doi.org/10.1007/978-3-319-93707-6

3. Tlustý J. Manufacturing processes and equipment / J. Tlustý. Prentice-Hall, 2000. – 928 p.

4. Кудинов В. А. Динамика станков / В. А. Кудинов. Машиностроение, 1967. – 357 с.

5. Tryshyn P. Theory of the Cutter-oscillators Design. Shock and Vibration / P. Tryshyn // Shock and Vibration. – 2025. – 6679342. https://doi.org/10.1155/vib/6679342

6. Manufacturing process monitoring using time-frequency representation and transfer learning of deep neural / Y. Liao, I. Ragai, Z. Huang, S. Kerner // Journal of Manufacturing Processes. – 2021. – 67. – P. 231–248. https://doi.org/10.1016/j.jmapro.2021.05.046

7. Active chatter suppression for milling process with sliding mode control and electromagnetic actuator / W. Shaoke, L. Xiaohu, S. Wenjun, Y. Junpeng, H. Jun // Mechanical Systems and Signal Processing. – 2020. – 136. – 106528. https://doi.org/10.1016/j.ymssp.2019.106528

8. An adaptive chatter signal enhancement approach for early fault diagnosis in machining process / L. Cao, Zh. Xiaoming, H. Tao, Zh. Xiaojian, D. Han // Procedia CIRP. – 2019. – 82. – P. 308–313. https://doi.org/10.1016/j.procir.2019.03.273

9. Development of a generalized chatter detection methodology for variable speed machining / P. Albertelli, L. Braghieri, M. Torta, M. Monno // Mechanical Systems and Signal Processing. – 2019. – 123. – P. 26–42. https://doi.org/10.1016/j.ymssp.2019.01.002

10. Bayesian uncertainty quantification and propagation for prediction of milling stability lobe / K., Li, S. He, H. Liu, X. Mao, B. Li, B. Luo // Mechanical Systems and Signal Processing . – 2020. – 138. – 106532. https://doi.org/10.1016/j.ymssp.2019.106532

11. A comparative study of EMD and EEMD approaches for identifying chatter frequency in CNC turning // Y. Shrivastava, B. Singh // European Journal of Mechanics. – 2019. – 73. – P. 381–393. https://doi.org/10.1016/j.euromechsol.2018.10.004

12. Surface roughness diagnosis in hard turning using acoustic signals and support vector machine: A PCA-based approach / J. Pedro, E. Papandrea, P. Frigieri, P. Maia, G.

DOI 10.15588/1607-6885-2025-4-5

Oliveira, P. Paiva // Applied Acoustics. – 2020. – 159. – 107102. https://doi.org/10.1016/j.apacoust.2019.107102

13. Taylor C. M. Chatter, process damping, and chip segmentation in turning: A signal processing approach / C. M Taylor, S. Turner, N. D. Sims // Journal of Sound and Vibration. – 2010. – 329 (23). – P. 4922–4935. https://doi.org/10.1016/j.jsv.2010.05.025

14. Theoretical and experimental study of the chatter vibration in wet and MQL machining conditions in turning process / M. Emami, A. Karimipour // Precision Engineering – 2021. – 72. – P. 41–58. https://doi.org/10.1016/j.precisioneng.2021.04.006

15. Ma H. Active chatter control in turning processes with input constraint / H. Ma, J. Wu, Z. Xiong // Int. J Adv. Manuf. Technol. – 2020. – 108. – P. 3737–3751. https://doi.org/10.1007/s00170-020-05475-8

16. Nam S. Proposal of novel chatter stability indices of spindle speed variation based on its chatter growth characteristics // S. Nam, T. Hayasaka, H. Jung, E. Shamoto // Precision Engineering. – 2020. – 62. – P. 121–133. https://doi.org/10.1016/j.precisioneng.2019.11.018

17. Gök F. The effect of cutting tool material on chatter vibrations and statistical optimization in turning operations / F. Gök, S. Orak, M. A. Sofuoğlu // Soft Computing. – 2020. – 24. – P. 17319–17331. https://doi.org/10.1007/s00500-020-05022-3

18. Modeling of processes in metallurgy and mechanical engineering / P. Tryshyn, O. Kozlova, N. Honchar, A. Levchenko // Нові матеріали і технології в металургії та машинобудуванні. – 2025.– №3 – С. 49-56 https://doi.org/10.15588/1607-6885-2025-3-7

19. Research of natural frequencies of the cutter-oscillator during turning. Tryshyn P., Kozlova, O., Kazurova A. // Нові матеріали і технології в металургії та машинобудуванні. – 2025. – №2 – С. 75–83 https://doi.org/10.15588/1607-6885-2025-2-9

DOI 10.15588/1607-6885-2025-4-5

UDC 537.621.4:620.17:53.082.7

Gennadii Snizhnoi — Doctor of Technical Sciences, Professor, Professor of the Department of Information Security and Nanoelectronics, National University Zaporizhzhia Polytechnic, Zaporizhzhia, Ukraine, *e-mail: snow@zp.edu.ua*, ORCID: 0000-0003-1452-0544

Volodymyr Sazhnev — Candidate of Technical Sciences, Associate Professor of the Department of Machines and Foundry Technology, National University Zaporizhzhia Polytechnic, Zaporizhzhia, Ukraine, *e-mail: sajhnev@zp.edu.ua*, ORCID: 0000-0002-2095-4958

Olga Vasylenko — Candidate of Technical Sciences, Associate Professor of the Department of Information Security and Nanoelectronics, National University Zaporizhzhia Polytechnic, Zaporizhzhia, Ukraine, *e-mail: drvasylenkoolga@gmail.com*, ORCID: 0000-0001-6535-3462

Denys Onyshchenko — Postgraduate student of the Department of Physical Materials Science, National University Zaporizhzhia Polytechnic, Zaporizhzhia, Ukraine, *e-mail: denys.onyshchenko@zp.edu.ua,* ORCID: 0009-0008-4766-7052

Kristina Snizhna — Student of the Faculty of Construction, Architecture and Design, National University Zaporizhzhia Polytechnic, Zaporizhzhia, Ukraine, *e-mail: snowshade66@gmail.com.* ORCID: 0009-0005-1230-0283

ON THE POSSIBILITY OF MONITORING SMALL DEFORMATIONS OF AUSTENITIC MEDIUM-MANGANESE STEELS USING THE MAGNETOMETRIC METHOD

Purpose. *Development of a methodology for monitoring small deformations of austenitic medium-manganese steels using magnetometric methods. Determination of the paramagnetic parameter of austenitic steel, the value of which uniquely correlates with the degree of plastic deformation by compression.*

Research methods. *Determination of the specific magnetic susceptibility of the sample, the resulting specific magnetic susceptibility of the paramagnetic austenite of the sample, and the paraprocess of α-phase of the sample were performed on an automated Faraday magnetometric balance. Uniaxial plastic compression deformation at room temperature was performed on a laboratory setup.*

Results. *Based on the results of experimental studies, the amounts of α'-martensite arising during plastic deformation by compression of 110G8L steel were determined. The resulting (paramagnetic austenite of the sample and the paraprocess of α-phase of the sample) specific magnetic susceptibility of deformed samples of 110G8L steel was experimentally found.*

Scientific novelty. *The idea of the relationship between the degree of deformation of austenitic steel and the value of the resulting specific magnetic susceptibility $\chi_{\propto}$ (paramagnetic austenite of the sample and the paraprocess of α-phase of the sample) is proposed and experimentally confirmed.*

Practical value. *During operation, parts made of austenitic medium-manganese steels are subjected to static or dynamic loads under abrasive wear conditions. This operating mode is accompanied by plastic deformation due to compression. The degree of deformation is an important parameter for assessing the reliability of the product. Determining the degree of deformation by measuring geometric dimensions is not always appropriate, as the configuration of cast parts can be quite complex. At the same time, magnetometric deformation monitoring, specifically the correlation found between the degree of plastic deformation due to compression and the resulting specific magnetic susceptibility, allows to determine the degree of deformation of a part of any configuration.*

Key words*: austenitic steel, magnetic susceptibility, deformation, strain-induced martensite.*

Introduction

Austenitic manganese steels possess a range of valuable properties, leading to their use as structural materials in the mining industry for crushing and grinding equipment [1-3]. Good ductility, strain-hardening ability, and high wear resistance are essential requirements for components operating under intense dynamic loads [4]. However, in practice, depending on the intended use of the components, the optimal chemical composition of the steel is determined, primarily the manganese and carbon content [5, 6]. For low-medium impact loads, metastable 110G8L steel is used [7].

DOI 10.15588/1607-6885-2025-4-6

This steel is metastable and undergoes a martensitic transformation $\gamma \rightarrow \alpha'$ (strain-induced α′-martensite) during plastic deformation. The martensitic transformation is significantly affected by the steel chemical composition, microstructure, deformation temperature, mechanical stress, particle irradiation, etc. This strain-induced transformation is one of the main factors affecting the wear resistance of steel during service [3, 4, 8]. Martensitic transformation provides additional hardening and thus increases the strength and uniform elongation of materials. Thus, the degree of austenite stability is a key factor in martensitic transformation and is related to its morphology, size, carbon and manganese content [9].

Analysis of research and publications

In [10], a magnetometric method was proposed to assess the structural changes occurring during deformation of austenitic steel. That is, changes in the atomic-crystalline structure of steel during operation are reflected in its magnetic state, which will be determined by the ratio of paramagnetic austenite (γ) and ferromagnetic α′-martensite.

Moreover, if the regularities of γ→α′ transformations at comparatively large plastic deformations have been studied quite well [11, 12], however experimental data at small plastic deformations are practically absent. This is due to the fact that when determining low contents of the α-phase, which arises during deformation, the magnetization of the paramagnetic austenitic matrix is not taken into account, which leads to large errors. For example, the relative error is over 1000% with an α-phase content within 0.005 %, 80 % at 0.1%, and only with an α-phase content of approximately 2.5...3.0% does the error reach ~3%.

Therefore, to study relatively small deformations of austenitic medium-manganese steels, at which a very low content of deformation-induced martensite arises, the integral physical method of α-phase identification [13] was used, which takes into account the magnetization of the paramagnetic austenitic matrix.

The purpose of the work

The aim of the study is to develop a method for monitoring small deformations of austenitic medium-manganese steels using the magnetometric method and to determine a parameter that can be used for estimation of the degree of plastic deformation by compression.

Research material and methodology

The object of the study was cast manganese steel 110G8L with the following chemical composition (wt.%): 1.14 C, 8.60 Mn, 0.66 Si, 0.04 S, 0.088 P, 0.10 Cr, 0.019 Al. Steel ingots of 100×100×200 mm^3 were obtained in induction crucible electric furnaces by the smelting method in the foundry laboratory of National University Zaporizhzhia Polytechnic. The steel was preliminarily annealed at a temperature of 1323 *K* (30 min.) and quenched in water. Then, samples with dimensions of ~3×3×1 mm^3 were cut out using a cold mechanical method. To remove surface damage, the samples were ground on abrasive powders and then polished to a mirror shine with diamond pastes and an electrochemical method. The degree of plastic uniaxial compression strain *D* at room temperature was calculated from the ratio of the thicknesses before (d_0) and after (d) deformation $D=(d-d_0)/d_0$. At all stages of sample preparation, special attention was paid to ensuring that the sample surface was not contaminated with any ferromagnetic impurities.

The very low content of ferromagnetic carbides and deformation α′-martensite in volume percent was determined by a sensitive magnetometric method, taking into account the magnetization of the paramagnetic austenite matrix [10]. The amount *P* of ferrophase was determined by the formula [10]:

$$P = \frac{\sigma_m}{\sigma_\alpha} \cdot 100\% = \frac{\left[\chi - (\chi_0 + \chi_p)\right] \cdot H}{\sigma_\alpha} \cdot 100\%, \quad (1)$$

where σ_m is the ferromagnetic component of the specific saturation magnetization of the sample; σ_α is the specific saturation magnetization of the α- phase; χ is the specific magnetic susceptibility of the sample; χ_∞ is the resulting specific magnetic susceptibility χ_0 of the paramagnetic austenite of the sample and the paraprocess χ_p of the α-phase of the sample: $\chi_\infty = \chi_0 + \chi_p$; *H* is the magnetic field strength.

From the experimental dependence curves $\chi = f(1/H)$, the values χ_∞ were found by extrapolation and the amount of ferromagnetic phase was determined in volume percent.

Research results

In the cast state, the structure of the steel that was investigated was an austenitic base with inclusions of large carbides. After quenching, 110G8L steel samples exhibited an austenitic structure with a small amount of residual carbides. Measurements of magnetic parameters and the amount of ferrophase were performed on the sample after each act of compression. Figure 1 shows typical experimental dependences of the specific magnetic susceptibility χ on the reciprocal magnetic field (1/*H*) of 110G8L steel at various degrees of relative compression strain *D*.

As can be seen from Figure 1, extending the straight lines with the ordinate axis ($H \rightarrow \infty$) yields χ_∞ values, and the resulting ferrophase content P_α in volume percent after each specimen deformation is calculated using the formula (1) (are listed in the Table 1). The presence of ferromagnetic carbides in the initial state at zero strain ($D = 0$) of 110G8L steel is confirmed by the slope of the experimental dependence of the specific magnetic susceptibility χ on the reciprocal of the magnetic field 1/*H* (Fig. 1a, line 1).

DOI 10.15588/1607-6885-2025-4-6

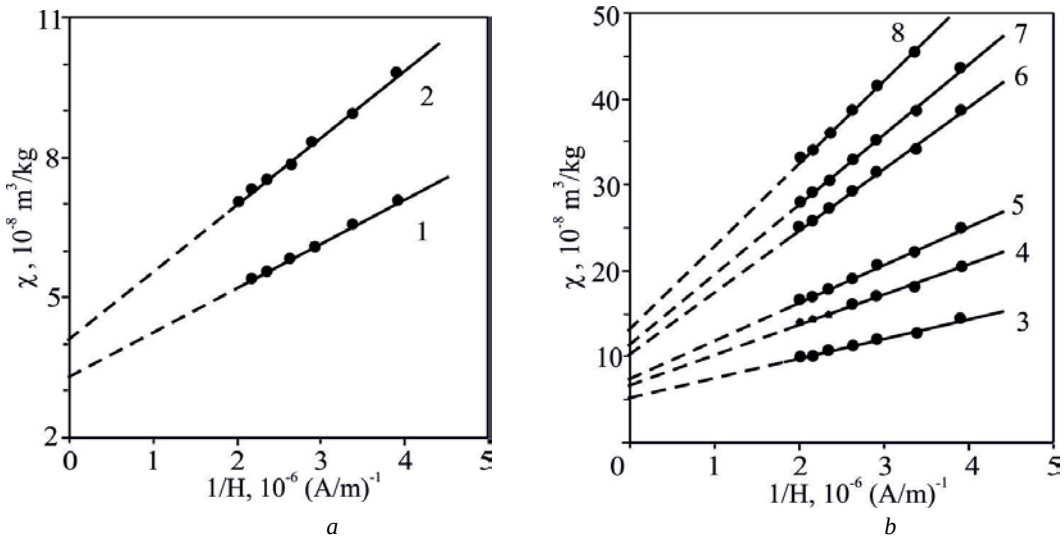

Figure 1. Dependence of the specific magnetic susceptibility χ of a 110G8L steel sample on the reciprocal value of the magnetic field strength *H* at different values of deformation *D*:
a – 1 – 0, 2 – 2.48 %; *b* – 3 – 5.82 %, 4 – 8.80 %, 5 – 10.57, 6 – 14.01 %, 7 – 16.49 %, 8 – 17.91 %

The determined amount of ferromagnetic carbides P_c = 0.071% are listed in the Table 1.

For different degrees of relative strain *D*, the total amount of ferromagnetic phases P_α was calculated. It was taken into account that $P_\alpha = P_c + P_{\alpha'}$, where P_c and $P_{\alpha'}$ are the amounts of ferromagnetic carbides and deformation-induced α′- martensite in volume percent (Table 1).

It is assumed that at a carbon content of less than 2 wt.% and moderate deformations, carbides do not form. If we assume that this amount of ferromagnetic carbides (0.071%) does not participate in the formation of deformation-induced α′-martensite and subtract it from the resulting amount of ferrophase P_α, we obtain the amount $P_{\alpha'}$ of deformation-induced α′- martensite.

Table 1 – Values of the total specific magnetic susceptibility of the sample χ (at $H = 2.55\ 10^5$ A/m), the resulting (paramagnetic austenite and paraprocess) specific magnetic susceptibility χ_∞ and the amount $P_{\alpha'}$ of α′-martensite deformation depending on the degree of deformation of the 110G8L steel sample

D, %	χ, 10^{-8} m^3/kg	χ_∞, 10^{-8} m^3/kg	P_α, %	$P_{\alpha'}$, %
0	7.03	3.29	0.071	0
2.48	9.75	4.10	0.107	0.036
5.82	1.41	5.23	0.168	0.098
8.80	2.04	6.58	0.261	0.190
10.57	2.46	7.39	0.326	0.255
14.01	3.84	1.03	0.532	0.461
16.49	4.33	1.13	0.604	0.533
17.91	5.05	1.40	0.689	0.619

Figure 2 shows the dependence of the formed amount $P_{\alpha'}$ of α′-martensite on the degree of compression deformation *D*. The relationship between these quantities is well described by a second-degree polynomial $P_{\alpha'} = 13.51 \cdot D^2 + 1.1621 \cdot D - 0.0044$ with a confidence level of $R^2 = 99.38$. Note that for 110G8L steel, deformation-induced α′-martensite is formed immediately after the first small compression events.

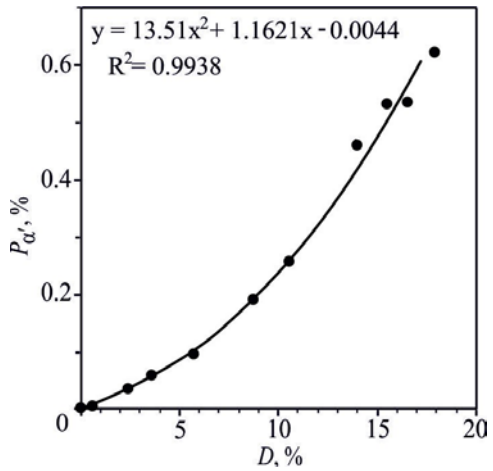

Figure 2. Dependence of the amount of $P_{\alpha'}$ of α′- martensite in 110G8L steel vs the degree *D* of compression deformation

The operation of 110G8L steel parts under dynamic loading is accompanied by plastic deformation. Determining the degree of deformation by measuring geometric dimensions is not always appropriate, as the configuration of cast parts can be quite complex. To create a deformation map of a part during operation, it is necessary to cut samples with dimensions of 1–5 mm from its structure at different points. The magnetic susceptibility of the sample is

DOI 10.15588/1607-6885-2025-4-6

then measured using a Faraday balance (or another magnetometric method) to obtain a dependence similar to Fig. 1. The resulting specific magnetic susceptibility χ_∞ is determined by extrapolation.

Using the correlation between the degree D of plastic deformation and the resulting specific magnetic susceptibility χ_∞ shown in Fig. 3, the degree of deformation of the 110G8L steel sample can be monitored.

Using the equation (the trend line) $D = 0.1288 \cdot ln(\chi_\infty) + 2.2172$ will allow us to determine the degree of plastic deformation by compression with a confidence level of $R^2 = 99.65\%$. For example, if the value of the resulting specific magnetic susceptibility $\chi_\infty = 6 \cdot 10^{-8}$ m^3/kg, then the degree of plastic deformation by compression of this sample (part fragment) $D = 0.075\%$ (Fig. 3).

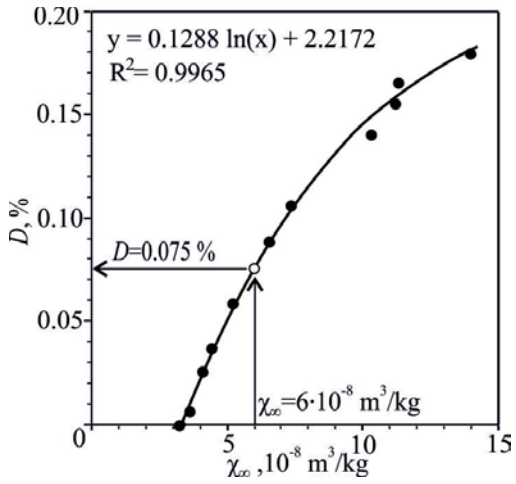

Figure 3. Determination (control) of small deformations (relative degree of compression) of 110G8L steel by the value of the resulting (paramagnetic austenite and paraprocess) specific magnetic susceptibility χ_∞

Discussion

Using χ_∞ as an evaluation criterion is more appropriate than using the specific magnetic susceptibility χ of the sample. This is because using the specific magnetic susceptibility of the sample χ requires an exact match to the magnetic field strength H, which may be technically incompatible for different magnetic setups (due to the different magnetic field strength ranges).

The resulting specific magnetic susceptibility χ_∞ can be determined from two χ values at different magnetic fields. Therefore, using the parameter χ_∞ is more appropriate.

Conclusions

1. To determine the actual, very low volume percent content of strain-induced α′-martensite, a method was used that takes into account the magnetic moment of paramagnetic austenite. Uniaxial compression of 110G8L steel produces strain-induced α′-martensite, the amount of which, depending on the degree of deformation, can be mathematically described by a second-degree polynomial.

2. A correlation was found between the magnitude of small deformations (relative compression ratio) of 110G8L steel and the resulting (paramagnetic austenite and paraprocess) specific magnetic susceptibility χ_∞. This correlation enables strain monitoring using magnetometric methods.

Reference

1. Yan, J., Zhou, M., Wu, H., Liang, X., Xing, Z., Li, H., Zhao L., Jiao, S., Jiang, Z. (2023). A Review of Key Factors Affecting the Wear Performance of Medium Manganese Steels. Metals, 13, 7, art. no. 1152. DOI: https://doi.org/10.3390/met13071152

2. Machado, P., Pereira, J., Penagos, J., Yonamine, T. and Sinatora, A. (2017). The effect of in-service work hardening and crystallographic orientation on the microscratch wear of Hadfield steel. Wear. 376–377, B, 1064-1073. DOI: https://doi.org/10.1016/j.wear.2016.12.057.

3. Sazhnev, V. M., Snizhnoi, H. (2023). The influence of technological parameters on the physical, mechanical and operational properties of wear-resistant austenitic high-mannan steel. Metallofizika i Noveishie Tekhnologii, 45, 4, 503-522. DOI: https://doi.org/10.15407/mfint.45.04.0503

4. Snizhnoi, H., Sazhnev, V., Snizhnoi, V., Mukhachev, A. (2024). Details of mining beneficiation equipment made of medium manganese wear-resistant steel. IOP Conference Series: Earth and Environmental Science, 1348, art. no. 012027. DOI: https://doi.org/10.1088/1755-1315/1348/1/012027

5. Gürol, U., Kurnaz, S. (2020). Effect of carbon and manganese content on the microstructure and mechanical properties of high manganese austenitic steel. Journal of Mining and Metallurgy, Section B: Metallurgy, 56, 2, 171-182. DOI: https://doi.org/10.2298/ JMMB191111009G

6. Bhattacharya, A., Biswal, S., Barik, R., Mahato, B., Ghosh M., Mitra, R., Chakrabarti, D. (2024). Comparative interplay of C and Mn on austenite stabilization and low temperature impact toughness of low C medium Mn steels. Materials Characterization, 208, art. no. 113658, ISSN 1044-5803, DOI: https://doi.org/10.1016/j.matchar.2024.113658.

7. Li, J., Xu, L., Feng, Y., Wu, S., Li ,W., Wang, Q., Zhang, P. and Tu, X. (2023). Hardening mechanism of high manganese steel during impact abrasive wear. Engineering Failure Analysis. 154, art. no. 107716. DOI: https://doi.org/10.1016/j.engfailanal.2023.107716.

8. Ding, F., Guo, Q., Hu, B. and Luo, H. (2022). Influence of softening annealing on microstructural heredity and mechanical properties of medium-Mn steel. Microstructures. 2. art. no. 2022009. DOI: https://doi.org/10.20517/microstructures.2022.01

9. Ol'shanetskii, V. E., Snezhnoi, G. V., Sazhnev, V. N. (2016). Structural and magnetic stability of austenite

DOI 10.15588/1607-6885-2025-4-6

in chromium-nickel and manganese steels with cold deformation. Metal science and heat treatment. 58, 5-6, 311-317. DOI: https://doi.org/10.1007/s11041-016-0009-5

10. Snizhnoi, G. and Rasshchupkyna, M. (2012). Magnetic state of the deformed austenite before and after martensite nucleation in austenitic stainless steels. Journal of Iron and Steel Research, International. 19 (6), 42–46. DOI: https://doi.org/10.1016/S1006-706X(12)60125-3

11. Ning, Guo, Renjie, Chen, Jiyuan, Liu, Bingtao Tang, Guangchun, Xiao. (2024). Plasticity enhancement and sustainable strain hardening mechanism of a novel developed medium Mn steel. Materials Letters. 364, art. no.136388, ISSN 0167-577X, DOI: https://doi.org/10.1016/j.matlet.2024.136388.

12. Snizhnoi, H. and Sazhnev, V. (2025). Classification of austenitic manganese steels for parts of mining and processing equipment. IOP Conference Series: Earth and Environmental Science. 1491, 1. art. no. 012028. DOI : https://doi.org/10.1088/1755-1315/1491/1/012028.

13. Ol'shanetskii, V. Snizhnoi, G., Vasylenko, O., Onyshchenko, D. (2025). Quality control of high-manganese steels by the paramagnetic state of austenite. New materials and technologies in metallurgy and mechanical engineering. 1, 24-29. DOI: https://doi.org/10.15588/1607-6885-2025-1-3.

Received 30.10.2025
Accepted 03.11.2025

ПРО МОЖЛИВІСТЬ КОНТРОЛЮ МАЛИХ ДЕФОРМАЦІЙ АУСТЕНІТНИХ СЕРЕДНЬОМАРГАНЦЕВИХ СТАЛЕЙ МАГНЕТОМЕТРИЧНИМ МЕТОДОМ

Геннадій Сніжной — д-р техн. наук, професор, професор кафедри інформаційної безпеки та наноелектроніки, Національний університет «Запорізька політехніка», Запоріжжя, Україна, *e-mail: snow@zp.edu.ua*, ORCID: 0000-0003-1452-0544

Володимир Сажнєв — канд. техн. наук, доцент, доцент кафедри машин та технології ливарного виробництва, Національний університет «Запорізька політехніка», Запоріжжя, Україна, *e-mail: sajhnev@zp.edu.ua*, ORCID: 0000-0002-2095-4958

Ольга Василенко — канд. техн. наук, доцент, доцент кафедри інформаційної безпеки та наноелектроніки, Національний університет «Запорізька політехніка», Запоріжжя, Україна, *e-mail: drvasylenkoolga@gmail.com*, ORCID: 0000-0001-6535-3462

Денис Онищенко — аспірант, Національний університет «Запорізька політехніка», Запоріжжя, Україна, *e-mail: denys.onyshchenko@zp.edu.ua*, ORCID: 0009-0008-4766-7052

Крістіна Сніжна — студентка факультету будівництва, архітектури та дизайну, Національний університет «Запорізька політехніка», Запоріжжя, Україна, *e-mail: snowshade66@gmail.com*, ORCID: 0009-0005-1230-0283

Мета роботи. *Розробка методики контролю малих деформацій аустенітних середньомарганцевих сталей магнетометричним методом. Визначення парамагнітного параметра аустенітної сталі, величина якого однозначно корелює зі ступенем пластичної деформації стисненням.*

Методи дослідження. *Визначення питомої магнетної сприйнятливості зразка, результуюча питома магнетна сприйнятливість парамагнітного аустеніту зразка та парапроцесу α -фази зразка здійснювалося на автоматизованих магнетометричних вагах Фарадея. Пластична одновісна деформація стиском при кімнатній температурі виконувалася на лабораторній установці.*

Отримані результати. *Виходячи з результатів експериментальних досліджень, визначено кількість α′-мартенситу, що виникає при пластичній деформації стисненням сталі 110Г8Л. Експериментально знайдено результуючу (парамагнетного аустеніту зразка та парапроцесу α′ -фази зразка) питому магнетна сприйнятливість деформованих зразків сталі 110Г8Л.*

Наукова новизна. *Запропоновано та експериментально підтверджено ідею про зв'язок між ступенем деформації аустенітної сталі та величиною результуючої питомої магнетної сприйнятливості χ_∞ (парамагнетного аустеніту зразка та парапроцесу α-фази зразка).*

Практична цінність. *Деталі з аустенітних середньомарганцевих сталях у процесі експлуатації зазнають статичного чи динамічного навантаження в умовах абразивного зносу. Такий режим роботи деталей супрово-*

DOI 10.15588/1607-6885-2025-4-6

джується пластичною деформацією стисненням. Ступінь деформації є важливим параметром оцінки надійності вироби. Визначення ступеня деформації виміром геометричних розмірів не завжди прийнятний, так як конфігурація литих деталей може бути досить складною. В той час, магнетометричний метод контролю деформації, а саме знайдена кореляція між ступенем пластичної деформації стисненням і величиною результуючої питомої магнетної сприйнятливості дозволить визначити ступінь деформацій деталі будь-якої конфігурації.

Ключові слова: *аустенітна сталь, магнетна сприйнятливість, деформація, мартенсит деформації.*

Список літератури

1. Review of Key Factors Affecting the Wear Performance of Medium Manganese Steels / Yan J., Zhou M., Wu H. et al. // Metals. – 2023. – Vol.13, 7, art. no. 1152. DOI: https://doi.org/10.3390/met13071152

2. The effect of in-service work hardening and crystallographic orientation on the micro-scratch wear of Hadfield steel / Machado P., Pereira J., Penagos J.,et al. // Wear. – 2017. – 376–377, B. – P. 1064–1073. DOI: https://doi.org/10.1016/j.wear.2016.12.057.

3. Сажнєв В. Вплив технологічних параметрів на фізико-механічні і експлуатаційні властивості зносостійкої аустенітної високоманганової криці / Сажнєв В., Сніжной Г. // Металофізика та новітні технології. – 2023. – Т. 45. – № 4. – С. 503–522.

4. Snizhnoi H. Details of mining beneficiation equipment made of medium manganese wear-resistant steel / Sazhnev V., Snizhnoi H., Mukhachev V. / IOP Conference Series: Earth and Environmental Science. – 2024. – 1348, art. no. 012027. DOI: https://doi.org/10.1088/1755-1315/1348/1/012027

5. Gürol U. Effect of carbon and manganese content on the microstructure and mechanical properties of high manganese austenitic steel / Gürol U., Kurnaz S. // Journal of Mining and Metallurgy, Section B: Metallurgy. – 2020. – Vol. 56, 2. – P. 171–182. DOI: https://doi.org/10.2298/JMMB191111009G

6. Comparative interplay of C and Mn on austenite stabilization and low temperature impact toughness of low C medium Mn steels / Bhattacharya A., Biswal S., Barik R. et al. // Materials Characterization. – 2024. – 208, art. no. 113658, ISSN 1044-5803, DOI: https://doi.org/10.1016/j.matchar.2024.113658.

7. Hardening mechanism of high manganese steel during impact abrasive wear / Li J., Xu L., Feng Y. Et al. // Engineering Failure Analysis. – 2023. – 154, art. no. 107716. DOI: https://doi.org/10.1016/j.engfailanal.2023.107716.

8. Influence of softening annealing on microstructural heredity and mechanical properties of medium-Mn steel / Ding F., Guo Q., Hu B. and Luo H. // Microstructures. – 2022. – 2. art. no. 2022009. DOI: https://doi.org/10.20517/microstructures.2022.01

9. Ol'shanetskii V. E. Structural and magnetic stability of austenite in chromium-nickel and manganese steels with cold deformation / Ol'shanetskii V. E., Snezhnoi G. V., Sazhnev V. N. // Metal science and heat treatment. – 2016. – Vol. 58, 5–6, – P. 311–317. DOI: https://doi.org/10.1007/s11041-016-0009-5

10.Snizhnoi G. Magnetic state of the deformed austenite before and after martensite nucleation in austenitic stainless steels / Snizhnoi G., Rasshchupkyna M. // Journal of Iron and Steel Research, International. – 2012. – Vol. 19 (6). – P. 42–46. DOI: https://doi.org/10.1016/S1006-706X(12)60125-3

11. Plasticity enhancement and sustainable strain hardening mechanism of a novel developed medium Mn steel / Ning Guo, Renjie Chen, Jiyuan Liu et al. // Materials Letters. – 2024. – 364, art. no.136388, ISSN 0167-577X, DOI: https://doi.org/10.1016/j.matlet.2024.136388.

12.Snizhnoi H. Classification of austenitic manganese steels for parts of mining and processing equipment / Snizhnoi H., Sazhnev V. // IOP Conference Series: Earth and Environmental Science. – 2025. – 1491, 1. art. no. 012028. DOI: https://doi.org/10.1088/1755-1315/1491/1/012028.

13. Quality control of high-manganese steels by the paramagnetic state of austenite / Ol'shanetskii V., Snizhnoi G., Sazhnev V. et al. // Нові матеріали і технології в металургії та машинобудуванні. – 2025. – № 1. – С. 24–29. DOI : https://doi.org/10.15588/1607-6885-2025-1-3.

DOI 10.15588/1607-6885-2025-4-6

UDC 621.45-253:534.1:621.753:620.179

Yurii Kovalenko — Leading Research Engineer, Strength Analysis Section, Experimental Testing Complex, JSC "Ivchenko-Progress", Zaporizhzhia, Ukraine, *e-mail: turbina_vd@icloud.com*, ORCID: 0009-0009-6572-1339

Oleksandr Zanin — Leading Engineer, JSC "Ivchenko-Progress", Zaporizhzhia, Ukraine, *e-mail: ZaninAE@zmdb.ua*, ORCID 0000-0003-0440-606X

Ruslan Shakalo — Head of the Compressor Department Group, JSC "Ivchenko-Progress", Zaporizhzhia, Ukraine, *e-mail: shakaloryu@ivchenko-progress.com*, ORCID: 0000-0003-4324-9191

Olha Lazarieva — Senior Teacher of the Department of Aircraft Engine Technology, National University Zaporizhzhia Polytechnic, Zaporizhzhia, Ukraine, *e-mail: lazarevaolha@gmail.com*, ORCID: 0000-0002-3417-6309

Yuriy Torba — Candidate of Technical Sciences, Deputy Director for Research, Head of the Experimental Testing Complex, JSC "Ivchenko-Progress", Zaporizhzhia, Ukraine, *e-mail: torba.yuriy@gmail.com*, ORCID: 0000-0001-8470-9049

Dmytro Pavlenko — Doctor of Technical Sciences, Professor, Head of the Department of Aircraft Engine Technology, National University Zaporizhzhia Polytechnic, Zaporizhzhia, Ukraine, *e-mail: dvp@zp.edu.ua*, ORCID: 0000-0001-6376-2879

INFLUENCE OF MANUFACTURING DEVIATIONS ON NATURAL FREQUENCIES AND MODE SHAPES OF TURBINE BLISKS

Purpose. *To establish the vibration characteristics of cast turbine blisks (monowheels) and to determine the influence of inevitable manufacturing deviations on their natural frequencies and mode shapes by combining computational and experimental methods.*

Research methods*. A comprehensive computational-experimental approach was applied. The computational part included finite element modal analysis of two models: 1) an idealized cyclically symmetric model with nominal geometry, and 2) a full model reproducing the actual geometry of the manufactured product, obtained via high-precision 3D scanning. The experimental part consisted of two stages: preliminary determination of the amplitude-frequency spectrum using the impact excitation method (tap testing) and a detailed investigation of natural frequencies and mode shapes using a piezo-probe.*

Results. *It was confirmed that manufacturing deviations cause significant changes in the dynamic behavior of the blisk. Frequency spectrum splitting and asymmetry of mode shapes, which are not predicted by nominal geometry models, were established. The computational model built from 3D scanning data demonstrates significantly better correlation with experimental data. A shift in nodal diameters relative to the axis of symmetry was experimentally recorded, which is direct proof of the influence of asymmetry caused by manufacturing tolerances.*

Scientific novelty. *For the first time, an approach to blisk quality control has been proposed and tested, based not on static geometric comparison, but on the analysis of the product's integral dynamic "signature" – its natural frequencies and mode shapes. It has been proven that the discrepancies between the nominal geometry calculation and the experiment are not an error, but a quantitative measure of the manufacturing deviations' impact on the structure's dynamic behavior.*

Practical value. *A rationale for a new non-destructive testing (NDT) method has been developed, which allows for objective decisions regarding the serviceability of both new and in-service blisks. The creation of a "reference" vibrational passport is proposed for the objective quality assessment of series-produced products and for diagnosing component degradation during inter-repair maintenance, thereby increasing the reliability and safety of aircraft engine operation.*

Key words: *turbine blisk, natural frequencies, mode shapes, manufacturing deviations, computational-experimental method, 3D scanning, non-destructive testing, blisk asymmetry.*

Introduction

The competitiveness of modern aircraft gas turbine engines is determined not only by the perfection of thermodynamic parameters, such as the compressor pressure ratio, turbine inlet gas temperature, and specific fuel consumption, but also by the economic efficiency of production. In the struggle for sales markets, the cost of the finished pro-

DOI 10.15588/1607-6885-2025-4-7

duct becomes critical, prompting designers to search for innovative technological solutions. One such solution is the transition from traditional assembled structures, consisting of a disk and separate blades, to compressor and turbine blisks (bladed disks) manufactured as a single unit [1, 2].

However, the introduction of blisks imposes a qualitatively new level of requirements for production and quality control. Unlike assembled structures, where a defective blade can be replaced, any deviation or defect in a blisk leads to the rejection of the entire product or the need for expensive repairs. This problem is particularly acute for turbine blisks manufactured by investment casting. Unlike compressor blisks, which are machined on high-precision five-axis machines, cast turbine blisks are characterized by significantly larger manufacturing deviations in geometric parameters.

Manufacturing deviations lead to blade mistuning within the blisk, which directly affects its dynamic characteristics and operability [3–5]. The presence of even slight asymmetry can cause splitting of the natural frequency spectrum, changes in mode shapes, and the appearance of resonant regimes in the operating speed range. This creates an increased risk of fatigue failures during operation [6], especially under conditions of unsteady thermal states and significant centrifugal loads.

Existing blisk quality control practices, which include frequency testing of individual blades, geometric dimension measurements, and defect detection, do not allow for a full assessment of the combined influence of manufacturing deviations on the dynamic behavior of the blisk as an integral oscillating system. Modern 3D scanning methods open new possibilities for detailed modeling of the actual geometry of products; however, there is a lack of methodology for a comprehensive computational-experimental study of the influence of manufacturing deviations on the natural frequencies and mode shapes of turbine blisks.

The purpose of this work is to establish the vibration features of turbine blisks and determine the influence of manufacturing deviations on their dynamic characteristics through the comprehensive application of 3D scanning, finite element modeling, and experimental studies. The developed methodology will increase the objectivity of blisk quality assessment and decision-making regarding their serviceability.

Literature Review

The problem of mistuning in turbomachinery blisks has attracted the attention of researchers for over five decades. Early fundamental works by Dye and Henry (1969) [7], El-Bayoumy and Srinivasan (1975) [8], and Ewins (1969, 1973, 1984) [9–11] laid the foundations for understanding the impact of discrepancies in the mechanical properties of blades on the dynamic behavior of bladed disks. It is well known that inevitable variations in mechanical properties from blade to blade, referred to as mistuning, can cause frequency splitting and a significant increase in forced vibration amplitudes compared to a tuned structure with identical blades [12].

At the current stage of research in this field, several main directions can be distinguished. It has been established that vibrations of blades with lower inter-blade coupling, such as torsional modes or modes with a large number of nodal diameters, are characterized by increased sensitivity to mistuning. The obtained results allowed for the formulation of criteria for evaluating the level of mode localization depending on the parameters of real high-pressure compressor systems.

Particular attention is paid to the issues of experimental identification of mistuning. One modern approach is the method of individual blade excitation using a miniature impact tool followed by non-contact vibration velocity measurement using laser Doppler vibrometry, which ensures high accuracy in determining frequency characteristics [13]. At the same time, traditional methods require collecting modal information from many points around the disk or isolating individual blades, which complicates experiments [14].

One of the key research directions is the application of intentional mistuning as an effective method for reducing vibration levels. It was found that this approach can weaken the coupling between blades by separating their frequencies. It is proposed that the mistuning pattern should be designed to primarily separate the frequencies of those blades that demonstrate the strongest coupling [15].

A separate group consists of works on the identification of mistuning caused by defects. In work [16], experimental and numerical studies of cracks in blades were conducted, comparing the natural frequencies and mode shapes of defective and defect-free blades to identify the main differences in modal behavior. These studies are important for understanding the mechanisms of the influence of operational damage on the dynamic characteristics of blisks.

A revolutionary aspect in production quality control has been the introduction of 3D scanning technologies. Modern 3D scanning systems, especially those using blue light, provide high-precision measurements, reducing errors and guaranteeing strict compliance with design specifications, significantly reducing inspection time compared to traditional methods. The implementation of automated 3D scanning systems has reduced the inspection time for blisks from 18 hours using a coordinate measuring machine (CMM) to approximately 45 minutes, achieving test repeatability below five microns [17]. Laser scanning can create CAD data for legacy blades that lack documentation, allowing for reverse engineering or data usage to review specific characteristics [18].

However, despite significant achievements in understanding the mistuning phenomenon and the development of geometry control methods, there is a substantial gap in the comprehensive computational-experimental study of the influence of manufacturing deviations on the natural frequencies and mode shapes of turbine blisks. Specifically, the following aspects remain unsolved:

- Methodology of comprehensive analysis: There is no systematic approach combining 3D scanning of actual

DOI 10.15588/1607-6885-2025-4-7

geometry, finite element modeling taking into account all manufacturing deviations, and experimental verification of results for turbine blisks.

- Specifics of cast blisks: Most studies focus on compressor blisks manufactured on high-precision machine tools. Turbine blisks made by casting are characterized by a fundamentally different nature and magnitude of deviations, the influence of which on dynamic characteristics has not been sufficiently studied.

- Criteria for serviceability assessment: Existing control methods (frequency control of individual blades, 3D scanning, defect detection) do not allow for an objective assessment of the serviceability of a blisk with manufacturing deviations based on a comprehensive analysis of its dynamic characteristics.

- Comparison of models of varying accuracy: There is a lack of systematic studies comparing the results of calculations for cyclically symmetric models with nominal geometry, full models with actual geometry, and experimental data to establish the degree of adequacy of simplified approaches

Purpose

To establish the vibration characteristics of cast turbine blisks (monowheels) and to determine the influence of inevitable manufacturing deviations on their natural frequencies and mode shapes by combining computational and experimental methods.

Materials and Methods

The object of the study is an aircraft gas turbine engine turbine blisk manufactured by investment casting with subsequent machining of the attachment points. The blisk consists of three main elements: the hub, the flange for attachment to the shaft, and the blade rim. A feature of this design is the inseparable connection of the disk and blades, which leads to increased requirements for production quality, as deviations in the geometric parameters of individual blades affect the dynamic characteristics of the entire blisk.

To conduct strength calculations and determine natural frequencies and mode shapes, a three-dimensional nominal model of the turbine blisk was built using the Unigraphics NX system. The model corresponds to the design geometry without taking into account manufacturing tolerances and deviations.

In the first stage of calculations, a cyclically symmetric model consisting of one sector with a single blade was used (Figure 1).

This model contained 845874 nodes and 319783 second-order elements. The application of the cyclically symmetric approach is based on the assumption of mathematically strict symmetry of the structure, where all blades have identical geometry. An isotropic material model was used for the calculations.

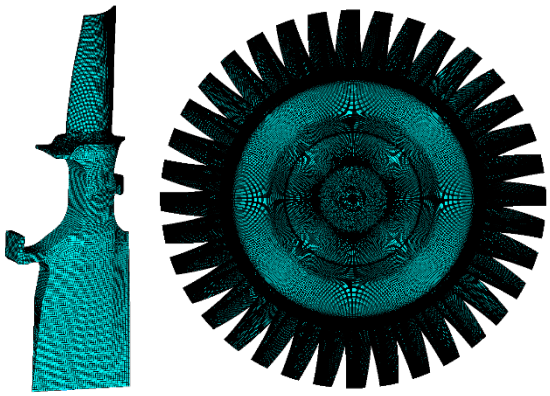

Figure 1. Cyclically symmetric computational model of the blisk

To determine the real influence of manufacturing deviations on the dynamic characteristics of the blisk, a 3D scan of the manufactured wheel was performed using an Atos Core 300 scanner. This control method allows obtaining complete geometric information about the part, including individual deviations of each blade. The obtained file in .stl format was loaded into the Unigraphics NX system, after which the actual geometry of the blisk was reconstructed. The modeled geometry corresponded to the actual one with an accuracy of up to 0.03 mm. The error is due to the shadowing effect of certain areas of the blisk during the scanning process, which makes complete scanning of some parts of the structure impossible.

Based on the 3D scanning data, a full computational model of the turbine wheel was built, which takes into account all manufacturing deviations, including geometric variations of each individual blade. The model contained 794784 nodes and 380485 second-order elements (Figure 2). Using the full model instead of the cyclically symmetric one allows accounting for the real asymmetry of the structure arising from the technological manufacturing process.

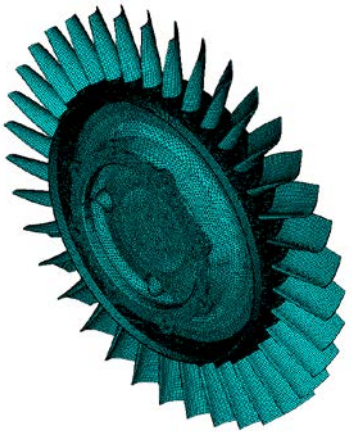

Figure 2. Full computational model of the turbine wheeli

DOI 10.15588/1607-6885-2025-4-7

The determination of natural frequencies and mode shapes was carried out using the finite element method. For both models (nominal cyclically symmetric and full with deviations), modal calculations were performed in a specified frequency range. The results were presented in the form of frequency diagrams and visualizations of mode shapes (Figures 3, 4).

In the first stage of experimental research, the amplitude-frequency spectrum of the investigated blisk was obtained. To ensure free vibration conditions, the blisk was suspended between two stands on a cable passed through one of the through-holes in the hub. This mounting scheme minimizes the influence of additional stiffnesses and added masses on the natural frequencies and mode shapes. Excitation of natural frequencies and mode shapes was performed by striking the web on the outlet side of the blisk with a rubber mallet. The signal was registered using a microphone located near the rim part on the outlet side. The signal was recorded on a portable computer with subsequent processing to obtain the frequency spectrum (Figure 5).

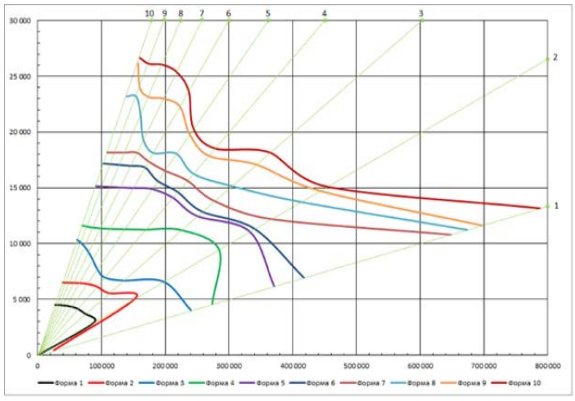

Figure 3. Resonance frequency diagram of the turbine wheel

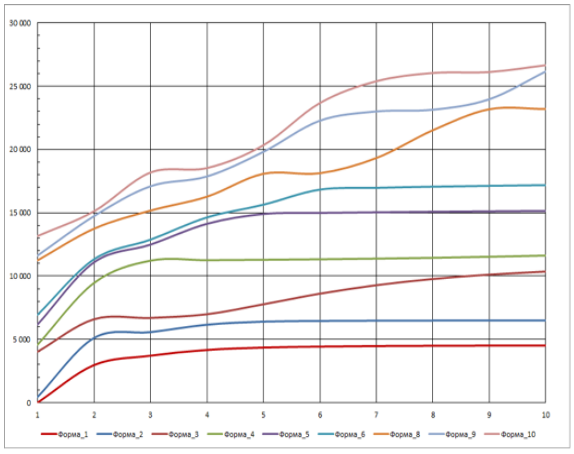

Figure 4. Frequency function of the turbine wheel

In the second stage, taking into account the previously obtained frequency spectrum, an equipment setup was assembled for a detailed study of natural frequencies and mode shapes. The setup included: a signal generator for excitation; oscilloscopes for signal visualization; a frequency counter for precise frequency measurement; a microphone for non-contact vibration registration; and a piezo-probe for contact investigation (Figure 6).

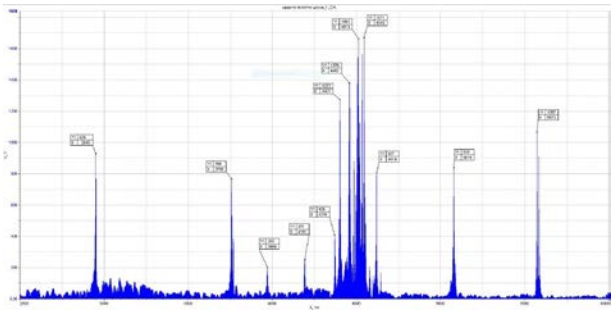

Figure 5. Spectrum of natural frequencies and mode shapes

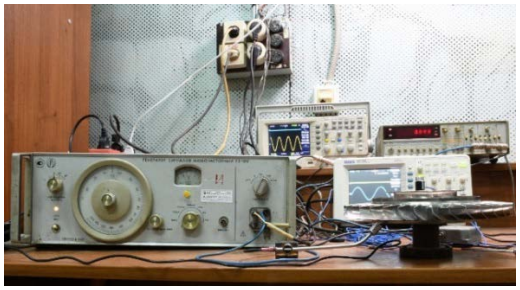

Figure 6. Equipment setup for investigating natural frequencies and mode shapes

The laboratory research methodology provided for the possibility of free movement of the blisk during resonant vibrations and the exclusion of the influence of any additional stiffnesses and added masses. The blisk was placed with its hub part under its own weight on a textolite stand. The use of a textolite stand ensured minimal influence on the intrinsic characteristics of the test object due to the low stiffness of the material.

Vibration excitation was provided by a vibration transducer installed through one of the holes in the flange using a threaded connection. The vibration transducer allowed ensuring a constant excitation level in the frequency range f = 0...25 kHz. For the research, a frequency range of f = 2500...6000 Hz was established, covering the most intense mode shapes of the blisk. The first six most intense mode shapes were investigated.

The determination of resonant mode shapes was carried out by a combined method using a piezo-probe and a microphone. The piezo-probe allowed determining local vibration amplitudes at various points of the structure, while the microphone provided non-contact registration of the overall vibration picture. The excitation frequency was smoothly changed manually using the generator in the selected range to tune precisely to the peaks of resonant vibration frequencies. To determine the vibration phases at resonant modes, the generator's output reference signal with a

DOI 10.15588/1607-6885-2025-4-7

constant sign was used. This allowed identifying the location of nodes and antinodes, as well as determining the number of nodal diameters and circles for each mode shape.

For a comprehensive assessment, a comparative analysis of the obtained results by three methods was applied:

- Calculation of the cyclically symmetric nominal model (ideal geometry).
- Calculation of the full model taking into account manufacturing deviations.
- Experimental determination of natural frequencies and mode shapes.

Comparisons were made both by natural frequency values and by the configuration of mode shapes , with special attention paid to the effect of blade spectrum splitting and general blisk asymmetry.

Results

The calculation of the cyclically symmetric nominal model allowed determining the natural frequencies for the idealized geometry. The results show a regular arrangement of natural frequencies corresponding to the mathematically strict symmetry of the structure. The following natural frequencies were determined: 2916 Hz, 3846 Hz, 4641 Hz, and 5127 Hz (Table 1).

Table 1 – Natural frequencies of the blisk

№	Nominal model of the blisk, Hz	Model of the manufactured blisk, Hz	Experiment, Hz
1	2916	2877	2940
2	3846	3847	3754
3			3966
4		4400	4192
5	4641	5011	5079
6	5127	5489	5574

For the nominal model, clear frequency separation without spectrum splitting is observed.

The calculation of the full model, built from 3D scanning results, revealed significant differences. The determined natural frequencies were: 2877 Hz, 3847 Hz, 4400 Hz, 5011 Hz, and 5489 Hz. The most significant features were:

-Natural frequency shift: both a decrease (for the first mode from 2916 Hz to 2877 Hz) and an increase (for the fifth mode from 4641 Hz to 5011 Hz, and for the sixth mode from 5127 Hz to 5489 Hz) in natural frequencies relative to nominal values were observed.

- Spectrum splitting: Mistuning of blades caused by individual geometric deviations is present. The frequencies of the working blades for the first bending mode are located in the range f = 4375...4651 Hz.
- Mode shape asymmetry: Arbitrary asymmetry in mode shapes was detected.
- Appearance of additional modes: The real geometry model revealed a mode at 4400 Hz (first bending, blade-disk), which was not observed in the nominal model.
- Nodal diameter shift: A shift in the location of nodal diameters relative to the center of the symmetry axis is characteristic, explained by the inevitable asymmetry of the blisk itself.

Experimental research registered six most intense mode shapes in the range f = 2500...6000 Hz. The measured frequencies were: 2940 Hz, 3754 Hz, 3966 Hz, 4192 Hz, 5079 Hz, and 5574 Hz. The grouping area of intense mode shapes of working blades (first bending mode) was observed in the range f = 4370...4619 Hz, which is consistent with the calculation data on spectrum splitting.

The following characteristic mode shapes were determined:

- Vibrations with two nodal diameters (fan-like vibrations) at 2940 Hz.
- Vibrations with one nodal circle at 3754, 3966, and 4192 Hz.
- Vibrations with multiple nodal diameters and a circle (complex shapes) at 5079 Hz and 5574 Hz.

A key feature is the passage of nodal diameters with a shift relative to the center of the symmetry axis, confirming the presence of inevitable asymmetry in the cast blisk. Qualitative analysis (Table 2) showed satisfactory correspondence between calculation and experiment.

Discrepancies are attributed to: neglecting real material properties (anisotropy), 3D scanning accuracy limits (0.03 mm), mass distribution differences due to crystallization, and FE model discretization . However, the model with manufacturing deviations showed significantly better convergence with experimental data than the nominal model.

Discussion

The results demonstrate a fundamental difference between the dynamic characteristics of cast turbine blisks and theoretical characteristics for nominal geometry. Unlike compressor blisks, the influence of manufacturing deviations on turbine blisks is significantly greater.

Analysis of existing control methods revealed their limitations. Traditional methods (frequency control of individual blades, 3D scanning) do not allow for an objective assessment of serviceability without analyzing natural frequencies and mode shapes. Based on the results, a methodology for comprehensive control is proposed:

- Creation of a reference sample: Using the spectrum of a blisk that meets technical. requirements and matches calculation data.
- Periodic sampling control: Comparing the spectrum signature of new blisks with the reference to detect systematic deviations.
- Serviceability assessment criteria: Decision-making based on geometry, spectrum, frequencies, and mode shapes (at least six intense forms).
- Control of in-service blisks: Applying this control during inter-resource repair for Auxiliary Power Units (APU), where harsh operating conditions (high static stress, thermal gradients) can lead to geometry changes.

This approach allows for a more objective decision on further operation without destructive testing. Future research should focus on automating the spectrum acquisition process and applying laser holography .

DOI 10.15588/1607-6885-2025-4-7

Table 2 – Experimentally determined and numerically calculated natural vibration mode shapes

	Nominal wheel model	Scanned wheel model	Experiment
1	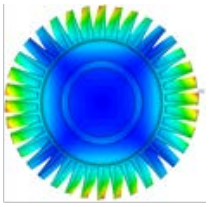 f =2916 Hz	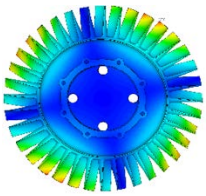 f =2877 Hz	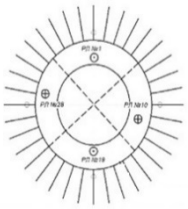 f =2940 Hz
2	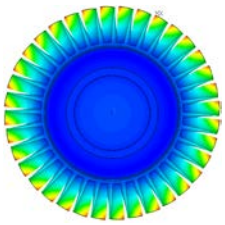 f =3846 Hz	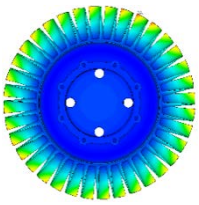 f =3847 Hz	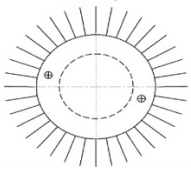 f =3754 Hz
3			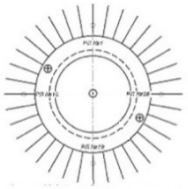 f =3966 Hz
4		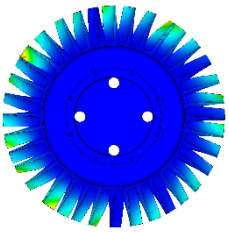 f =4400 Hz	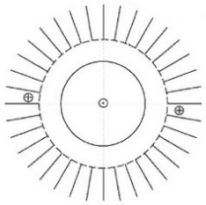 f =4192 Hz
5	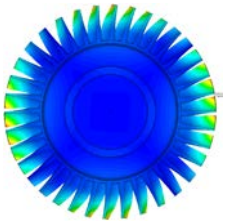 f =4641 Hz	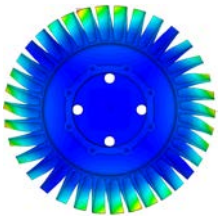 f =5011 Hz	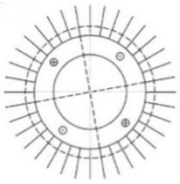 f =5079 Hz
6	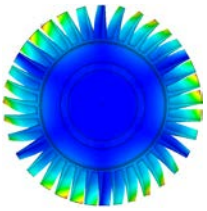 f =5127 Hz	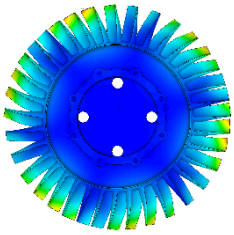 f =5489 Hz	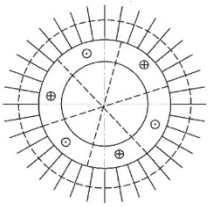 f =5574 Hz

DOI 10.15588/1607-6885-2025-4-7

Conclusions

Based on the conducted computational-experimental study of the influence of deviations allowed during the production of turbine blisks on their natural frequencies and mode shapes, the following has been established:

- Characteristic features of cast turbine blisk vibrations were identified, including mode shape asymmetry with a shift of nodal diameters relative to the axis of symmetry and the presence of complex mode shapes with multiple nodal diameters and circles.

- A significant influence of manufacturing deviations on dynamic characteristics was confirmed.

- The six most intense mode shapes of the investigated blisk were determined.

- The necessity of improving the turbine blisk quality control system was substantiated. It was found that traditional control methods (frequency control of individual blades, 3D scanning, defect detection, determination of actual geometric dimensions) without investigating natural frequencies and mode shapes and comparing calculation data with actual data do not allow for an objective assessment of the blisk's serviceability.

- A methodology for periodic control of turbine blisk natural frequencies and mode shapes using the spectrum and a computational-research method was proposed. The methodology involves: creating a reference sample with confirmed compliance with technical requirements and calculation data; periodic comparative analysis of the spectrum signature of sample blisks from a new batch; and decision-making on serviceability based on a set of criteria (geometry, spectrum, natural frequencies, and mode shapes) for at least six intense mode shapes .

- It is recommended to apply the proposed methodology for blisks in operation on auxiliary power units during inter-resource repair. This allows for a more objective decision on further operation without destructive testing, taking into account possible changes in geometry and stiffness under the influence of static, thermal, and dynamic loads.

Directions for further research have been defined:

- Automation of the process of acquiring amplitude-frequency characteristics and obtaining the natural frequency spectrum with the elimination of the human factor.

- Application of laser holography to determine mode shapes for a wide range of investigated parts.

- Investigation of the influence of material anisotropy and temperature fields on the dynamic characteristics of blisks.

- Study of changes in dynamic characteristics during long-term operation to establish criteria for residual life.

Practical significance of the work lies in the development of a methodology for comprehensive quality assessment of turbine blisks, which allows increasing the objectivity of decision-making regarding installation on an engine or rejection of both newly manufactured and in-service blisks. Ultimately, this increases the reliability of aircraft gas turbine engines and reduces the risks of operational failures.

References

1. Kulyk, M., Koveshnikov, M., Petruk, Y., Petruk, B., & Yakushenko, O. (2022). Thermocyclic fatigue and destruction of high pressure turbine blades in their critical sections. Transportation Research Procedia, 63, 2812–2819. https://doi.org/10.1016/j.trpro.2022.06.326

2. Zinkovskyi, A. P., Merkulov, V. M., Tokar, I. H., Derkach, O. L., & Shakalo, R. Yu. (2020). Doslidzhennia vplyvu hnuchkosti pera na optymalni umovy spriahennia polyts popарно bandazhovanykh lopatok turbin [Research of the influence of pen flexibility on optimum requirements linkings of shelves pairwise shrouded blades of turbines]. Aviatsiino-kosmichna tekhnika i tekhnolohiia [Aerospace Technic and Technology], 7(167), 41–49. https://doi.org/10.32620/aktt.2020.8.06

3. Singh, H. P., Rawat, A., Manral, A. R., Yadev, V., Singh, T., Saxena, P., & Chohan, J. S. (2020). Computational analysis of a gas turbine blade with different materials. Materials Today: Proceedings. https://doi.org/10.1016/j.matpr.2020.06.486

4. Pridorozhnyi, R. P., Zinkovskii, A. P., Merkulov, V. M., Sheremet'ev, A. V., & Shakalo, R. Yu. (2019). Calculation-and-experimental investigation on natural frequencies and oscillation modes of pairwise-shrouded cooled turbine blades. Strength of Materials, 51(6), 817–827. https://doi.org/10.1007/s11223-020-00133-6

5. Poursaeid, E., Aieneravaie, M., & Mohammadi, M. R. (2008). Failure analysis of a second stage blade in a gas turbine engine. Engineering Failure Analysis, 15(8), 1111–1129. https://doi.org/10.1016/j.engfailanal.2007.11.020

6. Shakalo, R. Yu., Pridorozhnyi, R. P., Yakushev, Yu. V., Merkulov, V. M., & Zinkovskii, A. P. (2019). Dempfirovanie kolebanii okhlazhdaemykh poparno bandazhirovannykh rabochikh lopatok turbin [Damping of vibrations of pairwise shrouded cooled turbine blades]. Aviatsionno-kosmicheskaia tekhnika I tekhnologiia [Aerospace Technic and Technology], *7*(159), 109–113. https://doi.org/10.32620/aktt.2019.7.15

7. Dye, R. C. F., & Henry, T. A. (1969). Vibration characteristics of bladed disc assemblies. *ASME Paper 69-VIBR-56*. American Society of Mechanical Engineers.

8. El-Bayoumy, L. E., & Srinivasan, A. V. (1975). Influence of mistuning on the vibration of turbomachine blades. AIAA Journal, 13(4), 460–464. https://doi.org/10.2514/3.49731

9. Ewins, D. J. (1969). The effects of detuning upon the forced vibrations of bladed disks. Journal of Sound and Vibration, 9(1), 65–79. https://doi.org/10.1016/0022-460X(69)90264-8

10. Ewins, D. J. (1973). Vibration characteristics of bladed disc assemblies. Journal of Mechanical Engineering Science, 15(3), 165–186. https://doi.org/10.1243/JMES_JOUR_1973_015_032_02

11. Ewins, D. J. (1984). Modal testing: Theory and practice. Research Studies Press.

DOI 10.15588/1607-6885-2025-4-7

12. Liao, H., Huang, X., & Li, J. (2010). Mistuning forced response characteristics analysis of mistuned bladed disks. Journal of Engineering for Gas Turbines and Power, 132(12), 122501. https://doi.org/10.1115/1.4001054

13. Judge, J. A., Pierre, C., & Ceccio, S. L. (2011). Method for detecting mistuning in integrally bladed rotors (U.S. Patent No. 8,024,137 B2). U.S. Patent and Trademark Office. https://patents.google.com/patent/US8024137B2/en

14. Imregun, M., & Ewins, D. J. (1991). A study of the experimental difficulties in the modal analysis of mistuned bladed disks. Proceedings of the 9th International Modal Analysis Conference (IMAC), 536–542.

15. Martel, C., & Sánchez-Álvarez, J. (2018). Intentional mistuning effect in the forced response of rotors with aerodynamic damping. Journal of Sound and Vibration, 433, 212–229. https://doi.org/10.1016/j.jsv.2018.07.020

16. Zhang, M., Valentin, D., Valero, C., Presas, A., Egusquiza, M., & Egusquiza, E. (2020). Experimental and numerical investigation on the influence of a large crack on the modal behaviour of a Kaplan turbine blade. Engineering Failure Analysis, 110, 104389. https://doi.org/10.1016/j.enfailanal.2020.104389

17. Jeschke, K. (2020, October 14). 3D scanners measure and inspect aerospace turbine blades. Vision Systems Design. https://www.vision-systems.com/cameras-accessories/article/14181385/3d-imaging-measures-and-inspects-aerospace-turbine-blades

18. Mohaghegh, K., Sadeghi, M. H., & Abdullah, A. (2007). Reverse engineering of turbine blades based on design intent. The International Journal of Advanced Manufacturing Technology, *32*(9–10), 1009–1020. https://doi.org/10.1007/s00170-006-0406-9

Received 28.11.2025
Accepted 09.12.2025

ВПЛИВ ВИРОБНИЧИХ ВІДХИЛЕНЬ НА ВЛАСНІ ЧАСТОТИ ТА ФОРМИ КОЛИВАНЬ МОНОКОЛІС ТУРБІН

Юрій Коваленко — провідний інженер-дослідник експериментально-випробувального комплексу, сектору міцності АТ «Івченко-Прогрес», м. Запоріжжя, Україна, *e-mail: turbina_vd@icloud.com*, ORCID: 0009-0009-6572-1339

Олександр Занін — провідний інженер, АТ «Івченко-Прогрес», м. Запоріжжя, Україна, *e-mail: ZaninAE@zmdb.ua*, ORCID: 0000-0003-0440-606X

Руслан Шакало — керівник групи відділу компресорів, АТ «Івченко-Прогрес», м. Запоріжжя, Україна, *e-mail: shakaloryu@ivchenko-progress.com*, ORCID : 0000-0003-4324-9191

Ольга Лазарєва — ст. викладач кафедри технології авіаційних двигунів Національного університету «Запорізька політехніка», м. Запоріжжя, Україна, *e-mail: lazarevaolha@gmail.com*, ORCID: 0000-0002-3417-6309

Юрій Торба — канд. техн. наук, заступник директора підприємства з наукової роботи, начальник експериментально-випробувального комплексу АТ «Івченко-Прогрес», м. Запоріжжя, Україна, *e-mail:torba.yuriy@gmail.com*, ORCID: 0000-0001-8470-9049

Дмитро Павленко — д-р техн. наук, професор, завідувач кафедри технології авіаційних двигунів Національного університету «Запорізька політехніка», м. Запоріжжя, Україна, *e-mail: dvp@zp.edu.ua*, ORCID: 0000-0001-6376-2879

Мета роботи. *Встановлення особливостей коливань моноколіс турбіни, виготовлених методом лиття, та визначення впливу неминучих виробничих відхилень на їхні власні частоти і форми коливань шляхом поєднання розрахункових та експериментальних методів.*

Методи дослідження. *Застосовано комплексний розрахунково-експериментальний підхід. Розрахункова частина включала модальний аналіз методом скінченних елементів двох моделей: 1) ідеалізованої циклосиметричної моделі з номінальною геометрією та 2) повної моделі, що відтворює фактичну геометрію виготовленого виробу, отриману за допомогою високоточного 3D-сканування. Експериментальна частина складалася з двох етапів: попереднього визначення амплітудно-частотного спектра методом ударного збудження та детального дослідження власних частот і форм коливань з використанням п'єзощупа.*

Отримані результати. *Підтверджено, що виробничі відхилення спричиняють значні зміни в динамічній поведінці моноколеса. Встановлено розшарування частотного спектра та асиметрію форм коливань, що не прогнозуються моделями з номінальною геометрією. Розрахункова модель, побудована за даними 3D-сканування, демонструє значно кращу кореляцію з експериментальними даними. Експериментально зафіксовано зміщення вузлових діаметрів відносно осі симетрії, що є прямим доказом впливу асиметрії, спричиненої виробничими допусками.*

DOI 10.15588/1607-6885-2025-4-7

Наукова новизна. *Вперше запропоновано та апробовано підхід до контролю якості моноколіс, що базується не на статичному геометричному порівнянні, а на аналізі інтегральної динамічної «сигнатури» виробу – його власних частот та форм коливань. Доведено, що розбіжності між розрахунком для номінальної геометрії та експериментом є не похибкою, а кількісною мірою впливу виробничих відхилень на динамічну поведінку конструкції.*

Практична цінність. *Розроблено обґрунтування для нового методу неруйнівного контролю, що дозволяє приймати об'єктивні рішення про придатність до експлуатації моноколіс. Запропоновано створення «еталонного» вібраційного паспорта для об'єктивної оцінки якості серійних виробів та діагностики деградації компонентів під час міжремонтного обслуговування, що підвищує надійність та безпеку експлуатації авіаційних двигунів.*

Ключові слова: *моноколесо турбіни, власні частоти, форми коливань, виробничі відхилення, розрахунково-експериментальний метод, 3D-сканування, неруйнівний контроль, асиметрія моноколеса.*

Список літератури

1. Thermocyclic fatigue and destruction of high pressure turbine blades in their critical sections / M. Kulyk, M. Koveshnikov, Y. Petruk M. // Transportation Research Procedia. – 2022. – Vol. 63. – P. 2812–2819. – https://doi.org/10.1016/j.trpro.2022.06.326

2. Дослідження впливу гнучкості пера на оптимальні умови спряження полиць попарно бандажованих лопаток турбін / А. П. Зіньковський, В. М. Меркулов, І. Г. Токарь та ін. // Авіаційно-космічна техніка і технологія. – 2020. – № 7 (167). – С. 41–49. – https://doi.org/10.32620/aktt.2020.8.06.

3. Computational analysis of a gas turbine blade with different materials / H. P. Singh, A. Rawat, A. R. Manral [et al.] // Materials Today: Proceedings. – 2020. – https://doi.org/10.1016/j.matpr.2020.06.486.

4. Pridorozhnyi, R. P., Zinkovskii, A. P., Merkulov, V. M., Sheremet'ev, A. V., & Shakalo, R. Yu. Calculation-and-Experimental Investigation on Natural Frequencies and Oscillation Modes of Pairwise-Shrouded Cooled Turbine Blades [Electronic resource]. – Strength of Materials. – 2019. – Vol. 51, No. 6. – P. 817–827. – https://doi.org/10.1007/s11223-020-00133-6

5. Poursaeid, E., Aieneravaie, M., & Mohammadi, M. R. Failure analysis of a second stage blade in a gas turbine engine [Electronic resource] // Engineering Failure Analysis. – 2008. – Vol. 15. – P. 1111–1129. – https://doi.org/10.1016/j.engfailanal.2007.11.020.

6.. Демпфирование колебаний охлаждаемых попарно бандажированных рабочих лопаток турбин [Електронний ресурс] / Шакало, Р. Ю., Придорожный, Р. П., Якушев, Ю. В. та ін. // Авиационно-космическая техника и технология. – 2019. – № 7 (159). – С. 109–113. – DOI: https://doi.org/10.32620/aktt.2019.7.15

7. Dye R. C. F. Vibration characteristics of bladed disc assemblies / R. C. F. Dye, T. A. Henry // ASME paper 69-VIBR-56. – 1969.

8. El-Bayoumy L. E. Influence of mistuning on the vibration of turbomachine blades / L. E. El-Bayoumy, A. V. Srinivasan // AIAA Journal. – 1975. – Vol. 13, № 4. – P. 460–464. – https://doi.org/10.2514/3.49731.

9. Ewins D. J. The effects of detuning upon the forced vibrations of bladed disks / D. J. Ewins // Journal of Sound and Vibration. – 1969. – Vol. 9, № 1. – P. 65–79. – DOI: https://doi.org/10.1016/0022-460X(69)90264-8.

10. Ewins D. J. Vibration characteristics of bladed disc assemblies / D. J. Ewins // Journal of Mechanical Engineering Science. – 1973. – Vol. 15, № 3. – P. 165–186. – DOI: https://doi.org/10.1243/JMES_JOUR_1973_015_032_02

11. Ewins D. J. Modal testing: theory and practice / D. J. Ewins. – Letchworth : Research Studies Press, 1984. – 269 p.

12. Liao H. Mistuning forced response characteristics analysis of mistuned bladed disks [Електронний ресурс] / Liao H. // Journal of Engineering for Gas Turbines and Power. – 2010. – Vol. 132. – Paper 122501. – DOI: 10.1115/1.4001054. – Режим доступу: https://doi.org/10.1115/1.4001054

13. Method for detecting mistuning in integrally bladed rotors [Електронний ресурс] : пат. US 8024137 B2 / United States Patent and Trademark Office. – Опубл. 20 вер. 2011 р. – Режим доступу: https://patents.google.com/patent/US8024137B2/en

14. Imregun M. A study of the experimental difficulties in the modal analysis of mistuned bladed disks / M. Imregun, D. J. Ewins // Proceedings of the 9th International Modal Analysis Conference (IMAC). – 1991.

15. Martel C. Intentional mistuning effect in the forced response of rotors with aerodynamic damping / C. Martel, J. Sánchez-Álvarez // Journal of Sound and Vibration. – 2018. – Vol. 433. – P. 212–229. – DOI: https://doi.org/10.1016/j.jsv.2018.07.020

16. Experimental and numerical investigation on the influence of a large crack on the modal behaviour of a Kaplan turbine blade [Електронний ресурс] / Zhang M., Valentin D., Valero C. et al. // Engineering Failure Analysis. – 2020. – Vol. 110. – P. 104389. – DOI: https://doi.org/10.1016/j.engfailanal.2020.104389

17. 3D scanners measure and inspect aerospace turbine blades [Electronic resource] // Vision Systems Design. – 2020. – 14 October. – Access mode: https://www.vision-systems.com/cameras-accessories/article/14181385/3d-imaging-measures-and-inspects-aerospace-turbine-blades. – (date of access: 30.10.2025).

18. Mohaghegh K. Reverse engineering of turbine blades based on design intent / K. Mohaghegh, M. H. Sadeghi, A. Abdullah // The International Journal of Advanced Manufacturing Technology. – 2007. – Vol. 32. – P. 1009–1020. – DOI: 10.1007/s00170-006-0406-9.

DOI 10.15588/1607-6885-2025-4-7

p-ISSN 1607-6885 New materials and technologies in metallurgy and mechanical engineering. 2025/4
e-ISSN 2786-7358 New materials and technologies in metallurgy and mechanical engineering. 2025/4

UDC 621.73

Anton Matiukhin — Candidate of Technical Sciences, Associate Professor, Head of the Department of Metal Forming of National University Zaporizhzhia Polytechnic, Zaporizhzhia, Ukraine, *e-mail: matiukhin85@gmail.com*, ORCID: 0000-0002-2261-0577

Volodymyr Tovstiuchenko — Postgraduate student, Department of Metal Forming of National University Zaporizhzhia Polytechnic, Zaporizhzhia, Ukraine, *e-mail: azazelo1315@gmail.com*, ORCID: 0009-0008-0353-8101

STUDY OF THE FORGING PROCESS OF HIGHLY ALLOYED STEEL FORGINGS ON HYDRAULIC PRESSES

Purpose. *To conduct a chronometric study of the forging process of high-alloy steel grades on hydraulic presses to identify ways of applying resource-saving technologies, which will ultimately reduce the cost of manufacturing products and increase the competitiveness of domestic manufacturers of forged products.*

Research methods. *To achieve the set goal and objectives of the study, a set of complementary scientific methods was used to obtain empirical data and analyse it. In particular, the main empirical method used in the study was chronometry, namely, the accurate measurement and recording of the duration of individual technological operations in the free forging process. To form a complete picture of the technological process and compare actual data with planned data, an analysis of technological documentation was used.*

Data processing and analysis methods made it possible to calculate the time norm fulfilment coefficient. This set of methods made it possible not only to quantitatively assess the time spent, but also to qualitatively analyse the organisation and technology of the forging process in order to develop recommendations for its optimisation.

Results. *The timing of all components of the forging technological process and subsequent analysis revealed the trends in improving the forging process of high-alloy steel grades.*

Scientific novelty. *The step-by-step timing of the forging process was accompanied by an analysis of the characteristics of the technological process, the equipment used, the mass of the ingot and the mass of the finished forging, and the working records made by the technological personnel in the forging cards after the process was completed.*

Practical value. *The results of the chronometric study of the existing technological process of forging large ingots on hydraulic presses make it possible to identify and apply technical solutions to reduce resource costs.*

Keywords: *stress-strain state of metal, highly alloyed steel, forging, hydraulic press, operation timing, resource-saving technologies.*

Introduction

Forging is the basis for the automotive, aviation and aerospace industries, shipbuilding, mechanical engineering, electrical engineering and energy.

The development of resource-saving technologies for forging expensive high-alloy steel grades can only be implemented if as many factors as possible that affect the quality of the finished product are taken into account. These factors include shape, kinematic, temperature and structural factors.

Synergistic consideration of the impact of the factors discussed will ensure a high level of technological preparation of the forging process, the quality of forgings, and their competitiveness in terms of cost.

Since consumption rates at domestic metallurgical enterprises are 15–20% higher than those of foreign manufacturers, metallurgical enterprises that pay due attention to improving production will be more competitive. Bringing forging processes at domestic enterprises up to international standards is an important and pressing task today.

Therefore, the main focus of this work is to analyse possible ways of implementing the latest approaches in the organisation and execution of heavy forging of alloyed stainless steels and heat-resistant alloys.

Analysis of research and publications

The work [1] considers the main methods of improving the quality of forging highly alloyed steels and alloys on hydraulic presses. In particular, the dependence of the stress-strain state of metal on the influence of various technological factors of the forging process was shown. The main factors include the shape of the tool (flat working surface, flat and with a bevelled surface, combined anvils, symmetrical and asymmetrical, profiled anvils, cut-out, convex, radial, stepped, anvils with crossed working surfaces, etc.) and the shape of the ingot (square, round cross-section, three-beam, multi-faceted forging, slab ingot, flat ingot, shortened, non-profit and others, round cross-section billets, for example, obtained in continuous casting machines).

The next factor affecting the distribution of the stress-strain state of metal is the kinematic factor, namely the

DOI 10.15588/1607-6885-2025-4-8

kinematics of the tool's impact on the blank. And, of course, the temperature factor, which has the most significant impact on the distribution of the stress-strain state of metal.

In turn, work [2] described the main stages of designing resource-saving technologies for deforming ingots on hydraulic presses and indicated the main factors affecting the plasticity of highly alloyed steels during forging. These include:

- the presence of obstacles to sliding: restriction or inhibition of intergranular or intragranular deformation;
- high alloying of the solid solution without the formation of an excess strengthening phase;
- supersaturation of the solid solution and the formation of a dispersed strengthening phase inside the grains and at their boundaries;
- formation of a network, a brittle excess component (more often eutectic) around relatively plastic grains of the main structure of the solid solution;
- presence of two or more structural components with different properties;
- weakening of intergranular bonds at hot plastic deformation temperatures.

When developing a resource-saving technological process, it is advisable to take into account another aspect related to the design and operation of hydraulic presses. The accuracy of the obtained cross-sectional dimensions of the forging is influenced both by the characteristics of the hydraulic press itself (rigidity of the structure, inertia of the hydraulic drive) and by the resistance of the blank to deformation, which, in turn, depends on the duration of the strengthening and weakening processes in the metal of the blank [3].

Purpose of the work

The aim of the work is to conduct a chronometric study of the forging process of highly alloyed steel grades on hydraulic presses in order to identify ways of applying resource-saving technologies, which will ultimately make it possible to reduce the cost of manufacturing products and increase the competitiveness of domestic manufacturers of forged products.

Material and research methods

The study of the manufacture of large forgings from highly alloyed steels by free forging was carried out at PJSC "DNIPROSPECSTAL" in the forging and pressing shop (hereinafter referred to as FPS). For forging, ingots with a square cross-section and a trapezoidal longitudinal cross-section weighing 7.15 t, 6.5 t, 4.8 t, 4.5 (4.52) t, 3.8 t (3.77 t) and 3.6 tons, obtained in electric arc furnaces of steel-making shops SPC-2, SPC-3, and cylindrical ingots weighing 0.9-6 tons, obtained in steel-making shop SPC-5, by the method of electroslag remelting (ESR) and vacuum arc remelting (VAR). The ingots are delivered to the blacksmith press shop in a hot and cold state.

PJSC “DNIPROSPECSTAL” produces metal products of 1,200 profile sizes from more than 800 steel grades. For optimal technological preparation of production, all steel grades are classified into 20 steel grade groups (hereinafter referred to as SGG).

To solve the research tasks set, the technological processes of production of cylindrical forged bars (forgings) from steel grades belonging to five SGG, which are in high demand among consumers and represent the technological capabilities of the enterprise, are considered (Table 1). Nickel-alloyed structural steels and alloyed tool steels are smelted in steelmaking shop No. 3, while stainless steels are produced in steelmaking shop No. 2. Steel is cast in moulds of various weights. Therefore, for the sake of accuracy in comparison and analysis of the forging process, one ingot is taken as the unit of measurement.

Table 1 – Steel grades considered in the technological process

SGG	Names of steel grade groups	Steel grade	Steel melting shop
22	Alloy structural steel	40Х2Н2МА	SPC-3
32	Alloy tool steel	4Х5МФ1С	SPTS-3
		Х12МФ	
		9Г2Ф	
40	Stainless steel	14Х17Н2	SPTS-2
40Н	Ni-alloyed stainless steel	12Х18Н10Т	SPTS-2
		03Х17Н12М2У	
49Н	Heat-resistant alloyed steel Ni	ХН77ТЮР ВД	SPTS-5

At SPC-2, steel is smelted in an open electric arc furnace with a capacity of 50 tonnes, followed by blowing in an argon-oxygen converter with a capacity of 60 tonnes and processing in a ladle furnace. This process allows low-carbon corrosion-resistant stainless steel to be obtained. The shop is equipped with an 8-tonne induction furnace for the production of heat-resistant steels and special alloys.

At SPC-3, high-quality steel is obtained by processing semi-finished products in a Daniel ladle furnace, followed by vacuuming the melt in a Mannesmann Demag vacuum furnace.

SPC-5 is equipped with ESR and VDP furnaces of various capacities, which allow the production of billets weighing 0.9-6.0 tonnes and sheet billets weighing 9.3-20.0 tonnes. ESR technology ensures the production of steel and special alloys used in the most critical industries: aviation, defence, as well as thermal and nuclear power.

Two hydraulic forging presses with a nominal force of 32 and 60 MN are used for direct forging.

Seven furnaces with a stationary hearth with an area of 13.5 m^2 and a maximum charge weight of 20.2 tonnes are used to heat the ingots before forging. five furnaces

DOI 10.15588/1607-6885-2025-4-8

with a roll-out hearth with an area of 18.6 m^2 and a maximum load capacity of 55 tonnes; two furnaces with a roll-out hearth with an area of 13.9 m^2 and a maximum load capacity of 44 tonnes. On these furnaces, a single TPP (S) model thermocouple with a length of 1.0 m is installed vertically in the centre of the vault (arch) of each furnace to control the heating temperature of the ingots before forging.

Research results

The study of the peculiarities of the forging process of high-alloy steels, shown in Table 1, was carried out using the example of manufacturing due to specific customer orders. For this purpose, the process of several order items was timed step by step, the applied technological charts for the manufacture of forgings in the KPC from the above-mentioned steel grades were reviewed with a description of the technological process, the equipment used, the weight of the ingot and the weight of the finished forging, and the work records made by the technological personnel in the forging charts after the completed process were analysed.

The consolidated data of the analysis of the optimality of the technological process are grouped in Table 2 and discussed in more detail in the following sections for each steel grade.

Eight grades from five steel groups were considered. For timing from current production, steel 03Х17Н12М2У with a billet weight of 6.8 t and a forging size of Ø365±5 and steel 9Г2Ф with a billet weight of 3.77 t and a forging size of Ø225±5 were selected, in terms of the parameters of the forging process, which could be grouped with other steels. Thus, the production of bars from 40Х2Н2МА and 12Х18Н10Т steels in terms of the sequence of operations was considered analogous to the technological process of forging cylindrical bars from 03Х17Н12М2У steel, and the production of bars from 4Х5МФ1С, Х12МФ, 14Х17Н2 steels was considered analogous to the forging of bars from 9Г2Ф steels based on the same factors. The features of the forging process of heat-resistant Ni- based alloy ХН77ТЮР ВД were considered based on the data provided by the author[3].

The step-by-step timing of the forging process for 03Х17Н12М2У and 9Г2Ф steel forgings at the blacksmith press shop PJSC “DNIPROSPECSTAL” was accompanied by an analysis of the features of the technological process, the upplied equipment, the weight of the ingot and the weight of the finished forging, and the work records made by the technological personnel in the forging cards after the process was completed . The main results of the research are presented below.

The forging chart was reviewed and the technological process of forging a Ø225+5 mm bar (forging size) to a finished size of Ø202+3 mm of 9Г2Ф steel from a 3.77 t ingot was analysed. The ingot has a square cross-section and a trapezoidal longitudinal cross-section with the following dimensions: 590x590 mm top, 480x480 mm bottom, length to the profitable part 1680 mm.

The results of the technological process analysis are given in Table 2, and the forging diagram is shown in Figure 1.

The data on the yield of Ø225+5 mm bars suitable for forging from 4Х5МФ1С, Х12МФ, and 9Г2Ф tool alloy steels are calculated and presented in Table 2.

A significant part of this time, about 23%, was spent on transport operations, namely transporting the ingot from the heating furnace to the press and back in seven trips, turning it over to forge the second half of the ingot, and preparing the workpiece.

The actual forging accounted for 77% of the forging complex's operating time, which in turn was divided between the main forging operations, when the press was operating at maximum load (sedimentation and drawing operations), i.e. the equipment was used with maximum efficiency, and the time of auxiliary operations (smoothing, ticket cutting, corner filling), when only 3-4% of the press capacity was used.

In the last finishing pass, auxiliary operations and, accordingly, unproductive use of the press capacity accounted for about 40% of the total forging time.

The forging diagram (Fig. 1) shows the technological stages of obtaining a finished forged bar:

- heating of the ingot;
- forging the trunnion;
- depositing the ingot on the sedimentation plate;
- drawing to an intermediate size of 450 mm square with cutting of the leading edge (it is possible to transfer the cutting to the trailing cut);
- drawing to an intermediate size of 350 x mm;
- cutting the workpiece into 2 parts, identified as bar A and bar H, taking into account their location relative to the head of the ingot;
- drawing rod A and rod H separately to an intermediate size of 280 mm square;
- final removal – forging to a finished forging size of 235 mm.

The yield of usable billets from 4Х5МФ1С, Х12МФ, and 14Х17Н2 steel ingots, the forging of which was considered analogous to the forging of 9Г2Ф steel bars, and actually from 9Г2Ф steel ingots, ranges from 58 to 65 %.

DOI 10.15588/1607-6885-2025-4-8

Table 2 – Technological process of forging a Ø230 mm bar (forging size) to a finished size of Ø202+3 mm of 9G2F steel from a 3.77 t ingot

No	Content of technological actions	No. of technological operation	Name of technological operation / forging start temperature Tn, forging end temperature Tk, ºC	Time of execution		
				of the main forging operation, s	auxiliary forging operation, s	transport operation, s
I	Settling, forging of the trunnion	1	Removing the ingot for forging Tn=1160ºC			60
		2	Forging of the trunnion	46		
		3	Settling on 630 mm square (compression up to 200 mm per press stroke)	543		
		4	Return to furnace for heating Tk=960ºC			60
		Total time for technological operations for the first removal 709 s (11 min 49 s)				
II	Forging from 630 mm square to 450 mm square	5	Removal of settled ingot 630 mm square for forging Tn=1160ºC			6
		6	Drawing (compression to 120 mm per press stroke)	443		
		7	Smoothing (compression up to 10 mm per press stroke)		13	
		8	Turning over for forging the second half of the ingot			8
		9	Returning a 450 mm square forging to the furnace for heating at 950ºC			60
		Total time for technological operations for the second removal 780 s (13 min)				
III	Forging of 450 mm square bar to 350 mm square bar	10	Removal of settled ingot 630 mm square for forging Tn=1160ºC			6
		11	Drawing (compression to 120 mm per press stroke)	29		
		12	Turning for forging the second half of the ingot			84
		13	Smoothing (compression to 10 mm per press stroke)		118	
		14	Cutting into two bars A and H	100		
		15	Returning bar A sq. 350 mm to the furnace for heating			60
		16	Return of rod H sq. 350 mm to the furnace for heating Tk = 950ºC			60
		Total time for technological operations for III removal 780 s (13 min)				
IV	Forging of rod A from 350 mm square to 280 mm square	17	Removal of rod A from the furnace Tn=1160ºC			6
		18	Drawing rod A	612		
		19	Smoothing bar A		262	
		20	Turning over to forge the second half of bar A			86
		21	Return of bar A sq. 280 mm to the furnace for heating Tk = 920ºC			60
		Total time for technological operations for IV removal 1080 s (18 min)				
V	Forging of bar H from 350 mm square to 280 mm square	22	Removal of bar H from the furnace Tn=1160ºC			60
		23	Drawing of bar H	618		
		24	Smoothing the rod H		269	
		25	Turn for forging the second half of the rod H			81
		26	Return of bar H sq. 280 mm to the furnace for heating Tk = 920ºC			60
		Total time for technological operations for V removal 1088 s (18 min 8 s)				
VI	Forging of bar A from 280 mm square to Ø230 mm (finished grade in forging dimensions)	27	Removal of bar A from the furnace Tn=1160ºC			6
		28	Drawing of the first half of bar A	25		
		29	Smoothing of the first half of bar A		151	
		30	Reversal for forging the second half of bar A			81
		31	Drawing of the second half of rod A	75		
		32	Smoothing of the second half of bar A Tk=920ºC		133	
		Total time for technological operations for VI removal 750 s (12 min 30 s)				
VII	Forging of bar H from 280 mm square to Ø230 mm (finished grade in forging dimensions)	33	Removal of bar A from the press area. Removal of bar H from the furnace Tn=1160ºC			6
		34	Drawing of the first half of bar H	202		
		35	Smoothing of the first half of the bar N		162	
		36	Turning over for forging the second half of the rod H			91
		37	Drawing of the second half of the rod H	77		
		38	Smoothing of the second half of the bar N		109	
		39	Removal of the barbell from the press zone H Tk=920ºC			60
		Total time for performing technological operations for VII removal 671 s (11 min 11 s)				
ANALYSIS OF TECHNOLOGICAL PROCESS PARAMETERS						
A. Total time of use of the forging complex (B + C) 5858 s (1 hour 37 min 38 s = 1.627 hours) Forged bar obtained in forging dimensions – 3130 kg. Productivity – 1.924 t/hour. Products shipped to the consumer – 2432 kg. Productivity – 1.495 t/hour.						
B. Transport operation time 1344 s (22 min 24 s) – 22.94% of A						
C. Forging time (main and auxiliary forging operations) 4514 s (1 hour 15 min 14 s) – 77.06% of A						
B.1 Time of main forging operations (operations 2, 3, 6, 11, 14, 18, 23, 28, 31, 34, 37) 3264 s (54 min 24 s) – 72.31% of B						
B.2 Time of all auxiliary forging operations (operations 7, 13, 19, 24, 29, 32, 34, 38) 1240 s (20 min 40 s) – 27.69% of B						
B.3 Time of main forging operations of the last finishing stroke (operations 28, 31, 34, 37) bar A – 750 s bar H – 671 s						
B.4 Time of auxiliary operations of the last finishing stroke (operations 29, 32, 34, 38) bar A – 284 s (37.87% of B.3) bar H – 271 s (40.39% of B.3)						

DOI 10.15588/1607-6885-2025-4-8

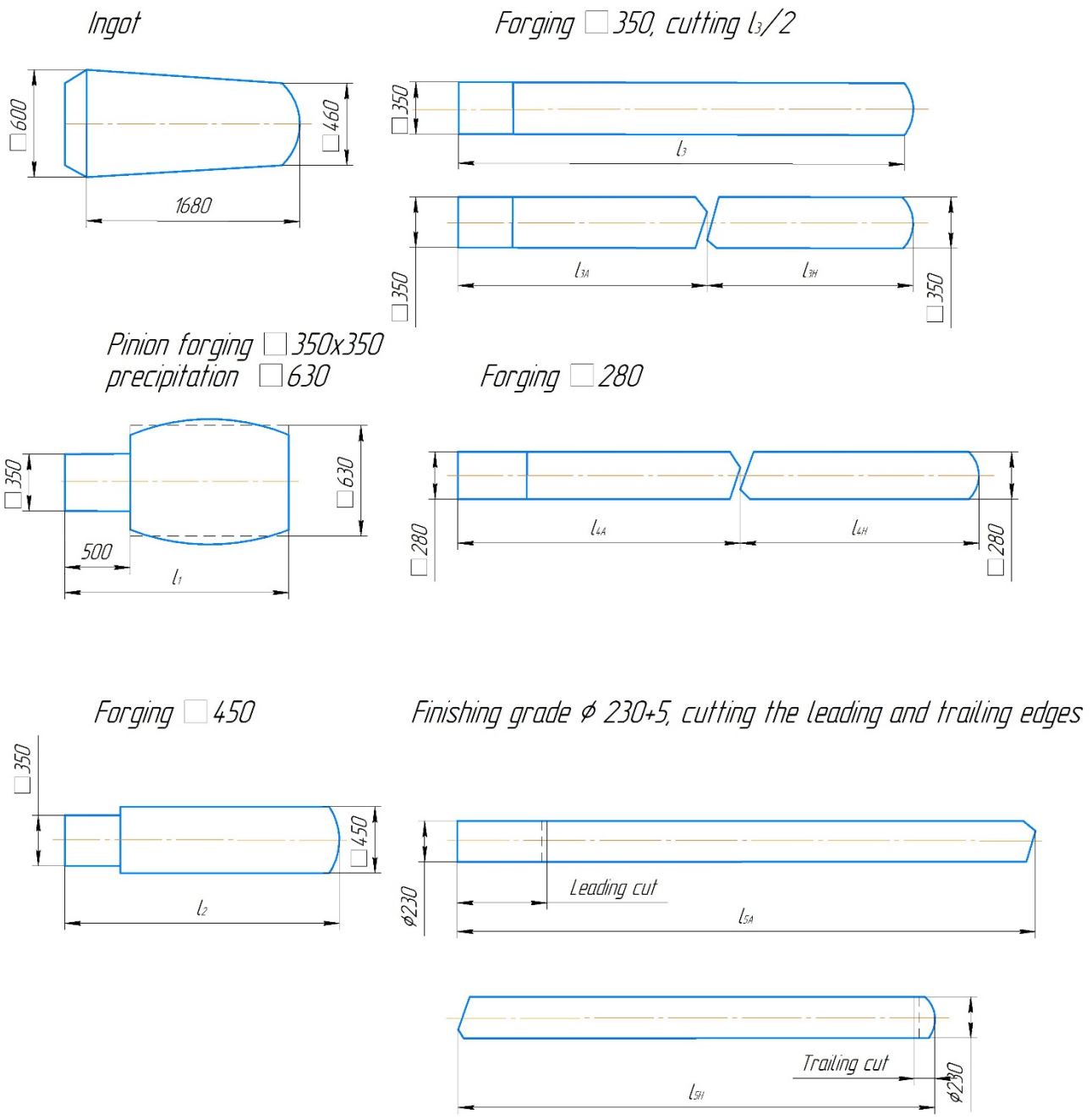

Figure 1. Diagram of forging cylindrical bars from tool alloy steel (using the example of steels 4Х5МФ1С, Х12МФ, 9Г2Ф)

Conclusions

The timing of forging large ingots of high-alloy steel grades on a hydraulic press indicates that forging accounted for 77% of the forging complex's operating time, which in turn was divided between the main forging operations, when the press was operating at maximum load (sedimentation, drawing), i.e. the equipment was used with maximum efficiency, and the time of auxiliary operations (smoothing, ticketing, corner filling), when only 3–4% of the press capacity was used. In the last finishing pass, auxiliary operations and, accordingly, unproductive use of the press capacity accounted for about 40% of the total forging time.

Thus, we can talk about the irrational use of high-cost equipment (hydraulic forging press), accompanied by increased resource costs. One way to apply resource-saving technologies could be introduction of additional equipment into the technological cycle to perform auxiliary forging operations or to replace these operations with other types of metal pressure processing while maintaining the final result of shaping.

DOI 10.15588/1607-6885-2025-4-8

References

1. A.Yu. Matyukhin, I.A. Alferov, T.A. Stefanenko et al. (2019). Methods for improving the quality of forging high-alloy steels and alloys on hydraulic presses. Bulletin of the National Technical University “KhPI”. Series: Innovative technologies and equipment for materials processing in mechanical engineering and metallurgy: collection of scientific papers. Kharkiv : NTU “KhPI”, 12 (1337), 36-41.

2. Matyukhin A.Yu., Knapinski M., Ben A.M. (2024). Main stages of designing resource-saving technologies for ingot deformation on hydraulic presses. New materials and technologies in metallurgy and mechanical engineering, 3, 66-71. https://doi.org/10.15588/1607-6885-2024-7-7

3. D.V. Obdul, V.D. Obdul, V.V. Duving, V.I. (2009). Tretyak Increasing the productivity of large-scale forging on hydraulic presses. New materials and technologies in metallurgy and mechanical engineering, 2, 73-75.

4. Kargin S.B. (2012). Improvement of shaft forging processes / Metal pressure treatment, 2(31), 101-106.

5. Kargin S.B. (2010). Innovative technologies for forging large forgings. Bulletin of the National Technical University of Ukraine “Kyiv Polytechnic Institute”. Series “Mechanical Engineering”, 60, 165-168.

6. Kargin S.B. (2013). Investigation of the forging of axial defects in ingots during shaft forging. Bulletin of the Priazovsk State Technical University. Series “Technical Sciences”, 27, 64–68.

7. V.K. Zablotsky, Ya.G. Zhbankov, A.A. Shvets, V.V. (2013). Panov Broaching of workpieces with a non-uniform temperature. Scientific Bulletin of the Dnipropetrovsk State Medical Academy, 2(12E), 52–62.

8. Y.S. Leea, S.U. Lee b, C.J. Van Tynec, B.D. Joo d, Y.H. Moon Internal void closure during the forging of large cast ingots using a simulation approach. Journal of Materials Processing Technology 211, 1136–1145. doi:10.1016/j.jmatprotec.2011.01.017.

9. Wang J, Fu P, Liu H, Li D, Li Y (2012). Shrinkage porosity criteria and optimised design of a 100-ton 30Cr2Ni4MoV forging ingot. Mater Design 35: 446–456. https://doi.org/10.1016/j.matdes.2011.09.056

10. Zhang X-X, Cui Z-S, Chen W, Li Y (2009). A criterion for void closure in large ingots during hot forging. J Mater Process Tech 209(4):1950–1959. https://doi.org/10.1016/j.jmatprotec.2008.04.051.

11. Feng C, Cui Z, Liu M, Shang X, Sui D, Liu J (2016). Investigation on the void closure efficiency in cogging processes of the large ingot by using a 3-D void evolution model. J Mater Proc Technol 237: 371–385. https://doi.org/10.1016/j.jmatprotec.2016.06.030.

12. Chen K, Yang YT, Liu KJ, Shao GJ (2010). Simulation of void defect evolution during the forging of steel ingots. In Adv Mater Res (Vol. 97, pp. 3079-3084). Trans Tech Publications Ltd. https://doi.org/10.4028/www.scientific.net/AMR.97-101.3079.

13. Kim Y, Cho J, Bae W (2011). Efficient forging process to improve the closing effect of the inner void on an ultra-large ingot. J Mater Proc Technol 211(6):1005–13. https://doi.org/10.1016/j.jmatprotec.2011.01.001.

14. Li Y, He T, Zeng Z (2013). Numerical simulation and experimental study on the tube sinking of a thin-walled copper tube with axially inner micro grooves by radial forging. J Mater Proc Technol 213(6):987–996. https://doi.org/10.1016/j.ijplas.2013.02.017

15. Banaszek G, Stefanik A (2006). Theoretical and laboratory modelling of the closure of metallurgical defects during forming of a forging. J Mater Proc Technol 177 (1–3):238-242

Received 27.11.2025
Accepted 04.12.2025

ДОСЛІДЖЕННЯ ПРОЦЕСУ КУВАННЯ ПОКОВОК ВИСОКОЛЕГОВАНИХ МАРОК СТАЛЕЙ НА ГІДРОПРЕСАХ

Антон Матюхін — канд. техн. наук, доцент, завідувач кафедри обробки металів тиском Національного університету «Запорізька політехніка», м. Запоріжжя, Україна, *e-mail: matiukhin85@gmail.com,* ORCID: 0000-0002-2261-0577

Володимир Товстюченко — аспірант кафедри обробки металів тиском Національного університету «Запорі-зька політехніка», м. Запоріжжя, Україна, *e-mail: azazelo1315@gmail.com*, ORCID: 0009-0008-0353-8101

Мета роботи. *Проведення хронометричного дослідження процесу кування високолегованих марок сталей на гідравлічних пресах для виявлення шляхів застосування ресурсозберігаючих технологій, що в кінцевому випадку дасть можливість знизити собівартість виготовлення продукції та підвищити конкурентну спроможність вітчизняних виробників кованої продукції.*

Методи дослідження. *Використано комплекс взаємодоповнюючих наукових методів, які дозволили отримати емпіричні дані та провести аналіз. Зокрема, основним емпіричним методом, застосованим у дослідженні, був хронометраж, а саме: точне вимірювання та фіксація тривалості окремих технологічних операцій у процесі*

DOI 10.15588/1607-6885-2025-4-8

вільного кування. Для формування повної картини технологічного процесу та порівняння фактичних даних з плановими було застосовано аналіз технологічної документації.

Методи обробки та аналізу даних дозволили розрахувати коефіцієнт виконання норм часу. Цей комплекс методів дозволив не лише кількісно оцінити витрати часу, але й якісно проаналізувати організацію та технологію процесу кування з метою розробки рекомендацій щодо його оптимізації.

Отримані результати. *Проведений хронометраж всіх складових технологічного процесу кування і подальший аналіз виявив тенденції з удосконалення процесу кування високолегованих марок сталей..*

Наукова новизна. *Пооперaційний хронометраж процесу кування поковок супроводжувався аналізом особливостей технологічного процесу, обладнання, що застосовувалося, маси злитка і маси готової поковки, робочих записів, що виконувалися технологічним персоналом в картах кування по факту виконання процесу.*

Практична цінність. *Отримані результати хронометричного дослідження існуючого технологічного процесу кування крупних злитків на гідропресах дають можливість виявити та застосувати технічні рішення для зниження ресурсовитрат.*

Ключові слова: *напружено-деформований стан металу, високолегована сталь, кування, гідравлічний прес, хронометраж операції, ресурсозберігаючі технології.*

Список літератури

1. Способи підвищення якості кування поковок високолегованих марок сталей та сплавів на гідропресах [Текст] / А. Ю. Матюхін, І. А. Альфьоров, Т. А. Стефаненко та ін. // Вісник Національного технічного університету «ХПІ». Серія: Інноваційні технології та обладнання обробки матеріалів у машинобудуванні та металургії: зб. наук. пр. – Харків : НТУ «ХПІ», 2019. – №12 (1337). – С. 36–41.

2. Основні етапи проектування ресурсозберігаючих технологій деформації зливків на гідропресах / Матюхін А. Ю., Кнапінські М., Бень А. М. // Нові матеріали і технології в металургії та машинобудуванні. – 2024. – № 3. – С. 66–71. https://doi.org/10.15588/1607-6885-2024-7-7

3. Підвищення продуктивності кування крупного сорту на гідравлічних пресах / Д.В. Обдул, В.Д. Обдул, В.В. Дувинг, В.І. Третяк //Нові матеріали і технології в металлургії та машинобудуванні. – 2009. – № 2. – С. 73–75.

4. Каргин С. Б. Совершенствование процессов ковки валов / Каргин С. Б. // Обработка металлов давлением. – 2012. – № 2(31). – С. 101–106.

5. Каргин С. Б. Инновационные технологии ковки крупных поковок / Каргин С. Б. // Вісник Національного технічного університету України «Київський політехнічний інститут». Серія «Машинобудування». – 2010. – № 60. – С. 165–168.

6. Каргин С. Б. Исследование заковки осевых дефектов в слитке при ковке валов / Каргин С. Б. //Вісник Приазовського державного технічного університету. Серія «Технічні науки». – 2013. – № 27. – С. 64–68.

7. Протяжка заготовок с неоднородным температурным полем // В.К. Заблоцкий, Я.Г. Жбанков, А.А. Швец, В.В. Панов // Научный вестник ДГМА. – 2013. – №2(12Е). – С. 52–62.

8. Moon Internal void closure during the forging of large cast ingots using a simulation approach / Y. S. Leea, S. U. Lee b, C. J. Van Tynec et al. // Journal of Materials Processing Technology. – 211. – P. 1136–1145. doi:10.1016/j.jmatprotec.2011.01.017.

9. Shrinkage porosity criteria and optimized design of a 100-ton 30Cr2Ni4MoV forging ingot. / Wang J., Fu P., Liu H. et al. // Mater Design 35. – P. 446–456. https://doi.org/10.1016/j.matdes.2011.09.056.

10. A crite-rion for void closure in large ingots during hot forging / Zhang X-X, Cui Z-S, Chen W, Li Y // J Mater Process Tech 209(4). – 2009. – P. 1950–1959. https://doi.org/10.1016/j.jmatprotec.2008.04.051.

11. Investigation on the void closure efficiency in cogging processes of the large ingot by using a 3-D void evolution model / Feng C, Cui Z, Liu M // J Mater Proc Technol 237. – 2016. – P. 371–385. https://doi.org/10.1016/j.jmatprotec.2016.06.030.

12. Simulation of void defect evolvement during the forging of steel ingot / Chen K, Yang YT, Liu KJ, Shao GJ // In Adv Mater Res. – 2010. – Vol. 97. – P. 3079–3084). Trans Tech Publications Ltd. https://doi.org/10.4028/www.scientific.net/AMR.97-101.3079.

13. Kim Y Efficient forging process to improve the closing effect of the inner void on an ultra-large ingot / Kim Y, Cho J, Bae W. // J Mater Proc Technol 211(6). – 2011. – P. 1005–13. https://doi.org/10.1016/j.jmatprotec.2011.01.001.

14. Li YNumerical simulation and experimental study on the tube sinking of a thin-walled copper tube with axially inner micro grooves by radial forging / Li Y, He T, Zeng Z //J Mater Proc Technol 213(6). – 2013. – P. 987–996. https://doi.org/10.1016/j.ijplas.2013.02.017.

15. Banaszek G.. Theoretical and laboratory modelling of the closure of metallurgical de-fects during forming of a forging / Banaszek G, Stefanik A // J Mater Proc Technol 177(1–3). – 2006. – P. 238–242.

DOI 10.15588/1607-6885-2025-4-8

ПАМ’ЯТІ КОЛЕГИ

DEAR COLLEAGUES

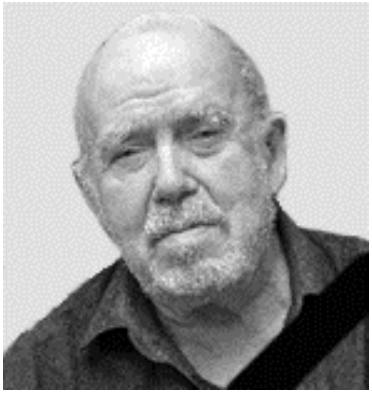

Смерть – це лише трансформація енергії,
що не зникає, а розквітає
в думках послідовників

Death is just a transformation of energy
that does not disappear, but flourishes
in the thoughts of followers

З глибоким сумом колектив редакційної колегії журналу «Нові матеріали і технології в металургії та машинобудуванні» повідомляє, що на 92-му році пішов з життя заступник головного редактора, доктор технічних наук, заслужений діяч науки і техніки України професор **Вадим Юхимович Ольшанецький**, який понад 25 років присвятив свої сили розвитку нашого видання та технічної науки в Україні.

Завідувач кафедри фізичного матеріалознавства Національного університету «Запорізька політехніка» В. Ю. Ольшанецький був не лише висококваліфікованим фахівцем, але й мудрим наставником, уважним колегою та невтомним популяризатором наукової думки. Його внесок у становлення та розширення змістової й методичної якості журналу важко переоцінити: завдяки його принциповості, інтелектуальній вимогливості та любові до науки наше видання стало одним з авторитетних майданчиків для технічної спільноти.

За роки співпраці він залишив по собі не тільки вагомий науковий спадок, а й людську теплоту – уміння підтримати словом, спрямувати до кращого рішення, надихнути на нові дослідження. Його професійність поєднувалася з гідністю й скромністю, що робило його постать особливо поважною серед колег, авторів та молодих учених.

Світла пам’ять про Вадима Юхимовича Ольшанецького назавжди залишиться в серцях тих, хто мав честь працювати поруч із ним.

Висловлюємо щирі співчуття рідним, друзям і всім, хто знав та цінував його.

With deep sorrow, the editorial team of the journal “New Materials and Technologies in Metallurgy and Mechanical Engineering” announces that at the age of 92, the Deputy Chief Editor, Doctor of Technical Sciences, Honored Worker of Science and Technology of Ukraine Professor **Vadym Ol’shanetskii**, has passed away. For more than 25 years, he devoted his efforts to the development of our publication and to the advancement of technical science in Ukraine.

Head of the Department of Physical Materials Science of the National University Zaporizhzhia Polytechnic Vadym Ol’shanetskii was not only a highly qualified specialist but also a wise mentor, an attentive colleague, and a tireless promoter of scientific thought. His contribution to shaping and enhancing the substantive and methodological quality of the journal is difficult to overestimate: thanks to his integrity, intellectual rigor, and love for science, our publication became one of the respected platforms for the technical community.

Throughout the years of cooperation, he left behind not only a significant scientific legacy but also human warmth – the ability to offer words of support, guide toward better decisions, and inspire new research. His professionalism was combined with dignity and modesty, which made him especially respected among colleagues, authors, and young scientists.

The bright memory of Vadym Ol’shanetskii will forever remain in the hearts of those who had the honor of working alongside him.

We express our sincere condolences to his family, friends, and all who knew and respected him.

Наукове видання

Нові матеріали і технології в металургії та машинобудуванні № 4/2025

Науковий журнал

Оригінал-макет підготовлено у редакційно-видавничому відділі НУ «Запорізька політехніка»

Комп’ютерний дизайн та верстання: Наталія Савчук

Реєстрація суб’єкта у сфері друкованих медіа:
Рішення Національної ради України з питань телебачення і радіомовлення
№ 3040 від 07.11.2024 року
Ідентифікатор медіа: R30-05583

Підписано до друку 18.12.2025. Формат 60×84/8
Папір офс. ризогр. Ум. др. арк. 8,1
Тираж 300 прим. Зам. № 1107

69063, м. Запоріжжя, НУ «Запорізька політехніка», друкарня, вул. Жуковського, 64

Свідоцтво суб’єкта видавничої справи
ДК № 6952 від 22.10.2019